

**PHYSICAL AND STRUCTURAL CHARACTERIZATION OF SUSTAINABLE
ASPHALT PAVEMENT SECTIONS AT THE NCAT TEST TRACK**

by

Adriana Vargas-Nordbeck

A dissertation submitted to the Graduate Faculty of
Auburn University
in partial fulfillment of the
requirements for the Degree of
Doctor of Philosophy

Auburn, Alabama
August 4, 2012

Approved by

David H. Timm, Chair, Brasfield & Gorrie Professor of Civil Engineering
Randy West, Director, National Center for Asphalt Technology
Rod Turochy, Associate Professor of Civil Engineering
John Fulton, Associate Professor of Biosystems Engineering

ABSTRACT

A sustainable pavement can be defined as a safe, efficient and environmentally friendly pavement that meets today's transportation needs without jeopardizing the ability to meet such needs in the future. Recent advances in this area include technologies that focus on low consumption of energy for production and placement, conservation of natural resources, noise reduction and improvement of the quality of stormwater runoff. As state agencies have begun to transition from an empirical pavement design method to a mechanistic-empirical (M-E) approach, it has become necessary to further evaluate the material properties and structural characteristics of these newer technologies. This research study evaluated physical and structural properties for different sustainable pavement sections placed at the National Center for Asphalt Technology (NCAT) Test Track.

The Test Track was reconstructed in the summer of 2009 and part of the experiment included six new structural sections built using several sustainable technologies, including warm mix asphalt (WMA), high RAP mixes and porous friction courses (PFCs). All pavement sections were embedded with a gauge array to measure horizontal asphalt strain, vertical aggregate base pressure and vertical subgrade pressure in the center of the outside wheelpath. During trafficking operations, falling weight deflectometer (FWD) testing was performed three times per month to quantify the seasonal behavior of the pavement layer moduli. Strain and pressure measurements were taken weekly under live traffic loads and under different environmental conditions. In general, the results indicated that pavement responses changed significantly for high RAP and PFC sections compared to the control, but not for virgin WMA sections.

Overall, laboratory tests performed on plant produced mixtures suggested that inclusion of high RAP percentages may increase susceptibility to fatigue and thermal cracking, while the use of WMA technologies could increase rutting susceptibility. However, some results varied depending on the test method used and did not correlate well with field performance. Caution must be taken when using laboratory test to evaluate the performance of sustainable mixes.

Field performance measurements showed that rut depths were influenced by the use of sustainable technologies, but all sections performed well overall with under 12.5 mm of rutting. No cracking or indication of moisture damage had been observed in any of the sections at the conclusion of the research cycle.

ACKNOWLEDGMENTS

The author would like to thank Dr. David H. Timm for his guidance and support in the development of this dissertation. The author would also like to acknowledge the advisory committee members including Dr. Randy West, Dr. Rod Turochy and Dr. John Fulton for their time and assistance during this project. Thanks are also due to the staff at the National Center for Asphalt Technology for all their assistance and to the State Departments of Transportation of Alabama, Florida, North Carolina, Oklahoma and Tennessee as well as the Federal Highway Administration for their continued cooperation and support of this research. Special thanks are due to her parents Mario and Shirley and to her sister Marcela, for all their love and support throughout all academic endeavors. Finally, to her husband Fabricio, for all of his encouragement and support in every step of the way.

TABLE OF CONTENTS

ABSTRACT	ii
ACKNOWLEDGMENTS.....	iv
LIST OF TABLES.....	x
LIST OF FIGURES	xii
LIST OF ABBREVIATIONS	xvi
CHAPTER 1 INTRODUCTION.....	1
BACKGROUND.....	1
MECHANISTIC EMPIRICAL PAVEMENT DESIGN.....	3
OBJECTIVES	5
SCOPE OF STUDY.....	5
ORGANIZATION OF DISSERTATION.....	6
CHAPTER 2 LITERATURE REVIEW	8
INTRODUCTION.....	8
WARM MIX ASPHALT	8
Advantages.....	10
Disadvantages	15
Design and Performance	15
HIGH RAP MIXTURES.....	20
Advantages.....	21

Disadvantages.....	22
Design and Performance	26
POROUS FRICTION COURSES	30
Advantages.....	30
Disadvantages	31
Design and Performance	33
SUMMARY	35
CHAPTER 3 EXPERIMENTAL PLAN	37
TEST SECTIONS.....	37
Mix Designs	39
Pavement Instrumentation	41
CONSTRUCTION	43
Cooling Rates.....	43
Density.....	44
LABORATORY TESTS.....	44
Binder Tests	45
Dynamic Modulus	46
Asphalt Pavement Analyzer.....	47
Flow Number	48
Hamburg Wheel Tracking Device.....	48
Tensile Strength Ratio	49
Beam Flexural Fatigue.....	50
Indirect Tension Test	51

PAVEMENT RESPONSES	52
Deflection Testing	52
Responses Under Dynamic Loading	53
Field Performance	56
SUMMARY	57
CHAPTER 4 CONSTRUCCION	58
COOLING RATES.....	58
MultiCool Software.....	59
MultiCool Simulation	61
Analysis of Results	64
IN-PLACE DENSITY	69
SUMMARY	72
CHAPTER 5 LABORATORY EVALUATION	73
EFFECT OF SUSTAINABLE TECHNOLOGIES ON BINDER PROPERTIES	73
Performance Grade.....	73
Performance Parameters	75
EFFECT OF SUSTAINABLE TECHNOLOGIES ON MIXTURE PROPERTIES	81
Dynamic Modulus.....	81
Asphalt Pavement Analyzer.....	85
Flow Number	87
Hamburg Wheel Tracking Device.....	88
Tensile Strength Ratio	91
Beam Flexural Fatigue.....	92

Thermal Cracking Analysis	95
SUMMARY	97
CHAPTER 6 ANALYSIS OF FIELD MEASURED PAVEMENT RESPONSES	99
AC Modulus – Temperature Relationships	99
Strain – Temperature Relationships	105
Pressure – Temperature Relationships.....	112
Significance of Differences.....	118
SUMMARY	123
CHAPTER 7 OBSERVED FIELD PERFORMANCE	125
RUTTING	125
CRACKING	131
MACROTEXTURE.....	132
ROUGHNESS.....	133
SUMMARY	134
CHAPTER 8 STRUCTURAL CAPACITY OF PFCs	136
FIELD MEASURED RESPONSES.....	136
ESTIMATING THE IN-PLACE MODULUS OF PFCs.....	137
EFFECT OF THICKNESS RATIO ON MODULUS REDUCTION	139
EFFECT OF THICKNESS RATIO ON STRAIN.....	140
SUMMARY	141
CHAPTER 9 CONCLUSIONS AND RECOMMENDATIONS	142
SUMMARY	142
CONCLUSIONS	143

RECOMMENDATIONS	145
REFERENCES	147
APPENDIX A	160

LIST OF TABLES

Table 2-1 Summary of WMA processes identified during NCHRP Project 09-43 (11).....	10
Table 2-2 Observed reduction (percent) in emissions with WMA (14).....	11
Table 2-3 Areas of HMA mixture design and analysis potentially requiring modification for WMA (11).....	16
Table 2-4 Minimum flow number requirements (11)	18
Table 2-5 Summary of test sections and binder test data (55).....	28
Table 2-6 Recommended gradation (68).....	34
Table 3-1 Section description.....	38
Table 3-2 Production temperatures.....	38
Table 3-3 Aggregate gradation – surface lift.....	40
Table 3-4 Aggregate gradation – intermediate lift.....	40
Table 3-5 Aggregate gradation – base lift.....	40
Table 3-6 Volumetric properties – surface lift.....	41
Table 3-7 Volumetric properties – intermediate lift	41
Table 3-8 Volumetric properties – base lift.....	41
Table 3-9 Dynamic modulus testing conditions	47
Table 4-1 Summary of Program Inputs.....	64
Table 5-1 Critical temperatures and performance grades – surface lift recovered binder.....	74
Table 5-2 Critical temperatures and performance grades – intermediate lift recovered binder....	74
Table 5-3 Critical temperatures and performance grades – base lift recovered binder.....	74
Table 5-4 Regression coefficients for master curve comparisons	84
Table 5-5 Regression coefficients for fatigue transfer functions.....	93

Table 5-6 IDT Test results for GE surface mixes	96
Table 6-1 Regression analysis for AC modulus as a function of mid-depth temperature	101
Table 6-2 Regression analysis for longitudinal strain as a function of mid-depth temperature .	108
Table 6-3 Regression analysis for vertical pressure as a function of mid-depth temperature	114
Table 6-4 Summary of differences in sustainable sections vs control	119
Table 7-1 Rutting resistance ranked by test method	128
Table 7-2 Predicted cycles to failure at 68°F	132
Table 7-3 Regression analysis for dense graded sections.....	133
Table 8-1 Dynamic and effective moduli data.....	138
Table 8-2 Software inputs – structural information	139

LIST OF FIGURES

Figure 1-1 M-E Design Schematic (8).....	4
Figure 2-1 Statistical Results of Interaction Between Aged and Virgin Binders Evaluated in NCHRP 9-12 Study (41).....	24
Figure 3-1 As-Built Pavement Cross-Sections.....	39
Figure 3-2 Schematic of Instrumentation.....	43
Figure 3-3 Temperature Measurements for (a) Surface and (b) Mid-depth.....	44
Figure 3-4 Sampling Mixtures.....	45
Figure 3-5 Asphalt Mixture Performance Tester (85).....	46
Figure 3-6 Asphalt Pavement Analyzer.....	47
Figure 3-7 Hamburg Wheel Tracking Device.....	49
Figure 3-8 Split Tensile Test Setup (85).....	50
Figure 3-9 Beam Fatigue Apparatus (85).....	51
Figure 3-10 Indirect Tension Test Setup (92).....	52
Figure 3-11 Falling Weight Deflectometer.....	53
Figure 3-12 Example Raw Response Traces for (a) Longitudinal Strain, (b) Transverse Strain and (c) Pressure.....	55
Figure 3-13 ALDOT Rut Depth Gauge Method.....	57
Figure 4-1 One-Dimensional Heat Transfer in a Pavement Structure (97).....	60
Figure 4-2 MultiCool Input Data Entry Window.....	62
Figure 4-3 Cumulative Distribution Function Plot for Temperature Differences.....	65
Figure 4-4 Main Effects Plot for Temperature Difference.....	66
Figure 4-5 Interaction Plot for Temperature Difference – Pavement Lift.....	67

Figure 4-6 Interaction Plot for Temperature Difference – Production Temperature.	67
Figure 4-7 Interaction Plot for Temperature Difference – Material Type.....	68
Figure 4-8 Average Temperature Differences for Control and PFC Mixtures.....	69
Figure 4-9 Average In-Place Density and Delivery Temperature – Surface Lift	70
Figure 4-10 Average In-Place Density and Delivery Temperature – Intermediate Lift.....	71
Figure 4-11 Average In-Place Density and Delivery Temperature – Base Lift.....	71
Figure 5-1 Rutting Parameter of Recovered Binders – Surface Lift.....	75
Figure 5-2 Rutting Parameter of Recovered Binders – Intermediate Lift.	76
Figure 5-3 Rutting Parameter of Recovered Binders – Base Lift.....	76
Figure 5-4 Fatigue Parameter of Recovered Binders – Surface Lift.....	77
Figure 5-5 Fatigue Parameter of Recovered Binders – Intermediate Lift.	78
Figure 5-6 Fatigue Parameter of Recovered Binders – Base Lift.....	78
Figure 5-7 Thermal Cracking Parameters of Recovered Binders – Surface Lift.....	79
Figure 5-8 Thermal Cracking Parameters of Recovered Binders – Intermediate Lift.	80
Figure 5-9 Thermal Cracking Parameters of Recovered Binders – Base Lift.....	80
Figure 5-10 Dynamic Modulus Comparison for Surface Lift Mixtures.....	82
Figure 5-11 Dynamic Modulus Comparison for Intermediate Lift Mixtures.....	82
Figure 5-12 Dynamic Modulus Comparison for Base Lift Mixtures.....	82
Figure 5-13 Dynamic Modulus at 10 Hz – Surface Lift.....	84
Figure 5-14 Dynamic Modulus at 10 Hz – Intermediate Lift.....	85
Figure 5-15 Dynamic Modulus at 10 Hz – Base Lift.....	85
Figure 5-16 APA Rut Depths.	86
Figure 5-17 Flow Number Results.....	88
Figure 5-18 Example of Hamburg Data (<i>104</i>).....	89
Figure 5-19 Hamburg Wheel Tracking Device Results for Rutting Susceptibility.	90
Figure 5-20 Hamburg Wheel Tracking Device Results for Moisture Susceptibility.....	91

Figure 5-21 Tensile Strength Ratio Results.....	92
Figure 5-22 Flexural Beam Fatigue Results at All Strain Levels.	93
Figure 5-23 95% Confidence Intervals for Regression Coefficients.	94
Figure 5-24 Fatigue Endurance Limit from Beam Fatigue Test.....	94
Figure 5-25 Thermal Stress versus Temperature.	96
Figure 5-26 Relationship between Critical Temperatures from Binder and Mix Testing.....	97
Figure 6-1 Relationship Between Backcalculated AC Modulus and Mid-depth Temperature...	100
Figure 6-2 95% Confidence Intervals for Regression Coefficients – AC Modulus.....	101
Figure 6-3 Temperature Normalized AC Modulus.....	103
Figure 6-4 Average Monthly Normalized AC Moduli at 68°F.....	104
Figure 6-5 Variation in AC Modulus Across Factors.	105
Figure 6-6 Relationship Between Longitudinal and Transverse Microstrain.....	106
Figure 6-7 Relationship Between Horizontal Longitudinal Microstrain and Mid-depth Temperature – Single Axles.	107
Figure 6-8 95% Confidence Intervals for Regression Coefficients – Longitudinal Strain.....	108
Figure 6-9 Temperature Normalized and Thickness Corrected Longitudinal Strains.	110
Figure 6-10 Average Monthly Thickness Corrected Longitudinal Strain Normalized at 68°F..	111
Figure 6-11 Variation in Longitudinal Strain Across Factors.	112
Figure 6-12 Relationship Between Vertical Base Pressure and Mid-depth Temperature – Single Axles.	113
Figure 6-13 Relationship Between Vertical Subgrade Pressure and Mid-depth Temperature – Single Axles.	113
Figure 6-14 95% Confidence Intervals for Regression Coefficients – Base Pressure.	115
Figure 6-15 95% Confidence Intervals for Regression Coefficients – Subgrade Pressure.	115
Figure 6-16 Temperature Normalized and Thickness Corrected Base Pressures.	116
Figure 6-17 Temperature Normalized and Thickness Corrected Subgrade Pressures.	117
Figure 6-18 Variation in Vertical Subgrade Pressure Across Factors.....	118

Figure 6-19 Change in Simulated Longitudinal Strain.	120
Figure 6-20 Change in Simulated Subgrade Pressure.	121
Figure 6-21 Difference in AC Modulus of Sustainable Sections Compared to the Control.....	122
Figure 6-22 Difference in Longitudinal Strain of Sustainable Sections Compared to the Control	122
Figure 6-23 Difference in Subgrade Pressure of Sustainable Sections Compared to the Control.	123
Figure 7-1 Rutting Progression of Test Sections.	126
Figure 7-2 Final Rut Depths.	127
Figure 7-3 Effect of Binder Stiffness on Rutting Potential.	128
Figure 7-4 Relationship between Last Measured Rut Depth and Vertical Pressures at 110°F...	129
Figure 7-5 Main Effects Plot for Rut Depth.	130
Figure 7-6 Interaction Plot for Rut Depth.	131
Figure 7-7 Change in Macrotexure over Time.	133
Figure 7-8 Change in IRI over Time.....	134
Figure 8-1 Difference in Measured Parameters at 68°F.....	137
Figure 8-2 Effect of Thickness Ratio on Modulus Reduction.	140
Figure 8-3 Effect of Thickness Ratio on Longitudinal Strain.....	141

LIST OF ABBREVIATIONS

AASHTO: American Association of State Highway and Transportation Officials

AC: Asphalt Concrete

ALDOT: Alabama Department of Transportation

AMPT: Asphalt Mixture Performance Tester

APA: Asphalt Pavement Analyzer

APT: Accelerated Pavement Testing

ARAN: Automated Road Analyzer

AWD: Asphalt Workability Device

BBR: Bending Beam Rheometer

CDF: Cumulative Distribution Function

DGIT: Design Guide Implementation Team

DOT: Department of Transportation

DP: Dust Proportion

DSR: Dynamic Shear Rheometer

EPA: Environmental Protection Agency

ESAL: Equivalent Single Axle Load

ETG: Expert Task Group

FEL: Fatigue Endurance Limit

FHWA: Federal Highway Administration

Fn: Flow Number

FWD: Falling Weight Deflectometer

GE: Group Experiment
GLWT: Georgia Loaded Wheel Tester
HMA: Hot-Mix Asphalt
HWTD: Hamburg Wheel Tracking Device
IDT: Indirect Tension Test
IRI: International Roughness Index
ITS: Indirect Tensile Strength
LEAB: Low-Energy Asphalt Concrete
LTPP: Long Term Pavement Performance
LVDT: Linear Variable Differential Transformer
MEPDG: Mechanistic-Empirical Pavement Design Guide
MTD: Mean Texture Depth
MTV: Material Transfer Vehicle
NAPA: National Asphalt Pavement Association
NCAT: National Center for Asphalt Technology
NCHRP: National Cooperative Highway Research Program
NMAS: Nominal Maximum Aggregate Size
OGFC: Open-Graded Friction Course
PAV: Pressure Aging Vessel
Pb: Binder Content
Pbe: Effective Binder
PCC: Portland Cement Concrete
PFC: Porous Friction Course
RAP: Reclaimed Asphalt Pavement
RMSE: Root-Mean-Square Error
RTFO: Rolling Thin Film Oven

SFE: Surface Free Energy

SGC: Superpave Gyratory Compactor

SIP: Stripping Inflection Point

TSR: Tensile Strength Ratio

Va: Air Voids

VFA: Voids Filled with Asphalt

VMA: Voids in the Mineral Aggregate

WMA: Warm Mix Asphalt

CHAPTER 1

INTRODUCTION

BACKGROUND

A sustainable pavement can be defined as a safe, efficient and environmentally friendly pavement that meets today's transportation needs without jeopardizing the ability to meet such needs in the future (1). The principal criteria for a sustainable pavement are as follows:

- Optimizing the use of natural resources and reducing energy consumption,
- Reducing impacts on the greenhouse effect (greenhouse gas emissions),
- Limiting pollution (air, water, ground, noise, etc.),
- Improving health, safety and risk prevention,
- Ensuring a high level of user comfort and safety.

The asphalt industry has been developing sustainable paving technologies and practicing green-build techniques since the 1960's through the reduction in emissions from asphalt plants (2). Since 1970, with the implementation of the Clean Air Act, total emissions from asphalt plants have dropped by more than 97% while annual production has increased by more than 250% (3). In 1973, the U.S. Environmental Protection Agency (EPA) established New Source Performance Standards (NSPS) to regulate air emissions of criteria pollutants and prevent the release of dust and smoke into the air.

In the 1980s the National Asphalt Pavement Association (NAPA) partnered with the EPA to conduct research on air emissions, including greenhouse gases from asphalt plants. In the 1990s the EPA conducted its own independent study of asphalt facilities. The results showed that emissions were low and well-controlled, leading EPA to declare in 2002 that asphalt plants are

not major sources of hazardous air pollutants. More recently, the asphalt industry has been implementing the use of warm mix asphalt (WMA) as means of reducing greenhouse gas emissions.

Another sustainable practice in the asphalt industry has been recycling. Asphalt pavement is the most recycled material in the nation, with about 100 million tons of asphalt pavement being reclaimed every year and approximately 80% of it being recycled back into new asphalt mixes (4). This initiative became popular in the 1970s due to the high cost of crude oil during the Arab oil embargo. The Federal Highway Administration (FHWA) provided partial funding to state agencies to construct paving projects using reclaimed asphalt pavement (RAP) and to document the results. As part of this effort, guidelines for pavement recycling were developed during the 1980s and 1990s (5).

Although the use of RAP provides environmental and economic benefits, many State transportation departments have limited the maximum amount of RAP allowed in asphalt mixes. This has been due to the lack of guidance on RAP use for special mixes and documented information about long-term performance of high RAP mixes. However, as asphalt binder costs continue to increase and more emphasis is given to sustainable technologies, the highway community is reassessing the use of higher percentages of RAP.

Finally, porous friction courses (PFCs), also called Open Graded Friction Courses (OGFC) have been used in the United States since the 1950s to improve skid resistance. The FHWA developed a mix design procedure in 1974, which was adopted by several state departments of transportation with mixed results. While many state agencies reported good performance, many others stopped using these types of mixtures due to unacceptable performance and/or inadequate durability (6, 7). However, significant improvements have been observed in the performance of PFCs since then thanks to the use of polymer modified binders and the development of better design and construction practices. PFCs are currently used as means of improving water quality, reducing noise and enhancing safety.

As state agencies have begun to transition from an empirical pavement design method to a mechanistic-empirical (M-E) approach, it has become necessary to further evaluate the material properties and structural characteristics of these sustainable technologies. This information is important for accurate performance prediction and design of efficient pavement structures because the M-E design method relies on mechanistic models that calculate structural responses (stresses, strains and deflections) based on material properties, environmental conditions and loading characteristics; as well as on empirical models that predict pavement performance from the calculated responses and material properties.

MECHANISTIC EMPIRICAL PAVEMENT DESIGN

From the early 1960s through 1993, all versions of the American Association for State Highway and Transportation Officials (AASHTO) Guide for Design of Pavement Structures were based on limited empirical equations developed at the AASHO Road Test in the late 1950s. As with any empirical method, the biggest disadvantage of the AASHTO method is that it can only be reliably applied to conditions similar to those for which it was developed. For this reason, the National Cooperative Highway Research Program (NCHRP) developed under Project 1-37A a mechanistic-empirical pavement design guide (known as the MEPDG) that incorporates nationally calibrated models to predict distresses induced by traffic load and environmental conditions.

The MEPDG uses material properties and climatic data to predict responses such as stresses, strains and deflections for a given pavement structure under traffic loads through the use of mathematical models. These responses are then used in empirically derived transfer functions to predict pavement performance through Miner's hypothesis. Figure 1-1 shows a schematic of the M-E design framework.

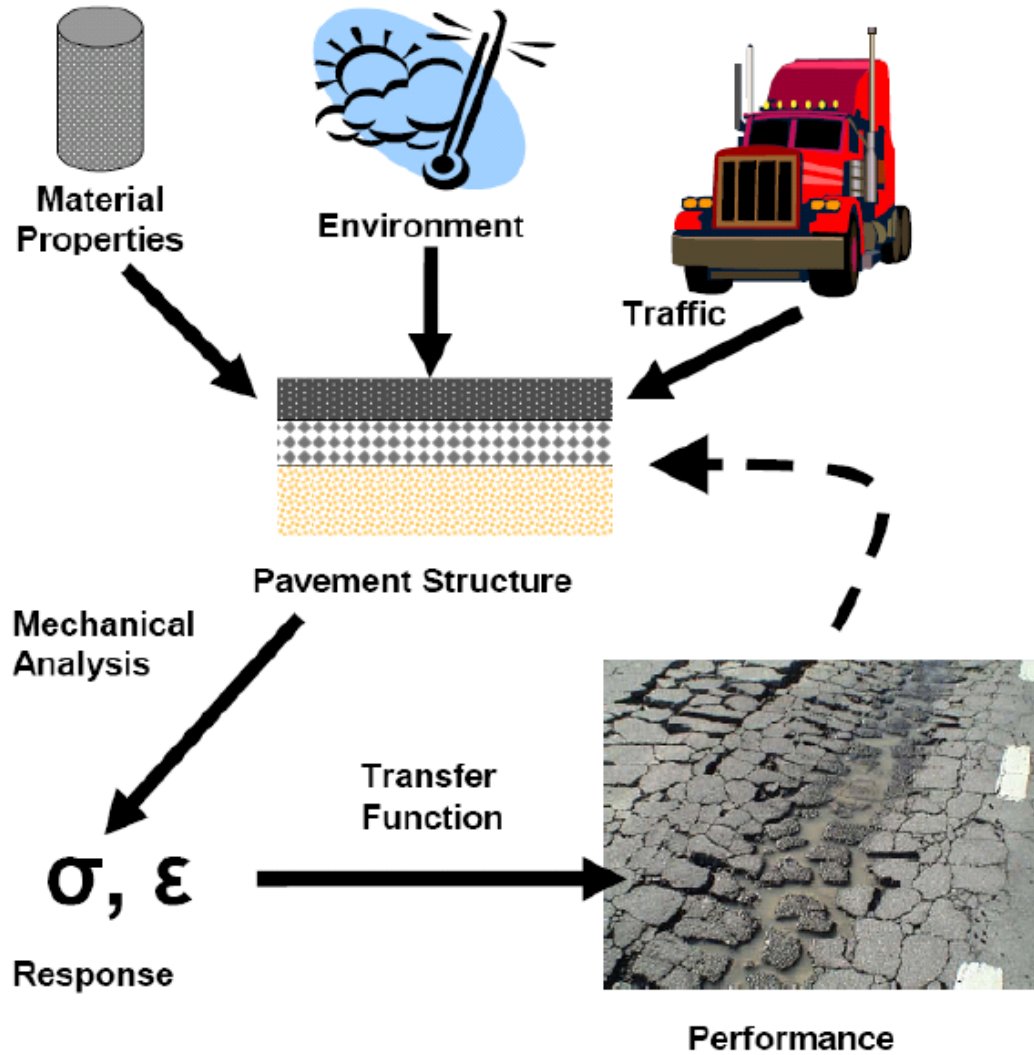


Figure 1-1 M-E Design Schematic (8).

There are many advantages of using an M-E design procedure over a purely empirical one. The analysis procedure relates not only pavement thickness, but also material properties to performance. Traffic is characterized in a more detailed manner, allowing for a more accurate prediction of its effect on performance. If the reliability analysis is properly formulated, the effect of construction and materials variability on performance can be estimated. Finally, the pavement can be designed specifically to address particular types of distresses (9).

A survey conducted by the Federal Highway Administration Design Guide Implementation Team (DGIT) indicated that, as of 2008, forty states use or are planning to use

the MEPDG. Additionally, the survey responses pointed out that the major hindrances to implementation included material characterization and local calibration (10). The use of sustainable technologies like WMA, high RAP mixes and PFCs is expected to produce changes in material properties which would in turn affect pavement responses, a pivotal part of the M-E procedure. The focus of this research was to determine the significance of those changes and how they affect pavement performance.

OBJECTIVES

The objectives of this research were to:

1. Characterize pavement properties of WMA, high RAP and PFC mixes using laboratory and field data.
2. Perform a statistical analysis to evaluate the effect of factors such as production temperature and high RAP content on pavement responses.
3. Assess the performance of WMA, high RAP and PFC mixes subjected to traffic.
4. Determine structural contribution of PFCs to the pavement section.

SCOPE OF STUDY

To accomplish the aforementioned objectives, six structural sections were built at the National Center for Asphalt Technology (NCAT) Test Track using several sustainable technologies. The NCAT Test Track is a 1.7 mile closed loop full-scale accelerated pavement testing (APT) facility located in Opelika, Alabama. A fleet of tractor-trailers operates five days per week for 16 hours per day, applying a total of 10 million 18,000 lb equivalent single axle loads (ESAL) to the 200-ft test sections over a two-year period of time. Sections at the Test Track can be classified as surface mix performance sections or structural sections. Structural sections are equipped with an embedded array of strain and pressure sensors to measure pavement responses under load for

validation and analysis of mechanistic-empirical design procedures. All sections are equipped with temperature sensors throughout the pavement depth.

Reconstruction for the fourth research cycle was carried out during the summer of 2009, with paving operations performed from July 3 to August 11. Traffic operations started on August 28, 2009 and concluded on September 30, 2011. A total of three WMA sections were placed including a foam-based section, an additive-based section and a foam-based section containing 50% RAP. Additionally, a control HMA section and a control HMA section with 50% RAP were also placed. A control section with permeable surface was also included. The mixtures placed in each of the sections were designed to have similar volumetric properties using the same virgin materials and had the same design cross-section.

During construction, plant produced mix samples were collected and used to conduct several laboratory tests to obtain material properties of the different mixes and to evaluate their performance. During operation, direct strain and pressure measurements were obtained weekly to compare the pavement responses under live traffic loads and different environmental conditions. Additionally, falling weight deflectometer (FWD) testing was performed several times per month to quantify the seasonal behavior of the pavement layer moduli. Finally, field performance was monitored throughout the experiment to determine if the differences observed in material properties and pavement responses had a significant effect on service life.

ORGANIZATION OF DISSERTATION

This dissertation is organized into nine remaining chapters. Chapter 2 presents a literature review of the different types of sustainable technologies evaluated in this study (warm mix asphalt, high RAP mixtures and porous friction courses), including a description, advantages and disadvantages, design methods and performance of each technology. Chapter 3 describes the experimental plan that includes a detailed description of the mixtures, pavement instrumentation, laboratory tests performed, and data collected during construction and traffic operations. Chapter

4 presents the findings from construction data, particularly a validation of the cooling curve prediction model for the asphalt mixtures and a comparison of the in-place densities obtained during construction. Chapters 5 and 6 provide the results of the laboratory tests and field-measured pavement responses, respectively. Chapter 7 describes the observed field performance of the test sections. In Chapter 8, the findings from the structural contribution of PFCs are presented. Finally, Chapter 9 discusses the conclusions and recommendations obtained from this study.

CHAPTER 2

LITERATURE REVIEW

INTRODUCTION

This chapter describes the different sustainable technologies included in this research, their advantages, disadvantages, design considerations and performance. The technologies include warm mix asphalt (WMA), reclaimed asphalt pavement (RAP) and porous friction courses (PFC).

WARM MIX ASPHALT

Warm-mix asphalt (WMA) describes a group of technologies which allow a reduction in the temperatures at which asphalt mixes are produced and placed. WMA originated in Europe with the German Bitumen Forum in 1997, in response to the requirements for greenhouse gas reduction that were being adopted by the European Union countries as part of the Kyoto treaty on climate change. In 2002, the National Asphalt Pavement Association (NAPA) led a study tour to Europe to examine WMA technologies. Since then, the interest in this type of technology has grown in the United States.

While hot-mix asphalt (HMA) is typically produced in the temperature range of 140° to 170°C (280° to 335°F), WMA mixes can be produced in the range of 105° to 135°C (220° to 275°F) thanks to the use of technologies that reduce mixture viscosity and improve workability. The technologies that are used to produce WMA can be classified into those that use foaming and those that use some form of chemical or organic additive(s). Foaming-based WMA introduces a small amount of water into hot asphalt. This water turns into steam dispersed in hot binder which results in an expansion of the binder and a corresponding reduction in the mix viscosity. The introduction of this small amount of water can be done by either a foaming nozzle, or adding a

hydrophilic material such as zeolite, or using moist aggregate. In most cases, additive-based WMA lowers the binder viscosity that enables relatively low mixing temperature and hence increases the mixture workability.

There are several WMA technologies available worldwide, and the number currently available in the United States continues to grow rapidly. Table 2-1 shows a summary of the technologies identified under NCHRP Project 09-43, which developed mixture design and analysis procedures to be used for the wide range of WMA processes currently available or likely to become available in the future (11). The reduction in production temperature obtained with these technologies can result in several economic, environmental and construction benefits, such as reduced emissions and energy consumption, extended paving seasons and improved working conditions at the paving site.

Table 2-1 Summary of WMA processes identified during NCHRP Project 09-43 (11)

WMA Technology	Process/Additive	Company
Accu-Shear Dual Warm Mix Additive System	Foaming system	Stansteel
Adesco/Madsen Static Inline Vortex Mixer	Foaming system	Adesco/Madsen
Advera	Zeolite	PQ Corporation
AQUABLACK	Foaming system	Maxam Equipment Company, Inc.
AquaFoil	Foaming system	Reliable Asphalt Products
Asphaltan-B	Montan Wax	Romonta
Aspha-min	Zeolite	Eurovia
Cecabase RT	Unspecified additive	Ceca
Double Barrel Green	Foaming system	Astec, Inc.
Evotherm ET	Emulsion with unspecified additives	MeadWestvaco
Evotherm DAT	Unspecified additive	MeadWestvaco
Evotherm 3G	Unspecified additive	MeadWestvaco
Licomont BS-100	Fatty acid derivative	Clariant
Low Emission Asphalt	Sequential coating using wet fine aggregate and unspecified additive	McConnaughay Technologies
Meeker Warm Mix Asphalt System	Foaming system	Meeker Equipment
Rediset WMX	Unspecified additive	Akzo Nobel
Sasobit	Fischer Tropsch wax	Sasobit
Terex Warm Mix Asphalt	Foaming system	Terex Roadbuilding
Thiopave	Sulfur plus compaction aid	Shell
TLA-X	Trinidad Lake Asphalt plus modifiers	Lake Asphalt of Trinidad and Tobago
Ultrafoam GX	Foaming system	Gencor Industries, Inc.
WAM Foam	Soft binder followed by hard foamed binder	Kolo Veidekke, Shell Bitumen

Advantages

The use of WMA technologies has the potential to provide a number of environmental, economic and operational benefits. Among the environmental benefits is the reduction of emissions, energy consumption savings and improved working conditions. The improved workability offers operational benefits like the ability to pave in cooler temperatures, longer haul distances, improved compaction and use of higher reclaimed asphalt pavement (RAP) percentages.

Reduced Emissions

The burning of fossil fuels required to generate heat needed to dry and heat the aggregates for asphalt concrete production results in the production of several combustion by-products, including sulfur dioxide (SO₂), nitrogen oxide (NO_x) and carbon dioxide (CO₂) (12). SO₂ and NO_x lead to the production of ground-level ozone (O₃) and particulate matter air pollution, which can be a health hazard. On the other hand, CO₂ is a greenhouse gas that absorbs infrared radiation and traps heat in the atmosphere. Reduction of CO₂ is a key element of sustainable development and is mandated as part of the European's Union ratification of the Kyoto Protocol (13).

Prowell and Hurley (14) reported that WMA emissions measurements range from 30 to 98% of that of HMA. The emission reduction depends upon several factors such as the degree of temperature reduction, type of fuel used, the plant's design and operation, aggregate moisture content and RAP use. Table 2-2 presents the range in reductions reported by several European countries and Canada.

Table 2-2 Observed reduction (percent) in emissions with WMA (14)

Emission	Norway	Italy	Netherlands	France	Canada
CO₂	31.5	30-40	15-30	23	45.8
SO₂	NA	5	NA ²	18	41.2
VOC	NA	50	NA	19	NA
CO	28.5	10-30	NA	NA	63.1
NO_x	62.5	60-70	NA	18 ¹	58.0
Dust	54.0	25-55	NA	NA	NA

¹Reported as NO₂

²Not Applicable

Mallick et al. (15) estimated CO₂ emission reductions of around 32% using 1.5% Sasobit®, which is the content typically used in the U.S. Middleton and Forfyflow (16) conducted emissions testing on warm mixes produced with the Double Barrel® Green process and found reductions of approximately 10% in CO₂, CO and NO_x. A slight increase in SO₂ emissions was identified, however these emissions are considered to be relatively low for both WMA and HMA

and the difference could be a result of testing variability. Davidson and Pedlow (17) found reductions of approximately 20% for CO, CO₂ and NO_x and a slight increase in SO₂ for WMA produced with Evotherm.

Reduced Fuel and Energy Usage

The reduced need to completely dry the aggregates and better coating at lower temperatures allow for lower mixing temperatures and hence less fuel consumption for WMA. Fuel savings with WMA typically range from 20 to 35% (14). These savings depend on several factors, such as the temperature reduction from the use of WMA, the moisture content of the aggregate, and details of the plant's design and operation. The savings could be higher (possibly 50% or more) with processes such as low-energy asphalt concrete (LEAB) and low-energy asphalt (LEA) where the aggregates (or a portion of the aggregates) are not heated above the boiling point of water.

Improved Workability

WMA technologies enhance workability through the addition of additives (organic, chemical, water-based, or hybrids). Some WMA technologies work by reducing the viscosity, allowing the aggregates to be properly coated with asphalt binder at lower temperatures. In general, mixture workability is determined based on subjective field observations. Austerman et al. (18) evaluated the workability of mixes containing various dosages of Advera® and Sasobit® using the Asphalt Workability Device (AWD). The AWD rotates the loose asphalt mixture at a constant speed and separately records the torque exerted on a pug mill style paddle shaft embedded into the mixture. Lower torque values are indicative of more workable mixes. The results showed that the addition of WMA additives at different dosages improved the workability of the mixtures.

Compaction of the mixtures may be improved thanks to several factors: a larger temperature bracket for WMA systems, lower binder viscosity within the compaction temperature bracket and the decreased rate of heat loss at lower temperatures. It is also suggested that a

lubrication effect may also be provided with certain additives (19). The reduction in viscosity also allows for each roller pass to provide more compaction, thus reducing the number of roller passes needed to achieve a specific density (20).

Cold Weather Paving and Longer Haul Distances

The reduced viscosity obtained with WMA technology in addition to a slower rate of cooling also have the potential to reduce the risks associated with cold-weather paving, allowing the extension of the paving season. Case studies were presented during the FHWA International Scanning Tour where, in Germany, paving was completed with various technologies when ambient temperatures were between -3 and 4 °C (27 and 39°F). The mix temperatures for the WMA behind the paver ranged from 102 to 139 °C (216 to 282°F). Better densities were obtained with the WMA than the HMA with the same or fewer roller passes (13).

Crews (21) reported that paving performed in New York City using mixes prepared with Evotherm™ at ambient temperatures below 0°C (32°F) compacted easily under normal compaction patterns using standard roller equipment. Density measurements substantiated the effectiveness of compaction: all measurements met the density specification of less than 8% air voids.

Reduced rate of cooling and reduced viscosity at lower compaction temperatures can also facilitate longer haul distances while maintaining workability. With WMA it is possible to increase mixing temperature above the “WMA mixing temperature” (but below the HMA mixing temperature) with limited binder damage. Consequently, mixing temperature may be adjusted to compensate for long transportation time, while workability of WMA remains acceptable at the end of the haul for placement and compaction (19).

FHWA’s WMA European Scanning Tour reported examples that included WAM-Foam stored in a silo for 48 hours and still had the ability to place and compact the mix. HMA

containing Sasobit® reportedly was hauled up to 9 hours in Australia and the material was still successfully unloaded (13).

In September 2008, Evotherm™ WMA was chosen for a long-haul Caltrans demonstration project, in which both dense-graded and open-graded asphalt mixes were produced at conventional hot mix temperatures at the Syar Industries, Inc., plant at Santa Rosa. The mix was hauled to California State Route 1 at Point Arena on the coast north of San Francisco, a four-hour drive through the mountains. For both mixes, a material transfer vehicle (MTV) was specified to receive mix from haul trucks and feed to the paver. Because of the long haul, the mix was produced at 149 to 152°C (300 to 305°F), temperatures higher than normal for warm mix. Typically the mix was leaving the hot mix plant at Santa Rosa at just above 149°C (300°F), and was arriving at the job site at about 127°C (260°F). After transition in the MTV, the mix was placed on the roadway at temperatures from 104 to 116°C (220 to 240°F) without any workability issues (22).

Increased Usage of RAP

The workability and compaction benefits mentioned above can be particularly favorable for the production of stiff mixes, such as those incorporating highly modified binders or large percentages of RAP. WMA technologies may be beneficial with mixes containing high proportions of RAP in two ways: 1) the viscosity reduction will aid in compaction, and 2) the decreased aging of the binder as a result of the lower production temperatures may help compensate for the aged RAP binder, similar to using a softer binder grade. In Germany, a case study was presented in which 45 percent RAP was used in the base course. In the Netherlands, both LEAB and HMA are routinely produced with 50 percent unfractionated RAP (13).

Mallick et al. (23) used a WMA additive to evaluate the feasibility of producing an asphalt mixture incorporating 75 percent RAP. Two HMA mixes and two WMA mixes were

produced using varying PG grades. The results showed that it was possible to produce mixes with high RAP with similar air voids as virgin mixes at lower than conventional temperatures using WMA technology.

Tao and Mallick (24) investigated the feasibility of using 100% RAP HMA as a base course with the aid of WMA additives. Workability of the mixes was evaluated with a torque tester, similar to the AWD. The tester measured the torque needed to move a paddle through a mix inside a bucket at different times after mixing. The results showed that workability of the 100% RAP HMA was improved with the addition of WMA additives at temperatures as low as 110°C (230°F).

Disadvantages

Because WMA technologies are relatively new, there may be some resistance from the paving industry to widely accept them in the U.S. The lack of long-term performance data is one of the major drawbacks to WMA implementation. Reducing the production temperature of asphalt mixtures has prompted concern by some that there is potential for greater moisture susceptibility, increased rutting, and delays in traffic due to cure time (25).

Finally, WMA technologies require some up-front investment in equipment modification, materials, and training. Although these costs can be eventually offset by reductions in fuel costs, without a commitment to use by owner agencies or specific contractual language allowing their use to the contractors' advantage, contractors may be unwilling to take on this additional up-front investment risk (26).

Design and Performance

Design

For most WMA projects constructed in the United States, WMA has been added into a mixture designed as HMA with no change to the job mix formula. NCHRP Project 09-43 was conducted

to develop a mixture design and analysis procedure for the wide range of WMA additives and processes that are currently in use or which may become used in the future (11).

HMA mixture design and analysis generally consists of five major steps: 1) materials selection, 2) design aggregate structure, 3) design binder content selection, 4) evaluate moisture susceptibility, and 5) performance analysis. NCHRP Project 09-43 identified potential areas of this design procedure requiring modification for WMA, as shown in Table 2-3. The research showed that only minor changes to current mixture design practice are needed to design WMA mixtures, which are summarized in the Draft Appendix to AASHTO R 35: Special Mixture Design Considerations and Methods for Warm Mix Asphalt (11).

Table 2-3 Areas of HMA mixture design and analysis potentially requiring modification for WMA (11)

Step	Item	Special Warm Mix Considerations
Materials Selection	Binder Selection	<ul style="list-style-type: none"> Potentially less aging during mixing and construction due to lower production temperatures. Effect of any warm mix additives and warm mix processing on binder properties.
	Aggregate Properties	<ul style="list-style-type: none"> None
	Recycled Asphalt Pavement	<ul style="list-style-type: none"> Effect of production temperature on the degree of commingling of recycled and new binders. Effect of warm mix additives and warm mix processing on the degree of commingling of recycled and new binders.
	Additives	<ul style="list-style-type: none"> Warm-mix additive selection. Effect of lower production temperatures and warm mix additives on anti-strip additives.
Design Aggregate Structure	Nominal Maximum Aggregate Size	<ul style="list-style-type: none"> None
	Trial Gradations	<ul style="list-style-type: none"> None
	Batching	<ul style="list-style-type: none"> WMA process specific
	Mixing	<ul style="list-style-type: none"> WMA process specific Method to determine appropriate mixing temperatures for warm mix processes. Method to assess workability of WMA.
	Conditioning	<ul style="list-style-type: none"> Verify that short-term conditioning per AASHTO R 30 applies to WMA processes.
	Compaction	<ul style="list-style-type: none"> Method to determine appropriate compaction temperatures for warm mix processes. Verification of compaction levels.
	Volumetric Analysis and Criteria	<ul style="list-style-type: none"> None
Design Binder Content Selection	Specimen Preparation	<ul style="list-style-type: none"> See considerations above for laboratory batching, mixing, conditioning, and compaction.
	Volumetric Analysis and Criteria	<ul style="list-style-type: none"> None
Evaluate Moisture Sensitivity	Specimen Preparation	<ul style="list-style-type: none"> See considerations above for laboratory batching, mixing, conditioning, and compaction.
	Testing and Analysis	<ul style="list-style-type: none"> None
Performance Analysis	Specimen Preparation	<ul style="list-style-type: none"> See considerations above for laboratory batching, mixing, conditioning, and compaction.
	Testing and Analysis	<ul style="list-style-type: none"> None

Key findings from this project are summarized below (11):

1. **Volumetric Properties.** For HMA mixtures with 1.0 percent binder absorption or less, the volumetric properties of WMA designed with the procedures developed under NCHRP Project 09-43 were essentially the same as those obtained from an HMA design.

2. **Binder Grade Selection.** The same grade of binder should be used in both WMA and HMA mixtures. High-temperature grade bumping may be necessary for WMA processes with extremely low production temperatures.
3. **RAP in WMA.** To ensure good mixing of RAP and new binders, it is recommended that the planned field compaction temperature for WMA exceed the high-temperature grade of the “as recovered” RAP binder.
4. **Short-Term Oven Conditioning.** The same short-term conditioning used for design of HMA mixtures (2 hours of oven conditioning at the compaction temperature) should be used for WMA.
5. **Coating, Workability and Compactability.** For the variety of WMA processes available, viscosity-based mixing and compaction temperatures cannot be used to control coating, workability and compactability. The draft appendix to AASHTO R 35 uses direct measurements of coating and compactability on laboratory-prepared mixtures. Several workability devices were evaluated and differences between WMA and HMA were detected, but only when the temperatures dropped to the compaction range of WMA. Therefore, the draft appendix to AASHTO R 35 does not include an evaluation of workability. The compactability of WMA mixtures is evaluated by determining the number of gyrations to 92 percent relative density at the planned field compaction temperature and 54°F below the planned field compaction temperature. A maximum increase in gyrations of 25 percent when the compaction temperature is reduced is recommended.
6. **Moisture Sensitivity.** The same process is used to evaluate WMA moisture susceptibility as is used with HMA. Moisture sensitivity will likely be different for WMA compared to HMA. Some WMA processes improve moisture resistance because they include anti-strip additives.
7. **Rutting Resistance.** The proposed evaluation of rutting resistance for WMA is done using the flow number test. Specimens should be short-term conditioned for 2 hours at the compaction temperature to simulate the binder absorption and stiffening that occurs during

construction. Current criteria for the flow number test for HMA are based on 4 hours of short-term conditioning at 275°F. However, since it is inappropriate to condition WMA mixtures at temperatures above their production temperature, the criteria for evaluating rutting resistance of WMA mixes were reduced compared to HMA mixes and are shown in Table 2-4.

Table 2-4 Minimum flow number requirements (II)

Traffic Level, Million ESALs	Minimum Flow Number ¹	
	HMA	WMA
< 3	NA	NA
3 to < 10	53	30
10 to < 30	190	105
≥ 30	740	415

¹ Average of four specimens tested using the following conditions: 7.0% air voids; 600 kPa repeated deviatoric stress with a contact deviatoric stress of 30 kPa; unconfined; design temperature at 50% reliability and appropriate depth.

8. **Performance Evaluation.** For the same aggregates and binders, WMA mixtures designed following the special considerations outlined in the report will have similar properties as HMA mixes. While volumetric properties will be similar, WMA mixes could have lower stiffness for as-constructed conditions.

Performance

There have been several laboratory and field studies aimed to assess the performance of WMA mixtures compared to HMA. These studies have focused primarily on areas of concern such as rutting resistance and moisture susceptibility.

Prowell et al. (27) evaluated the rutting potential of WMA mixes under accelerated loading. Laboratory and field tests were conducted on WMA mixes placed as surface courses on rehabilitated sections at the NCAT Test Track. The results indicated that the rutting potential of WMA and HMA mixes as measured by the Asphalt Pavement Analyzer (APA) compared well. Although the reduced aging of the binder in the WMA sections might tend to increase rutting potential, the improved density of the samples may tend to negate this to some extent. Field measured rut depths also indicated similar performance for WMA and HMA sections.

Hurley and Prowell (28, 29) evaluated the applicability of different processes for use in WMA mixes, including a zeolite and a synthetic wax. APA test results showed that addition of these products did not increase the rutting potential of the asphalt mixes. Xiao et al. (30) conducted a laboratory investigation of rutting resistance in WMA mixtures containing moist aggregates. The experimental design included two aggregate moisture contents, two lime contents, three WMA additives, and three aggregate sources. Results from the APA test indicated that mixtures containing WMA additives had lower or similar rut depths than the control. Rutting resistance was primarily affected by aggregate source regardless of WMA additive, lime content and moisture content.

In a similar experimental design, Xiao et al. (31) studied moisture damage in laboratory WMA mixes containing moist aggregates through conventional testing procedures such as indirect tensile strength (ITS) and tensile strength ratio (TSR). The authors found that dry ITS values are affected by the aggregate moisture and hydrated lime contents while the use of WMA additives had no significant effect on dry ITS and toughness values. The wet ITS values were similar for the control and WMA mixtures under identical conditions (same moisture and lime contents), but in general were statistically different for mixtures made with various aggregate sources.

Kvasnak et al. (32) compared moisture susceptibility test results for both laboratory and plant produced mixes. Mixtures were evaluated using three methods: tensile strength ratio, absorbed energy ratio and stripping inflection point. In general, lower moisture susceptibility results were observed for WMA specimens than for HMA, however most of the WMA samples passed all three moisture susceptibility criteria. In addition, WMA moisture susceptibility results improved from the laboratory to the plant while HMA performed better in the laboratory than in the plant.

Wasiuddin et al. (33) studied the effect of Sasobit® and Aspha-Min on wettability and adhesion using the surface free energy (SFE) method. Dynamic advancing–wetting contact angles

were measured for wettability (coating) and dewetting–receding contact angles were measured to evaluate adhesion. Moisture susceptibility was defined as the amount of spontaneously released free energy due to the breaking of the binder–aggregate bond with water. Two binders (PG 64-22 and PG 70-28) were evaluated at three selected percentages of Sasobit® (2%, 4%, and 8%) and Aspha-Min (1%, 4%, and 6%) based on the weight of the binder. It was observed that Sasobit increases the wettability of asphalt binders over aggregates and in general reduces the adhesion (free energy of adhesion) between asphalt binders and aggregates. The overall SFE results for Aspha-Min were not statistically significant. For PG 64-22, a small or no reduction in moisture susceptibility was observed; while for PG 70-28 an increase in moisture susceptibility was observed.

Hodo et al. (34) performed moisture susceptibility tests on cores extracted from a foamed asphalt project constructed in Chattanooga, TN, using the Hamburg wheel tracking device and AASHTO T 283. Results from the Hamburg wheel tracking device indicated that the stripping results marginally failed to meet the specifications, while AASHTO T 283 data indicated that the mix marginally met the specification requirements. The mixture continued to perform well after one year in place.

HIGH RAP MIXTURES

Asphalt materials removed during resurfacing, rehabilitation or reconstruction operations can be put back into new pavements since they contain asphalt binder and aggregates that can be reused. It is estimated that every year more than 100 million tons of asphalt pavement material is reclaimed and almost all of it is reused or recycled into new pavements (35). While RAP has been used for decades, increased production costs and limited aggregate and binder supply have generated interest in using higher RAP contents. High RAP is defined as using 25 percent or more RAP in an asphalt mixture by weight of the total mix (36).

The RAP Expert Task Group (ETG) was formed by the Federal Highway Administration in 2007 to encourage the use of RAP by agencies that do not currently optimize the amount of RAP in their mixtures or those that do not allow RAP at all in their HMA (2). As part of this initiative, the ETG conducts a RAP use survey in partnership with the American Association of State Highway and Transportation Officials (AASHTO) every two years. In 2007, RAP made up 12 percent of the average asphalt mix by volume. From 2007 to 2009, about 27 States increased the amount of RAP allowed in asphalt mixtures, and as of 2009, 23 States had experience with high RAP mixes. As of 2011, more than 40 State highway agencies allow more than 30 percent RAP, but only 11 report actually using 25 percent RAP or more (37).

Advantages

The two main factors that influence the use of RAP are economic savings and environmental benefits. Using RAP reduces costs associated with materials and transportation. Materials costs comprise about 70 percent of the total HMA production cost, with the most expensive and economically variable material being the asphalt binder (36). By replacing a portion of the virgin materials with RAP, especially in the intermediate and surface layers, where the binder is used to provide tensile strength, protect from moisture and provide a smooth, skid-resistant riding surface, more economical pavements can be built. Khandal and Mallick (38) estimated that savings of up to 34% could be generated for mixtures containing up to 50% RAP. McDaniel and Nantung (39) reported on a cost-benefit analysis conducted by the Indiana DOT that estimated savings in materials were nearly \$330,000 per year when adding only 5 percent RAP to more than 5 million tons of base and intermediate mixes, although RAP contents of 15 percent to 20 percent are more typical. The study also estimated a benefit-to-cost ratio of 220:1 in material cost savings alone.

The use of RAP also conserves energy, preserves natural resources and decreases the amount of construction debris placed into landfills. A study prepared for the New York State

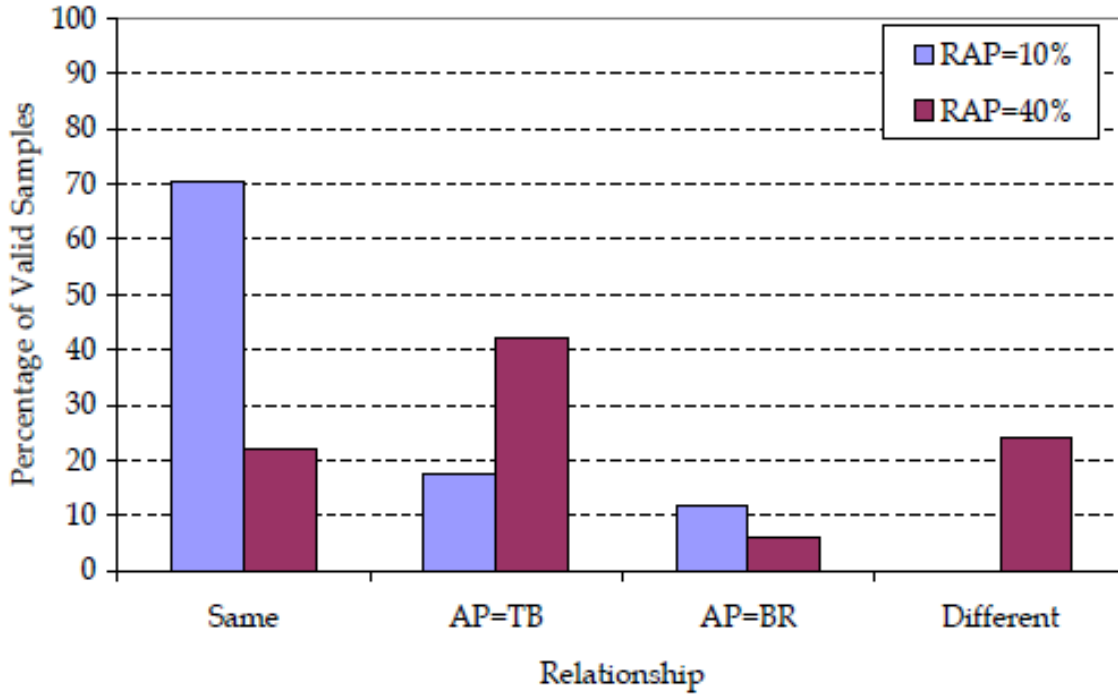
DOT (40) quantified the energy and environmental impacts of using RAP in HMA through several mathematical models that combined the drying/heating, transportation, and processing/calorific energies. It was found that using RAP in HMA resulted in energy savings, and that the difference in energy consumption was affected by RAP content, moisture in RAP, and HMA discharge temperature. In addition, it was estimated that at low RAP content, using RAP in HMA increases CO₂ emission while the opposite is true for high RAP content. However, the reduction of CO₂ emission from using RAP is primarily from the shorter hauling distance for RAP materials.

Disadvantages

One of the main concerns when using high RAP contents is the level of blending that occurs between the residual and virgin asphalt binders, which can affect the performance of the mixtures. If it is assumed that total blending occurs when the RAP is actually acting as a “black rock”, the binder will not be stiff enough and insufficient asphalt binder is used. Conversely, if it is assumed that RAP does not blend with the virgin asphalt binder when it is actually blending, the binder will be stiffer than expected and the mix will be rich (41). Kandhal and Foo (42) suggested that up to 15% RAP could be used without changing PG binder grade. Between 15% and 25% RAP, the virgin binder grade should be decreased by one increment on both the high- and low-temperature grades. Above 25% RAP, blending charts should be used to select virgin binder grade.

NCHRP Project 9-12 (43) studied the behavior of RAP materials when mixed with virgin aggregates and binders by comparing the performance of mixtures at three possible levels of interaction: black rock (no blending), total blending and actual practice. In all cases the overall gradation and total asphalt content were kept constant. Two RAP contents were used, 10 and 40%, which correspond to typical minimum and maximum percentages of RAP normally used in practice. Mixtures were compared using the results from the Frequency Sweep (FS), Simple

Shear (SS), and repeated Shear at Constant Height (RSCH) tests at high and intermediate temperatures, and the Indirect Tensile Creep (ITC) and Strength (ITS) tests at low temperatures. In most cases, the results indicated that at 10% RAP content there was no significant difference between the three cases. At 40% RAP content, the black rock case was different from the actual practice and total blending cases. These results suggest that no change in binder grade is required at low RAP contents and total blending can be assumed at high RAP contents. However, the statistical analyses of the study only partially support these findings, as shown in Figure 2-1. Out of 66 possible comparisons, 11 and 16 cases were inconclusive at a RAP content of 10% and 40%, respectively. At a RAP content of 10%, a majority of the cases (70%) supported the conclusion that all cases were similar. However, at a RAP content of 40%, only 42% of the comparisons supported the conclusion that the total blending cases are similar to the actual practice cases.



Same: Actual Practice = Total Blending = Black Rock
 AP = TB: Actual Practice = Total Blending \neq Black Rock
 AP = BR: Actual Practice = Black Rock \neq Total Blending
 Different: Actual Practice \neq Black Rock \neq Total Blending

Figure 2-1 Statistical Results of Interaction Between Aged and Virgin Binders Evaluated in NCHRP 9-12 Study (41).

Huang et al. (44) analyzed the blending process of RAP with virgin mixture under normal mixing conditions. Pure mechanical blending was evaluated by blending one type of screened RAP (only particles passing through a No. 4 sieve) at three proportions (10, 20 and 30%) with virgin coarse aggregates without adding any new virgin asphalt binder. Actual plant mixing was simulated by blending 20% screened RAP with virgin aggregates and PG 64-22 virgin asphalt binder. The results indicated that only a small portion of aged asphalt in RAP actually participated in the remixing process; other portions formed a stiff coating around RAP aggregates, and RAP functionally acted as “composite black rock.”

The presence of aged binder also makes design and construction of mixtures with a high RAP content challenging because it can cause problems with workability and compactability. In

addition, at high temperatures RAP materials tend to produce blue smoke, consisting of air pollutants. To prevent this, the RAP material is normally blended with superheated virgin aggregate before mixing with virgin binder. The superheated aggregate transfers heat to the RAP to soften the RAP binder and break the RAP material into smaller lumps. At high RAP percentages, higher temperatures are required for the virgin aggregate at the time of mixing since RAP is not heated, thus requiring higher energy consumption. These issues can be addressed by using additives or processes that improve workability and lower production temperature, such as WMA technologies.

Material variability is another obstacle for use of high RAP percentages. RAP variability makes it difficult to control the asphalt content, gradation and air voids of the production mixture, especially at higher percentages of RAP (45). The RAP variability may be caused by the following factors (46):

- When RAP is removed from an old roadway, it may include the original pavement materials, plus patches, chip seals, and other maintenance treatments.
- Base, intermediate, and surface courses from the old roadway may all be mixed together in the RAP.
- RAP from several projects is sometimes mixed in a single stockpile.
- RAP stockpiles may include waste trial batches of HMA mixes.
- RAP stockpiles may also include “deleterious material,” such as wood, concrete, trash, etc.

The use of proper techniques for stockpiling and processing RAP may help control RAP variability. These include eliminating contamination, separating RAP stockpiles from different sources, processing (crushing or fractionating) RAP stockpiles, storing the processed RAP using a paved, sloped surface to reduce the moisture content, and characterizing the processed RAP right after the stockpile is being built at its final location, and marking or numbering the stockpile (46).

Design and Performance

Design

When asphalt recycling became popular in the 1970's, FHWA provided funding to State transportation departments to build paving projects using recycled materials and document the effective use of resources. This effort resulted in the publication of several documents providing information and guidance on the use of recycled materials in highways from the late 1970's to the early 1990's (38, 47-49). When the Superior Performing Asphalt Pavements (Superpave) mixture design method was implemented in the late 1990's, the Strategic Highway Research Program did not provide guidance for the use of RAP in HMA, causing many State transportation departments to stop allowing the use of high amounts of RAP to reduce variability. In an effort to modify the Superpave design method to more effectively evaluate mixtures containing RAP, NCHRP Project 9-12 developed guidelines for testing and designing Superpave mixtures with RAP (50, 51).

The overall Superpave mix design process for mixtures incorporating RAP is similar to the mix design for all virgin materials, with the following exceptions (51):

- The RAP aggregate is treated like another stockpile for blending and weighing, but must be heated gently to avoid changing the RAP binder properties;
- The RAP aggregate specific gravity must be estimated;
- The weight of the binder in the RAP must be accounted for when batching aggregates;
- The total asphalt content includes the binder provided by the RAP; and
- A change in virgin binder grade may be needed depending on the amount of RAP, desired final binder grade, and RAP binder stiffness. For mixtures containing high RAP, this process involves the use of a blending chart or blending equation to determine the amount of RAP to use if the virgin binder grade is known or to select the grade of virgin binder if the percentage of RAP binder is known.

Performance

The use of high RAP contents has been the subject of several laboratory and field studies. More recently, studies have combined the use of high RAP and WMA processes in an effort to reduce the stiffening effect associated with aged RAP binder and maximize the benefits provided by both sustainable paving technologies.

Li et al. (52) investigated the effect of various types and percentages of RAP on asphalt binder and mixture properties. Two RAP sources, two asphalt binders (PG 58-28 and PG 58-34) and three RAP contents (0, 20 and 40%) were used to prepare ten different mixtures. Mixtures were subjected to moisture susceptibility tests, dynamic complex modulus testing and indirect tensile creep and strength testing. Results showed that all mixtures passed the minimum tensile strength ratio of 75%. The addition of RAP increased the complex modulus and the asphalt binder and RAP source had a significant effect on the mixture modulus. Additionally, increasing the amount of RAP in the mixture resulted in higher stiffness. Tests conducted on extracted binder samples indicated that as the percentage of RAP increased, the stiffness of the binder also increased.

Daniel and Lachance (53) studied the effect of RAP addition on the volumetric and mechanistic properties of asphalt mixtures. Mixtures included RAP contents of 15, 25 and 40% and two types of RAP (processed and unprocessed), with a Superpave 19-mm mixture containing 0% RAP being used as the control. Testing included dynamic modulus in tension and compression, creep compliance in compression, and creep flow in compression. Results indicated that at 15% RAP, the stiffness of the mixture increased and the compliance decreased, which suggests that the mixture will be more resistant to permanent deformation and less resistant to fatigue and thermal cracking due to the addition of aged binder contained in the RAP. However, mixtures containing 25 and 40% RAP did not follow the expected trends and behaved similar to the control mixture.

Huang et al. (54) conducted a laboratory study to evaluate the fatigue characteristics of HMA mixes containing varying percentages of RAP (0, 10, 20 and 30%). The tests performed included indirect tensile strength, semi-circular bending (SCB) and semi-circular notched fracture resistance. Results indicated that the inclusion of RAP generally increased the tensile strength and improved fatigue life of the mixes. However, mixture properties changed significantly for RAP contents of 30 percent.

West et al. (55) evaluated the constructability and performance of asphalt mixes containing moderate and high percentages of RAP under accelerated loading at the NCAT Test Track. The test sections included two with 20% RAP, four with 45% RAP and a control with no RAP. Table 2-5 summarizes the binder data for the test sections. Samples of the plant produced mixes were obtained during construction and used to fabricate specimens to test for APA rutting susceptibility, dynamic modulus and beam fatigue. Field cores were also taken to evaluate top down cracking using the energy ratio as a metric.

Table 2-5 Summary of test sections and binder test data (55)

Section	% RAP ^a	% RAP Binder ^b	Virgin Binder		Virgin Binder + RAP	
			PG Grade	True Grade	Predicted Grade	Recovered Grade
W3	20	18.2	PG 76-22	78.1-23.8	80.1-22.4	78.1-30.3
W4	20	17.6	PG 67-22	68.4-31.2	72.0-28.6	74.2-29.7
W5	45	42.7	PG 52-28	54.7-32.8	69.4-25.8	74.1-30.2
E5	45	41.0	PG 67-22	68.4-31.2	76.9-25.1	80.9-26.2
E6	45	41.9	PG 76-22	78.1-23.8	82.7-20.7	85.5-25.7
E7	45	42.7	PG 76-22 + 1.5% Sasobit	83.2-20.6	85.7-18.8	86.3-24.3
N5	0	0	PG 67-22	68.4-31.2	68.4-31.2	71.1-32.4

^aBy weight of aggregates.

^bBy weight of binder.

The results showed that as expected, mixes with softer binders and high VFA were more prone to rutting. The APA test results ranked the mixes in a way similar to the field results, with the exception of the control mix. The dynamic moduli results showed the effect of the binder

stiffnesses on mix stiffness. Softer grades of virgin binders substantially decreased the mix stiffness, which could play a role in durability of RAP mixes under high-strain conditions. The bending beam test results indicated that the 45% RAP mixes were less fatigue resistant than the 20% RAP and control mixes, but the differences appeared to be due to a lower effective volume of effective asphalt. The energy ratio results indicated that polymer modification was beneficial for the RAP mixes, but this was not evident with the bending beam results. All sections were performing well in the field after 9.4 million ESALs, with under 10 mm of rutting and only two sections showing minor cracking that could be due to reflection cracks and construction defects.

Another NCAT study compared virgin and recycled asphalt pavements using data from the Long Term Pavement Performance (LTPP) program (56). The study included data from 18 projects within the United States and Canada, and compared paired sections of virgin asphalt mix and recycled mix containing 30% RAP using seven pavement performance measurements: International Roughness Index (IRI), rutting, fatigue cracking, longitudinal cracking, transverse cracking, block cracking and raveling. The results showed that RAP mixes performed better than or equal to virgin mixes, except for fatigue cracking, longitudinal cracking and transverse cracking. It was concluded that using at least 30 percent recycled material in an asphalt pavement can provide the same overall performance as a virgin pavement.

Hong et al. (57) also investigated the in situ performance of HMA with a relatively high percentage of RAP (35% by weight) for Texas Specific Pavement Studies Category 5 experimental sections from the LTPP program. The performance monitoring period covered 16 years and the performance indicators included transverse cracking, rut depth and ride quality. Compared to virgin sections, sections containing RAP had higher cracking amounts, less rut depth and similar roughness change over time. The authors concluded that a well-designed mix with 35% RAP could perform as satisfactorily as a virgin mix during a normal pavement life span.

POROUS FRICTION COURSES

Porous friction courses (PFC), also known as open-graded friction courses (OGFC), are gap-graded HMA mixtures designed to have a large number of voids so that water can drain through and over their surface (58). The origin of porous mixtures dates back to the 1930s, when Oregon began experimenting with plant mix seal coats to improve frictional properties. In the 1940s, California began using plant mix seal coats as an alternative to chip seals and slurry seals, with the added benefits of noise reduction, increased durability and better ride quality. By 1950, a number of western states began to use these mixes to improve frictional properties. Their use did not become widespread until the 1970s, in response to FHWA's program to help increase the skid resistance on roadways, but the results were mixed (59). While many state DOTs reported good performance, many others stopped using PFCs due to unacceptable performance and lack of durability (60). However, significant improvements have been achieved in mixture design, construction and maintenance techniques of PFCs since their introduction, resulting in better performance and capturing the attention of transportation agencies thanks to their potential safety and environmental benefits.

Advantages

Safety Benefits

The large air voids content in PFCs allows for the removal of water from the road surface during rain events, improving safety through the reduction in splashing and hydroplaning. Less surface water also results in glare reduction, thus improving visibility of road markings under wet conditions. Higher wet frictional resistance, particularly at high speeds, has also been reported (61). As a result, PFCs have the potential to reduce wet weather accidents. Virginia, France and Canada have documented significant improvements (59). In Virginia, accidents on State Route 23 were reduced by approximately 50 percent. On the A7 Motorway in France, the number of accidents dropped from 52 between 1979 to 1985 to none in the following four years when a

dense-graded surface was replaced with a PFC. In Canada, wet weather accidents were reduced by 54 percent and the total number of accidents by 20 percent.

Environmental Benefits

PFCs have also been shown to reduce tire-pavement noise thanks to the sound absorbing negative texture generated by mixture air voids (62). Noise levels decrease in the range of 3 to 6 dB(A) as compared to dense-graded asphalt mixtures and up to 7.8 dB(A) as compared to Portland cement concrete (PCC) pavements (63). These reductions in tire/pavement noise can be compared to reducing the traffic volume in half or doubling the distance between the source of the noise and their location (59, 64).

The noise level is influenced by aggregate size, size distribution, permeability and the condition of the layer. PFC mixtures are more effective for noise reduction on high speed roadways, where tire-pavement interaction creates a hydraulic action which flushes the dirt from the pavement voids and reduces clogging, maintaining the noise reduction benefits for longer (65).

Additionally, PFCs reduce pollutants commonly observed in highway runoff such as total suspended solids, metals. The benefits obtained from the use of PFC mixtures are comparable with those attained from a vegetated filter (66, 67).

Disadvantages

The benefits of PFCs are diminished due to clogging of the voids, leading to accelerated loss of permeability and noise reduction capacity (65). Performance issues for this type of mixtures are generally related to moisture susceptibility and raveling. However, improvements in binders, admixtures (e.g. fibers) and gradation have enhanced performance in terms of longer life, reduction of failures, and conservation of functionality for longer periods (68, 69).

PFCs are typically assigned no or minimal structural contribution for pavement design. In a survey conducted as part of NCHRP Project 9-41 (59) in which sixty four percent of the U.S. states responded along with four Canadian provinces, Austria and Japan, only 27 percent of the respondents said that they assigned a structural value to the PFC pavement layer. Of those assigning a structural value, over 70 percent stated that the structural value was estimated from layer coefficients. In the Netherlands, Van Der Zwan et al. (70) indicated that the dynamic modulus of PFC is about 70 to 80 percent of dense-graded mixtures, which when input into their pavement design models results in a 10 to 20 percent increase in the thickness required to maintain a specific fatigue strain at the bottom of the pavement layer when using PFC as compared to dense-graded mixes. In Belgium, Van Heystraeten and Moraux (71) found that based upon modulus testing, porous asphalt constructed with an 80/100 penetration graded asphalt binder will contribute 73 to 79 percent of the structural capacity of typical dense-graded mixes. Bolzan et al. (72) indicated that Argentina adopted a 50 percent structural capacity for porous asphalt mixtures in the initial projects. The resilient modulus of porous asphalt mixtures was found to be approximately 60 percent of the conventional mixtures. The authors pointed out that at both higher and lower temperatures, polymer modified porous asphalt mixes perform better than unmodified conventional mixes and that further research needs to be conducted to reach at definitive conclusions.

Conversely, there are also some researchers who have indicated that PFCs are structurally comparable to conventional dense-graded mixes. Based on deflection measurements, the Oregon Department of Transportation assigns the same structural number for both OGFC and dense-graded layers (61). In Spain, PFC and dense-graded mixtures are also considered to have similar structural capacity (73). This conclusion was obtained from analysis of the reinforcement capacity and the reduction in deflection induced by PFC layers, which were similar to that produced by dense-graded asphalt mixtures.

Design and Performance

Design

The design of PFCs typically involves four primary steps: materials selection, selection of aggregate gradation, selection of optimum binder content and performance testing. However, there is not a unified methodology adopted by local agencies for the design of PFCs.

In 1990, the FHWA published complete guidelines for mixture design in Technical Advisory T5040.31 (74). This method was based on the evaluation of the surface capacity of the predominant aggregate fraction, defined as the material that passes the 3/8 inch sieve and is retained on the No. 4 sieve. The asphalt content is determined through an empirical formula that includes a surface constant value (K_c) and the apparent specific gravity of the predominant aggregate. The optimum content of fine aggregate is calculated based on the asphalt content and design percent air voids (suggested as 15%). The coarse aggregate gradation should be modified if the magnitude of its voids is not enough to contain the asphalt and the air voids. The procedure also requires a test to establish optimum mixing temperature and a test for resistance to effects of water.

In 2000, NCAT recommended a new mix design system based on a laboratory study that evaluated different gradations and types of additives (68). The new design system identified gradation bands, volumetric properties and performance related tests. The authors made the following recommendations based on the four design steps mentioned previously:

1. **Materials selection.** Guidance for suitable aggregates can be taken from recommendations for stone matrix asphalt (SMA). High stiffness binders made with polymers are recommended for hot climates or cold climates with freeze-thaw cycles, medium to high volume traffic conditions, and mixes with high air void contents (in excess of 22%). Addition of fibers is also desirable under such conditions. For low to medium volume traffic conditions, either polymer modified binders or fibers may be sufficient.

2. **Selection of aggregate gradation.** The master gradation band shown in Table 2-6 is recommended.

Table 2-6 Recommended gradation (68)

Sieve Size	Percent Passing
19 mm	100
12.5 mm	85-100
9.5 mm	55-75
4.75 mm	10-25
2.36 mm	5-10
0.075 mm	2-4

3. **Selection of optimum binder content.** Specimens are prepared at three binder contents in increments of 0.5 percent and subjected to draindown, Cantabro abrasion on aged and unaged samples, laboratory permeability and, if possible, APA rutting tests. The optimum binder content should meet the following criteria: 1) a minimum of 18 percent air voids, 2) abrasion loss on unaged specimens not exceeding 20 percent, 3) abrasion loss on aged specimens not exceeding 30 percent and 4) a maximum draindown of 0.3 percent by total mixture mass.
4. **Performance testing.** The mixture should be evaluated for moisture susceptibility using the modified Lottman method (AASHTO T283) with five freeze/thaw cycles and have a minimum TSR of 80 percent.

More recent research at NCAT (75) recommended that a design compaction effort (N_{design}) of 50 gyrations be used on SGC specimens, which provides approximately the same level of density as that of the 50-blow Marshall procedure. In addition, the CoreLock® procedure, using double bags, was recommended for determining the air voids content and bulk specific gravity of OGFC specimens. Lower air void magnitudes were obtained when using the CoreLok® method, therefore it was recommended that the target air voids be reduced by approximately 2.5% when using this procedure. Finally, the test parameters for the Cantabro loss test may need to be adjusted for SGC specimens. A maximum loss of 15% for unconditioned samples and 20% for conditioned samples was suggested.

Performance

The service life of PFCs is highly variable and can range from 7 to 10 years (73). While a number of European countries indicate an average service life of 10 years (59), in the United States a survey of state highway agencies conducted in 1998 by Kandhal and Mallick (60) showed that 73 percent of the state agencies obtained an estimated average service life of greater than 8 years. The most common distresses observed in PFCs are raveling and delamination (59, 73). Raveling in PFCs can be associated with the aging of the binder due to the open nature of the mix and binder draining from the mixture during transportation and laydown (draindown), which reduces the film thickness of the aggregates near the surface. Tolman and Gorkum (76) indicated that the increased hardening of the porous asphalt resulting from binder aging along with a drop in temperature can lead to fracture during the winter periods. However, these problems can be addressed by using polymer-modified binder and additives such as fibers.

Due to the stone-on-stone contact of the coarse aggregate, PFCs are considered to have high resistance to permanent deformation. Fortes and Merighi (77) evaluated the rutting potential of PFCs using an unconfined static creep test. The results indicated that PFC mixtures had less potential for permanent deformation than dense-graded mixtures and that PFCs containing polymer modified binders performed best. Generally, rutting should not be an issue unless there are mix design or construction problems (59).

SUMMARY

In the last decades, the asphalt industry has shown a growing interest in sustainable paving technologies. The potential environmental and economic benefits make these technologies attractive for contractors and transportation agencies, but questions still remain on how they may affect mixture properties and what, if any, is the effect on long term pavement performance. Although a number of laboratory studies regarding the types of sustainable pavements mentioned

in this chapter have been conducted, the limited information available on field studies continues to be one of the major hindrances for implementation.

CHAPTER 3

EXPERIMENTAL PLAN

TEST SECTIONS

As part of the fourth research cycle at the Test Track, the Group Experiment (GE) was created to include structural sections built using several sustainable technologies. The GE was sponsored by the Alabama, Florida, North Carolina, South Carolina, Oklahoma and Tennessee state departments of transportation and the Federal Highway Administration. A total of three WMA sections were placed including a foam-based section, an additive-based section and a foamed-based section containing 50% RAP. Additionally, a control HMA section, a control HMA section with 50% RAP and a control section with permeable surface course were also placed.

Table 3-1 shows a description of each section. The letters “S” and “N” in the section column denote the tangent of the Test Track in which the sections were located (South or North). All sections were paved in three lifts and paving was performed by the same contractor using the same crew. All mixtures were produced at the same plant. With the exception of the PFC surface lift in section S8, each lift of the south tangent sections were paved on the same day in a continuous process, keeping the plant settings constant while varying the production temperature. Similarly, both north tangent sections were placed in the same manner. Table 2 shows the production temperature for each mixture.

Table 3-1 Section description

Section	Description	Abbreviation	Lift	NMAS (mm)	Virgin Binder
S8	Control with PFC surface	PFC	Surface	12.5	PG 76-22
			Intermediate	19.0	PG-76-22
			Base	19.0	PG-67-22
S9	Control	Control	Surface	9.5	PG 76-22
			Intermediate	19.0	PG-76-22
			Base	19.0	PG-67-22
S10	Foam-Based WMA	WMA-F	Surface	9.5	PG 76-22
			Intermediate	19.0	PG-76-22
			Base	19.0	PG-67-22
S11	Additive-Based WMA	WMA-A	Surface	9.5	PG 76-22
			Intermediate	19.0	PG-76-22
			Base	19.0	PG-67-22
N10	50% RAP HMA	HMA-RAP	Surface	9.5	PG-67-22
			Intermediate	19.0	PG-67-22
			Base	19.0	PG-67-22
N11	50% RAP WMA (Foam-Based)	WMA-RAP	Surface	9.5	PG-67-22
			Intermediate	19.0	PG-67-22
			Base	19.0	PG-67-22

Table 3-2 Production temperatures

Lift	Production Temperature, °F					
	PFC	Control	WMA-F	WMA-A	HMA-RAP	WMA-RAP
Surface	335	335	275	250	325	275
Intermediate						
Base	325	325				

All GE sections had a design asphalt thickness of seven inches over six inches of aggregate base and a stiff subgrade underneath. The as-built layer thicknesses at the gauge array determined from surveyed depths during construction are shown in Figure 3-1. These thicknesses were used to adjust the measured responses (horizontal strain levels and vertical pressures) to the design cross section to account for differences due to construction variability.

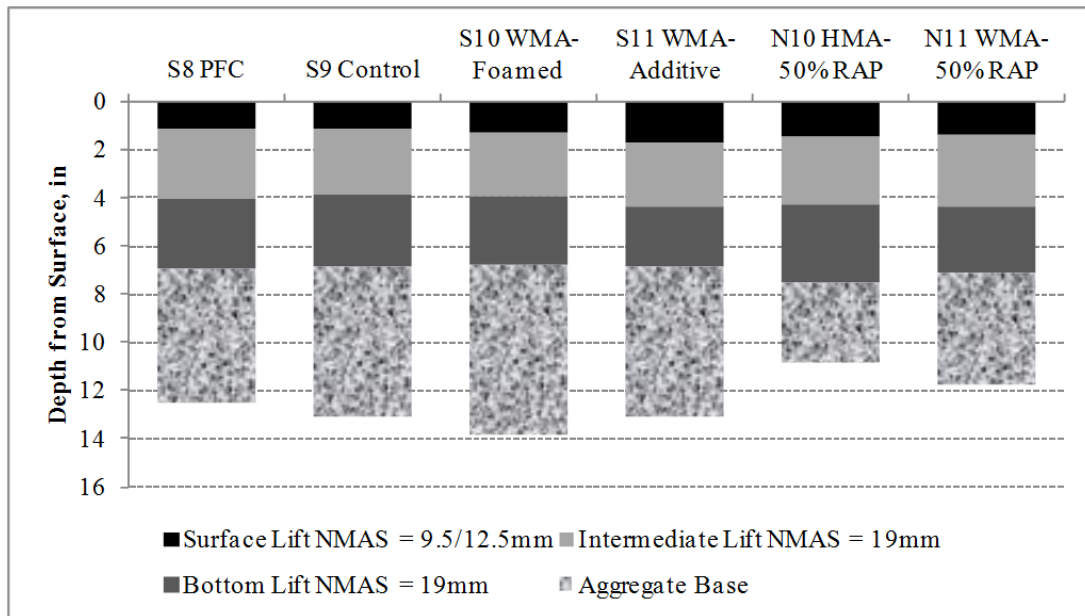


Figure 3-1 As-Built Pavement Cross-Sections.

Mix Designs

All mixes were designed using the Superpave method at 80 gyrations with the same virgin aggregates. The mixtures were designed so that all sections would have similar gradations and volumetric properties. Tables 3-3 through 3-5 show the as-built aggregate gradations and tables 3-6 through 3-8 show the as-built volumetric properties (binder content (P_b), effective binder (P_{be}), dust proportion (DP), air voids (V_a), voids in the mineral aggregate (VMA) and voids filled with asphalt (VFA)) as well as the average measured mat density. All mixes were within the acceptance criteria set by the researchers and section sponsors. More detailed information on mixture design and quality control for each section can be found in Appendix A.

Table 3-3 Aggregate gradation – surface lift

Sieve Size	Percent Passing					
	Control	PFC	WMA-F	WMA-A	HMA-RAP	WMA-RAP
1”	100	100	100	100	100	100
3/4”	100	100	100	100	100	100
1/2”	100	97	100	100	100	99
3/8”	100	71	100	100	95	95
#4	81	21	81	83	67	69
#8	59	11	60	61	48	51
#16	46	9	47	47	39	41
#30	31	7	32	31	27	27
#50	16	6	17	16	12	12
#100	9	4	10	9	7	7
#200	6.0	3.1	6.7	6.1	4.7	4.8

Table 3-4 Aggregate gradation – intermediate lift

Sieve Size	Percent Passing					
	Control	PFC	WMA-F	WMA-A	HMA-RAP	WMA-RAP
1”	99	98	99	98	98	99
3/4”	92	94	96	94	93	93
1/2”	84	87	89	87	86	86
3/8”	76	78	80	80	79	79
#4	57	59	60	60	56	58
#8	47	47	48	48	46	47
#16	38	37	39	38	37	39
#30	26	26	27	25	26	27
#50	15	15	14	13	13	14
#100	9	9	9	8	8	8
#200	5.3	5.2	5.3	4.9	5.6	5.7

Table 3-5 Aggregate gradation – base lift

Sieve Size	Percent Passing					
	Control	PFC	WMA-F	WMA-A	HMA-RAP	WMA-RAP
1”	99	98	99	99	99	97
3/4”	95	94	94	95	95	89
1/2”	87	87	85	87	89	83
3/8”	77	79	76	80	82	75
#4	56	59	57	61	58	54
#8	46	49	47	50	47	44
#16	37	39	38	40	39	37
#30	26	27	21	28	27	25
#50	15	15	12	16	14	13
#100	9	9	7	9	9	8
#200	5.1	5.3	5.1	5.3	5.8	5.3

Table 3-6 Volumetric properties – surface lift

Property	Control	PFC	WMA-F	WMA-A	HMA-RAP	WMA-RAP
Pb, %	6.1	5.1	6.1	6.4	6.0	6.1
Pbe, %	5.4	NA	5.5	5.7	5.2	5.3
DP	1.1	NA	1.2	1.1	0.9	0.9
Va, %	4.0	NA	3.3	3.4	3.8	3.2
VMA	16.5	NA	16.0	16.7	15.8	15.5
VFA	76	NA	80	80	76	79
Density, %	93.1	75.0%	92.5	93.6	92.6	92.0

Table 3-7 Volumetric properties – intermediate lift

Property	Control	PFC	WMA-F	WMA-A	HMA-RAP	WMA-RAP
Pb, %	4.4	4.6	4.7	4.6	4.4	4.7
Pbe, %	3.9	4.0	4.1	4.0	3.8	4.1
DP	1.4	1.3	1.3	1.2	1.5	1.4
Va, %	4.4	4.1	4.6	4.9	4.5	3.7
VMA	13.5	13.8	14.3	14.5	13.6	13.6
VFA	68	70	68	66	67	72
Density, %	92.7	93.7	93.0	92.8	92.9	93.2

Table 3-8 Volumetric properties – base lift

Property	Control	PFC	WMA-F	WMA-A	HMA-RAP	WMA-RAP
Pb, %	4.7	4.9	4.7	5.0	4.7	4.6
Pbe, %	4.2	4.4	4.2	4.5	4.1	4.0
DP	1.2	1.2	1.2	1.2	1.4	1.3
Va, %	4.0	3.6	4.1	3.0	4.2	4.1
VMA	13.9	14.0	14.0	13.7	13.8	13.7
VFA	71	75	71	78	70	70
Density, %	92.6	91.7	92.1	93.8	95.0	94.2

Pavement Instrumentation

During construction, all pavement sections included in this study were embedded with a gauge array that featured a total of fourteen structural response gauges. This instrumentation scheme has been employed in the 2003 and 2006 Test Track research cycles and has proven to be reasonably robust and effective in gathering the requisite pavement response data needed for M-E

investigations (78). Figure 3-2 shows a schematic of the gauge arrangement used in the test sections.

Twelve asphalt strain gauges measured both longitudinal and transverse horizontal strain (six in each direction). This configuration allows for redundancy in the system, so that in the event of gauge failure, paired gauges help ensure that at least one measurement is made. All the gauges were centered around the outside wheelpath, with gauges in the center and two feet on either side of the wheelpath. This distribution was used so that the maximum strain could be measured despite the effects of natural wheel wander.

The arrangement featured two earth pressure cells to measure vertical pressure in the center of the outside wheelpath at the top of the granular base and at the top of the subgrade. Additionally, in each section four temperature probes were bundled together and installed in the pavement to measure temperature at the top, middle and bottom of the AC and three inches into the underlying aggregate base layer. A detailed report on the instrumentation plan is documented elsewhere (78).

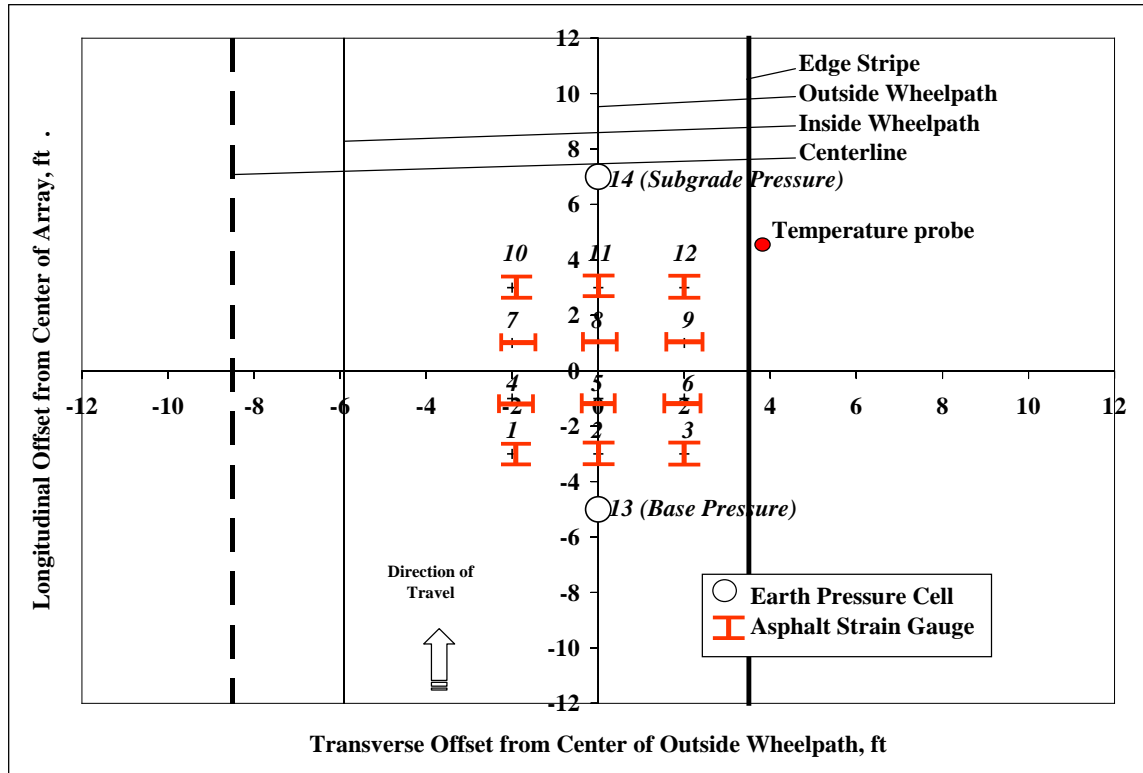


Figure 3-2 Schematic of Instrumentation.

CONSTRUCTION

Construction of the GE sections was carried out in July and August of 2009. The process was similar to that used in previous Test Track research cycles. Prior to placement on the Track, trial mixes were initially produced so that plant proportioning could be adjusted as necessary, and samples were collected for laboratory testing and evaluation.

Cooling Rates

Temperature readings were taken during delivery, laydown and compaction of each paving lift. Temperatures were measured at the surface and mid-depth of each lift to create cooling curves. Surface temperatures were measured with an infrared temperature device while mid-depth temperatures were obtained using a digital temperature probe, as shown in Figure 3-3. However, due to the difficulty in placing the temperature probe during compaction and obtaining consistent

readings only surface temperatures were used in the analysis. During construction, an area of the pavement was marked approximately 3 ft from the pavement edge and temperature readings were taken within that area approximately every 3 minutes until compaction was completed.



Figure 3-3 Temperature Measurements for (a) Surface and (b) Mid-depth.

Density

The compaction effort was achieved by first applying a Dynapac CC522 VHF breakdown steel-wheeled roller that had the capability of vibrating during compaction. After the steel-wheeled roller was removed from the pavement mat, the contractor continued compacting the mat with an Ingersoll Rand PT-125R pneumatic roller until the desired density was achieved. Finally, a Hypac C350D static smooth drum roller was applied to roll out roller marks and other imperfections.

Random locations were identified in every section for density testing. Nondestructive testing was conducted using a nuclear gauge and cores were extracted to develop mix-specific correlations, as required by ALDOT 350 (79).

LABORATORY TESTS

Plant produced mix samples were collected during construction and used to conduct several laboratory tests to evaluate the properties and performance of the GE mixes. Representative

samples were obtained from haul trucks prior to placement of the mixes on the Test Track, as shown in Figure 3-3. Tests were performed on laboratory compacted specimens as well as on extracted binder samples. For specimen fabrication, the mixtures were re-heated in the 5-gallon buckets obtained during sampling until the mixes were sufficiently workable and then split into appropriately-sized samples using a quartering device. The individual samples were returned to the oven and heated to the target compaction temperature. Once the loose mix samples reached the target compaction temperature, the mixes were compacted into the corresponding size testing sample. No short-term mechanical aging was conducted on the plant-produced mixtures.



Figure 3-4 Sampling Mixtures.

Binder Tests

Binder samples were extracted from the plant produced mixtures following the procedure in AASHTO T164 (80), recovered by the Rotovapor recovery method as described by ASTM D5404 (81) and tested according to AASHTO M320 (82) by means of the Dynamic Shear Rheometer (DSR) and Bending Beam Rheometer (BBR) to assess the effect of WMA

technologies and addition of high RAP percentages on binder properties. Since samples were obtained from plant produced mixtures, the extracted binders were assumed to be short-term aged and were not subjected to Rolling Thin Film Oven (RTFO) aging. Long-term aging was achieved through the use of the Pressure Aging Vessel (PAV) in accordance to AASHTO PP1 (83).

Dynamic Modulus

Mixtures were tested according to AASHTO TP 79-09 (84). Triplicate samples were compacted to 7.0 ± 0.5 percent air voids and subjected to a haversine compressive load using an Asphalt Mixture Performance Tester (AMPT), shown in Figure 3-5. The test was conducted at three temperatures (4, 20°C and a third temperature selected based on the high PG grade of the asphalt binder) and various frequencies. Samples were tested using a 138 kPa (20 psi) confining pressure as well as in unconfined mode. Table 3-9 summarizes the testing conditions for each mixture.



Figure 3-5 Asphalt Mixture Performance Tester (85).

Table 3-9 Dynamic modulus testing conditions

Lift	Temperature, °C	Mixture	Frequency, Hz
Surface	4, 20	All	0.1, 1, 10
	40	Control, WMA-A	0.01, 0.1, 1, 10
	45	WMA-F, HMA-RAP, WMA-RAP	
Intermediate	4, 20	All	0.1, 1, 10
	45	Control, WMA-F, WMA-A	0.01, 0.1, 1, 10
Base	4, 20	All	0.1, 1, 10
	40	Control, WMA-F, WMA-A	0.01, 0.1, 1, 10
	45	HMA-RAP, WMA-RAP	

Asphalt Pavement Analyzer

The Asphalt Pavement Analyzer (APA) was used to test the rutting susceptibility of the surface mixtures in accordance to AASHTO TP 63-07 (86). The APA is a modification of the Georgia Loaded Wheel Tester (GLWT), and it follows a similar rut-testing procedure. A wheel is loaded onto a pressurized linear hose and tracked back and forth over a testing sample to induce rutting, as shown in Figure 3-6. Six samples were compacted with a gyratory compactor to 7.0 ± 0.5 percent air voids for each of the surface mixtures and tested at 64°C using a vertical load of 100 lbs and a hose pressure of 100 psi for 8,000 cycles.

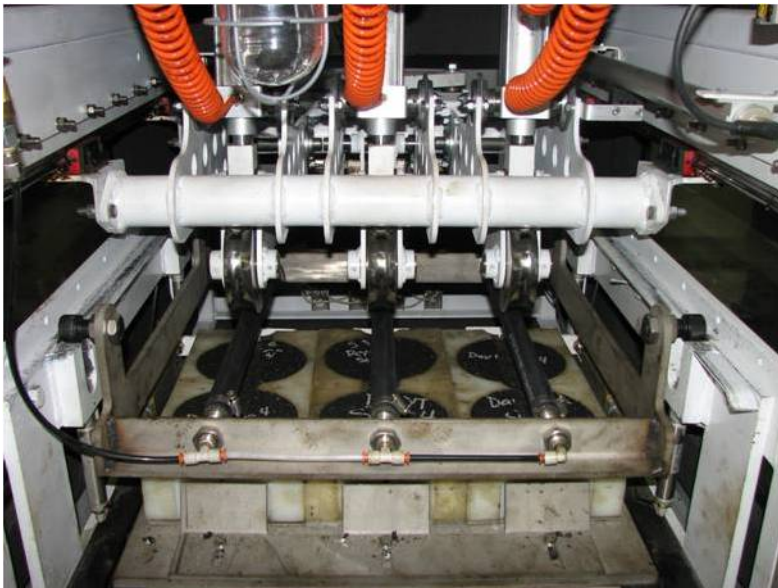


Figure 3-6 Asphalt Pavement Analyzer.

Flow Number

Flow number (F_n) testing was also performed for all surface mixes using the AMPT according to AASHTO TP 79 (84). Three replicate samples were compacted to $7 \pm 0.5\%$ air voids and tested at a temperature of 59.5°C . The specimens were tested at a deviator stress of 87 psi in unconfined mode until the axial strain reached 10%. Flow numbers (number of cycles to tertiary flow) were determined using the Francken model (87) shown in Equation 3-1.

$$\varepsilon_p(N) = aN^b + c(e^{dN} - 1)$$

(3-1)

where:

$\varepsilon_p(N)$ = permanent strain at 'N' cycles

N = number of cycles

a, b, c, d = regression coefficients

Hamburg Wheel Tracking Device

The Hamburg Wheel Tracking Device was used to evaluate the moisture damage and rutting susceptibility of the surface mixtures in accordance to AASHTO T 324-04 (88). The device, depicted in Figure 3-7, measures the combined effects of rutting and moisture damage by rolling a steel wheel across the surface of asphalt concrete specimens that are immersed in hot water. Specimens were compacted to 7.0 ± 1.0 percent air voids and conditioned in water for 30 minutes at 50°C . A fixed load 685 N and an average contact stress of 0.73 MPa, which simulates the stress produced by one rear tire of a double-axle truck, were applied for 20,000 passes (10,000 cycles). The rut depth in each specimen was measured automatically and continuously by a linear variable differential transformer (LVDT).



Figure 3-7 Hamburg Wheel Tracking Device.

Tensile Strength Ratio

Moisture susceptibility of all mixtures was evaluated by determining the diametral tensile strength on dry and wet specimens according to AASHTO T 283-07 (89). In this test, internal water pressures in the mixtures are produced by vacuum saturation followed by a freeze and a warm-water soaking cycle.

For each mixture, six specimens were compacted to 7.0 ± 1.0 percent air voids. A subset of three specimens were selected as the control and tested without moisture conditioning. The other subset was conditioned by saturating with water for 30 minutes and undergoing a freeze (-18°C for 15 hours) and thaw (60°C for 24 hours) cycle. Both subsets were then tested for indirect tensile strength by loading the specimens at a constant rate of 2 inches per minute. Figure 3-8 shows the test setup. The tensile strength of the conditioned specimens was compared to the control specimens to determine the tensile strength ratio (TSR).

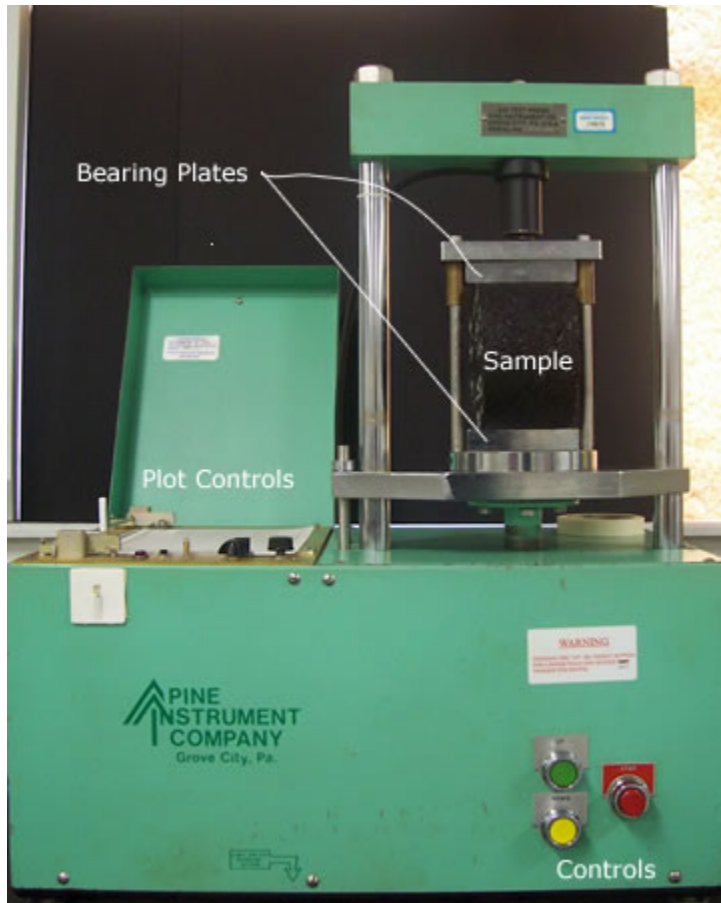


Figure 3-8 Split Tensile Test Setup (85).

Beam Flexural Fatigue

Fatigue resistance of the base mixes was evaluated using the beam flexural fatigue test, which simulates the bending that an asphalt concrete layer experiences in a pavement structure. The tests were performed under a constant-strain condition in accordance to AASHTO T 321-07 (90), at strain levels of 200, 400 and 800 microstrain.

For each strain level, three replicate beams were compacted with a kneading compactor to 6.0 ± 1.0 percent air voids and cut to dimensions of 380 mm long by 50 mm thick by 63 mm wide. Sinusoidal loads were applied at a frequency of 5 to 10 Hz at one-third points along the specimens at a test temperature of 20°C until a 50 percent decrease in stiffness from the initial stiffness at 50 cycles was reached. Figure 3-9 shows the test equipment setup.



Figure 3-9 Beam Fatigue Apparatus (85).

Indirect Tension Test

Thermal cracking resistance of the surface mixtures was evaluated through the Indirect Tension Test (IDT) according to AASHTO T 322-07 (91). Three replicate specimens were compacted to $7.0 \pm 0.5\%$ air voids and cut to dimensions of 150 mm diameter by 50 mm height. Creep compliance testing was conducted by applying a static load at a rate of 12.5 mm/min along the diametral axis of the specimens (Figure 3-10) for a period of 100 seconds at -20°C , -10°C and 0°C . The horizontal and vertical deformations measured near the center of the specimens were used to calculate tensile creep compliance as a function of time.

Since the creep compliance test is non-destructive, the same specimens were used to determine the tensile strength of the mixtures by applying the same static load at -10°C until failure. The intersection of the indirect tensile strength curve with the thermal stress curve yields the critical cracking temperature of the mixtures.



Figure 3-10 Indirect Tension Test Setup (92).

PAVEMENT RESPONSES

Pavement responses play a crucial role in the M-E design framework. Determining the effect of sustainable technologies on pavement responses is therefore valuable for the assessment of future pavement performance.

Deflection Testing

Falling weight deflectometer (FWD) testing was performed several times per month to quantify the seasonal behavior of the pavement layer moduli. FWD testing was conducted at three predetermined random locations per test section. At each random location, testing was performed in the inside, outside and between the wheelpaths. A Dynatest 8000 FWD was used with nine sensors spaced at 0, 8, 12, 18, 24, 36, 48, 60 and 72 inches from load center and a load plate with a radius of 5.91 inches and a split configuration to ensure good seating on the pavement surface (Figure 3-11). Three repetitions of the FWD at four load levels (approximately 6, 9, 12 and 16 kips) were completed at each location and mid-depth temperatures were obtained at the time of

testing. The pavement layer moduli were backcalculated from deflection data using EVERCALC 5.0 for a three-layer cross-section (asphalt concrete, aggregate base and subgrade soil). Data were filtered to eliminate results with root-mean-square error (RMSE) exceeding 3%. The RMSE represents the goodness-of-fit between the measured and computed deflection basins, and values under 3% are generally considered acceptable for backcalculation of layer moduli.



Figure 3-11 Falling Weight Deflectometer.

Responses Under Dynamic Loading

During trafficking operations, strain and pressure measurements were taken approximately once a week under live traffic loads and under different environmental conditions. A fleet of five triple-trailer vehicles operated 16 hours per day, five days a week. On each date of data collection, three passes of each truck traveling approximately 45 mph were obtained along with pavement temperatures.

Horizontal strains were measured at the bottom of the AC layer in the longitudinal and transverse directions, while vertical pressures were measured at the top of the granular base and at

the top of the subgrade. Data were subdivided by axle type (i.e., steer, single and tandem). For a given axle pass there were up to six longitudinal and six transverse strain measurements, depending on gauge functionality, along with one base and one subgrade pressure measurement.

The recorded data were analyzed using the graphical engineering software package DADiSP. Responses were recorded as changes in voltage over time, and the program used algorithms developed at the Test Track to clean and process the raw response traces into their corresponding units. This process has been previously documented by Priest and Timm (8). Figure 3-12 shows examples processed response traces. For a given truck pass, responses are recorded for each axle type, as shown in Figure 3-12 (a). For strain responses, positive values represent tension and negative values represent compression. Longitudinal strains (Figure 3-12 (a)) exhibit a compression wave as the tire approaches the gauge prior to the tensile peak, as well as full strain reversal between every axle. For transverse strains (Figure 3-12 (b)), there is no preceding wave due the perpendicular alignment of the gauge. Figure 3-12 (c) shows the vertical pressures experienced by the pavement as the truck passes over the pressure cell.

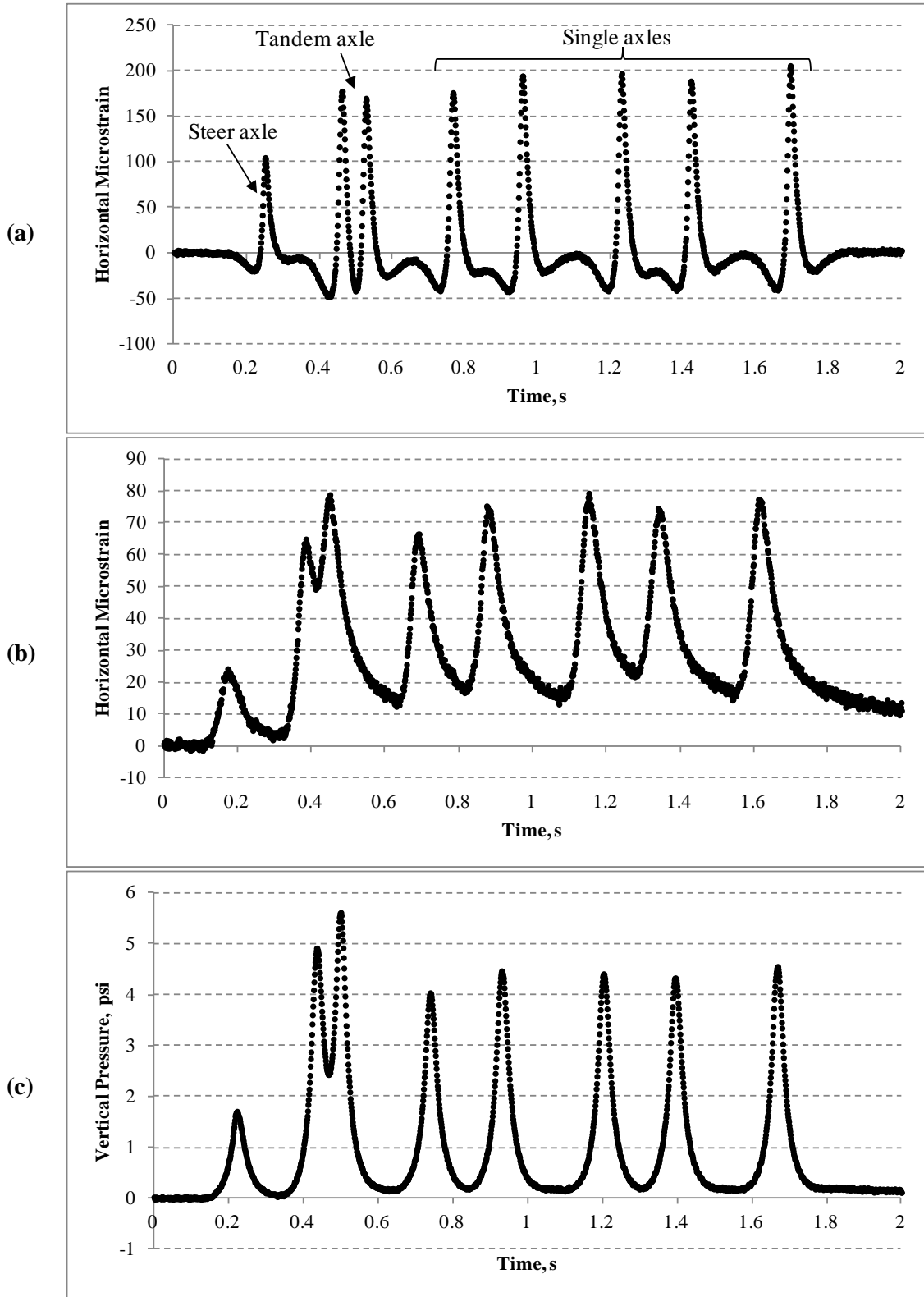


Figure 3-12 Example Raw Response Traces for (a) Longitudinal Strain, (b) Transverse Strain and (c) Pressure.

For each test section, the maximum reading per axle pass in each direction was tabulated to obtain the 95th percentile, which represents the “best-hit” of that particular test date. By using the 95th percentile, possible outliers due to voltage spikes, faulty gauges and processing errors were eliminated while maintaining values close to the maximum response measurement. This approach has been used previously at the Test Track to minimize errors in the development of response-temperature relationships (93).

Field Performance

All sections were tested on a weekly basis to assess pavement performance. Field performance evaluations focused on the middle 150 feet of each 200-foot test section to eliminate the effects of transitions near section ends. A high speed Automated Road Analyzer (ARAN) van was used to measure roughness and texture along the wheelpaths. Field rut depths were measured approximately once a month on each of the sections using the Alabama Department of Transportation (ALDOT) method. This method uses a 4-ft-long level with a dial gauge, shown in Figure 3-13. Readings were taken in each wheel path along three predetermined random locations within each section and the averages were computed. Sections were also manually inspected for cracking and crack maps were developed to determine the extent and monitor the progression of cracking.



Figure 3-13 ALDOT Rut Depth Gauge Method.

SUMMARY

An extensive number of laboratory tests and field measurements were obtained during this research cycle to compare the characteristics and structural behavior of conventional dense-graded HMA mixtures and alternative sustainable pavement technologies. Laboratory tests were conducted to obtain material properties of the different mixes and to evaluate their performance relative to the control in a laboratory setting. Field measured responses under dynamic loading were used to compare the structural behavior of the different pavement sections. Field performance was monitored and compared to laboratory results to determine the possible effects of sustainable technologies.

The data were used to perform a series of statistical analyses to determine whether the use of sustainable technologies could change pavement properties, and ultimately affect performance significantly. The results are discussed in the following chapters.

CHAPTER 4

CONSTRUCTION

COOLING RATES

As mentioned in Chapter 3, temperature readings were taken during delivery, laydown and compaction of each paving lift to evaluate the accuracy of existing models in predicting cooling curves during construction of sustainable mixtures relative to conventional AC mixtures. Asphalt concrete cooling rate predictions can help in the compaction planning process and with making field decisions during construction. The time required for AC to reach the proper compaction temperature and the time available for compaction decrease with an increased cooling rate. As the mix cools, the asphalt binder stiffens, which makes it difficult to gain density, regardless of the applied compaction effort. Inadequate compaction can affect pavement performance by reducing fatigue life as well as strength and stability, increasing permanent deformation, accelerating oxidation and increasing moisture susceptibility (94).

Studies have found that the most influential factors that affect pavement cooling rates are lift thickness and initial mix temperature. Other factors include wind speed, thickness of the existing pavement structure and ambient temperature (94, 95). These factors, in addition to time of day, latitude, type of underlying material, underlying material temperature and state of moisture in underlying material (if unbound), have been incorporated in a computer simulation tool, MultiCool. This computer program, as described below, predicts cooling rates of AC under a variety of conditions.

MultiCool Software

The concept of pavement cooling is related to heat transfer by conduction, convection and radiation. Conduction refers to energy transfer from the more energetic particles to adjacent particles that are less energetic. In a pavement structure, heat is exchanged with the base layer through conduction. Convection is the process of heat transfer between a solid surface and a fluid. Energy is transferred from the pavement to the surrounding air if the air temperature is lower than the pavement temperature. Radiation is the heat transfer between two bodies by electromagnetic waves or photon particles. In a pavement, this type of heat transfer is related to solar radiation.

MultiCool is a Windows-based computer program, originally developed in Minnesota (96) and adapted for multiple lift paving in California (97), which uses heat transfer theory to calculate cooling curves for AC mats during construction. The program assumes that heat conduction in the asphalt lift and underlying materials is one-dimensional through the depth of the structure. Heat conduction is computed using Fourier's second law (Equation 4.1), which states that the heat flux in a given direction is proportional to the temperature gradient in that direction.

$$k \frac{\partial^2 T}{\partial z^2} = \rho c \frac{\partial T}{\partial t}$$

(4.1)

Where:

k = thermal conductivity (W/mK)

T = temperature (K)

t = time (s)

c = specific heat (J/kg K)

ρ = density (kg/m³)

$z = \text{depth (m)}$

Figure 4-1 illustrates the one-dimensional heat transfer in the pavement structure. Equations 4.2 and 4.3 show special boundary conditions employed at the bottom and top of the pavement structure, respectively, to simulate the field condition. The bottom of the pavement is assumed to be perfectly insulated.

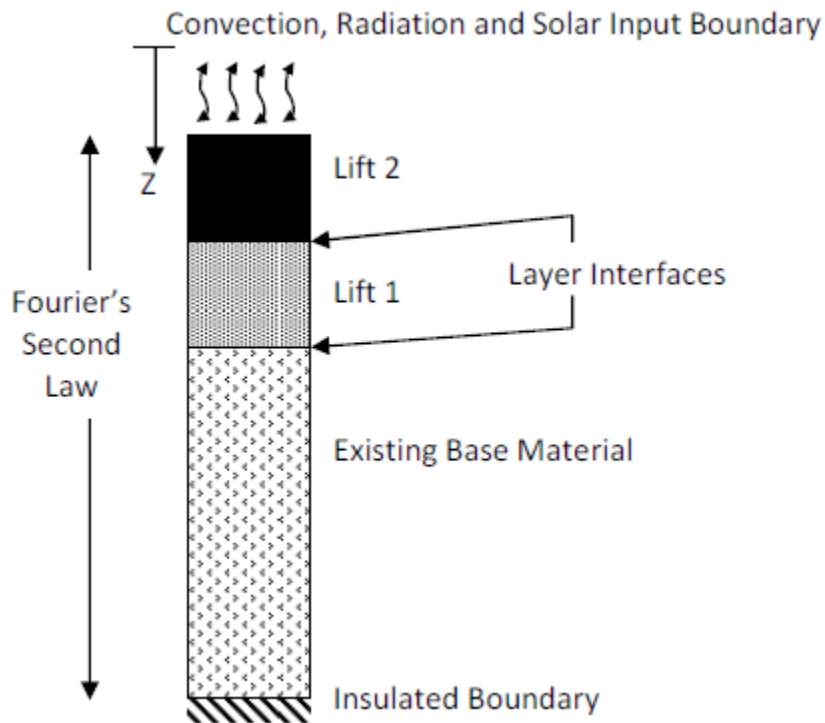


Figure 4-1 One-Dimensional Heat Transfer in a Pavement Structure (97).

$$q = h(T_a - T_p) - k \frac{\partial T}{\partial z} + \alpha H_s + \varepsilon \sigma (T_a^4 - T_p^4) \quad (\text{top of pavement}) \quad (4.2)$$

$$q = 0 \quad (\text{bottom of pavement}) \quad (4.3)$$

Where:

$q = \text{heat flux (W/m}^2\text{)}$

h = heat transfer coefficient ($\text{W}/\text{m}^2 \text{K}$)

T_a = ambient temperature (K)

T_p = pavement surface temperature (K)

α = total absorptency of asphalt

H_s = net solar flux at the surface (W/m^2)

ε = total pavement emittance

σ = Stefan-Boltzmann constant ($\text{W}/\text{m}^2 \text{K}^4$)

The model uses a finite difference approach to solve the above equations. This approach approximates the temperature at a point by applying thermal calculations to the temperatures at neighboring points. A node is placed at the surface of the lift being paved and the system of simultaneous equations is solved from the surface node to the bottom of the pavement structure. Placing a surface node at the surface of each pavement layer facilitates the simulation in multi-layer systems.

Although the accuracy of MultiCool has been previously demonstrated for conventional materials, where differences between simulated and measured temperatures were within 10°C (97), there is a need to evaluate the program with respect to non-conventional materials that are gaining in popularity, such as the sustainable technologies presented in this study.

MultiCool Simulation

The software inputs are divided into four main categories: start time, environmental conditions, existing surface and mix specifications, as shown in Figure 4-2. Each category is briefly described below.

Start Time (24-hour clock) Hour <input type="text" value="14"/> Minutes <input type="text" value="25"/> DATE Month <input type="text" value="7"/> Day <input type="text" value="16"/> Year <input type="text" value="2009"/>	Environmental Conditions Ambient Air Temp. <input type="text" value="93"/> F Average Wind Speed <input type="text" value="5"/> mph Sky Conditions <input type="text" value="Clear & Dry"/> Latitude (Deg North): <input type="text" value="33"/> <input type="button" value="Update to Current Time"/>	Mix Specifications Number of Lifts <input type="text" value="1"/> Lift Number 1 <input type="button" value="Next Lift"/> Mix Type <input type="text" value="Dense Graded"/> PG Grade <input type="text" value="64"/> <input type="text" value="-22"/> Lift Thickness <input type="text" value="3"/> in. Delivery Temp <input type="text" value="239"/> F Stop Temp <input type="text" value="175"/> F
Existing Surface Material Type <input type="text" value="Granular Base"/> State of Moisture <input type="text" value="Unfrozen"/>	Moisture Content <input type="text" value="Dry"/> Surface Temp. <input type="text" value="103"/> F	
Units <input type="radio"/> SI <input checked="" type="radio"/> English	<input type="button" value="Calculate"/>	<input type="button" value="Export Formatted Data"/>

Figure 4-2 MultiCool Input Data Entry Window.

Start Time

During construction, the start times were recorded for the software to determine the angle of the sun and incoming solar radiation.

Environmental Conditions

Environmental conditions such as ambient air temperature and average wind speed were obtained using data from a weather station located at the Test Track. Sky conditions were noted during data collection at the time of construction. These inputs affect the surface boundary conditions specified in Equation 4.2. The degree latitude of the job site corresponds to approximately 33 degrees north and is used by the software as part of the angle of sun calculation mentioned above.

Existing Surface Conditions

The existing material type was assigned as either granular base or AC depending on whether the lift was a bottom lift or an intermediate or surface lift, respectively. The moisture content was assumed to be “dry” and the state of moisture “unfrozen” for every lift. These inputs set default values for the thermal properties required for simulation. The surface temperature was measured in the field using an infrared temperature device. It is used by the program as an initial equilibrium condition and is assumed constant throughout the layer.

Mix Specifications

It is possible to enter multiple lifts in the simulation as long as they are paved in immediate succession. Since this was not the case at the Test Track, each lift was modeled individually. The mix type and PG grade of each lift were entered according to the mix design information. The gradation is related to the default thermal properties (i.e., thermal conductivity and specific heat) while the binder is used only to better identify the mixture. It should be noted that the thermal conductivity and specific heat were held constant amongst all the lifts simulated as these parameters are hard-coded within the program. Inaccuracies in the predicted cooling curves, since all other variables were entered based on conditions at the time of AC placement, would logically come from assuming these parameters.

As-built average lift thicknesses were used to minimize error. The delivery temperature was measured using an infrared temperature device when the asphalt concrete left the paver. The stop temperature represents the maximum temperature that the lift can reach before the next layer is added. Because only one layer was modeled at a time, this value was assigned in a way that the resulting cooling curve included the entire time period used in the paving operation. Table 4-1 shows a summary of the parameters used in the simulation for each pavement lift.

Table 4-1 Summary of Program Inputs

Section	Lift	Air Temp. (°F)	Wind Speed (mph)	Delivery Temp. (°F)	Surface Temp. (°F)	Lift Thickness (in)
Control	Bottom	85.9	2.9	254	145	3.0
	Intermediate	89.3	2.8	316	145	2.8
	Top	81.1	2.9	275	99	1.2
PFC	Bottom	84.4	2.8	274	145	2.6
	Intermediate	89.3	2.8	289	143	3.0
	Top	79.9	4.4	283	103	1.3
WMA-F	Bottom	87.7	3.2	239	145	3.0
	Intermediate	89.5	2.2	258	142	2.7
	Top	81.1	2.9	247	98	1.3
WMA-A	Bottom	87.7	3.2	230	145	2.6
	Intermediate	90.6	2.1	230	143	2.8
	Top	82.8	3.3	234	105	1.5
HMA-RAP	Bottom	91.0	3.2	289	110	3.0
	Intermediate	75.8	1.4	280	107	2.7
	Top	92.1	2.1	268	129	1.4
WMA-RAP	Bottom	90.0	3.2	241	115	2.9
	Intermediate	75.8	1.4	241	102	3.0
	Top	91.6	1.4	245	123	1.2

Analysis of Results

The difference between the measured and predicted temperatures was calculated and cumulative distribution functions (CDF) were determined to find the percentage of data points within the $\pm 10^{\circ}\text{C}$ (18°F) range found in the original validation. The average difference and standard deviation were also calculated for every section. Results indicated that, in general, the software tended to overpredict mix temperatures over time, but in the majority of cases the difference was within the accepted range. Figure 4-3 shows the CDF plots for each section, including all pavement lifts. It should be noted that the “control” curve includes section S9 as well as the intermediate and base lifts from section S8, all of which were dense graded control mixtures. The “PFC” curve includes only the surface lift from section S8, since this was the only porous mixture placed.

It was observed that the control section had the highest variability in temperature differences, which suggests that the data points outside the tolerance range found in the other

sections (sustainable mixes) are not caused solely by the unique characteristics (i.e., thermal conductivity and heat capacity) of such mixes. A hypothesis test performed on the absolute values of the differences showed that at a significance level of $\alpha=0.05$, there was no evidence that the differences exceeded 18°F in any of the sections.

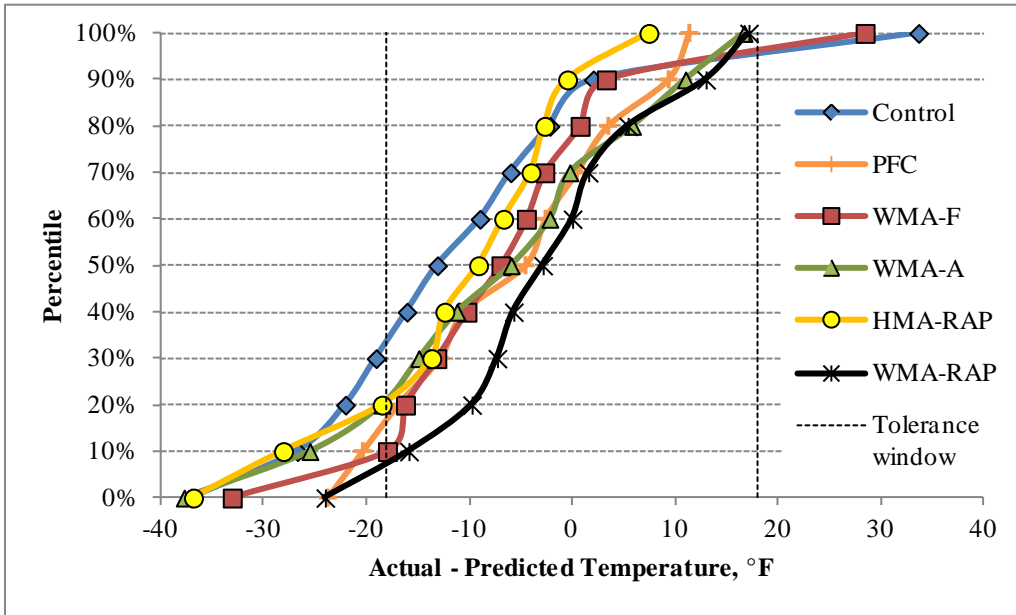


Figure 4-3 Cumulative Distribution Function Plot for Temperature Differences.

A factorial analysis was performed to determine the effect of factors such as production temperature (HMA or WMA), material type (virgin blend or high RAP) and lift (bottom, intermediate or top) had in the temperature difference between the actual and predicted cooling curves. The analysis did not include the PFC mixture because it did not contain information at all factor levels. The results showed that all three factors and their interactions were significant, meaning that certain combinations produced larger differences. Figure 4-4 shows the main effects plot for the average difference between measured and predicted temperatures. The points in the plot are the means of the temperature difference at the various levels of each factor. The dashed lines correspond to the grand mean (the mean of all observations across factor levels).

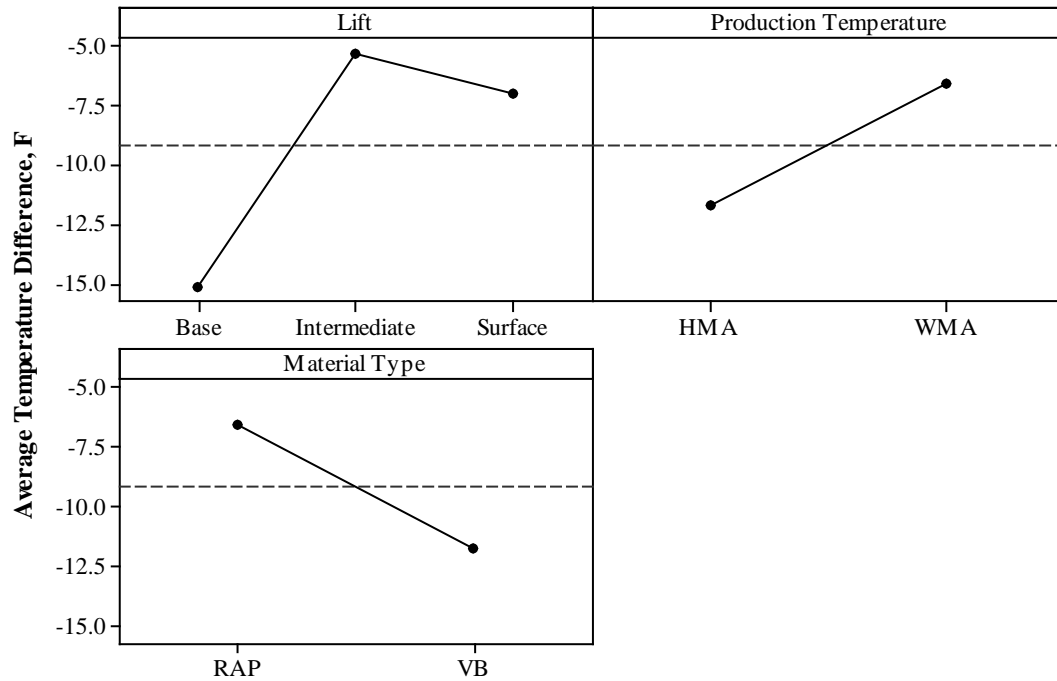


Figure 4-4 Main Effects Plot for Temperature Difference.

Based on the slopes from Figure 4-4, the factor pavement lift appears to vary more among its levels. Figure 4-5 shows the interaction between pavement lift and the other factor levels. The base lifts consistently showed the larger differences in temperature for both production temperature and material type. While the base and intermediate lifts vary similarly among temperature levels (similar slopes), the surface lift experienced an increased temperature difference from WMA to HMA. On the other hand, intermediate lifts were less affected by material type, while base lifts had the highest variation. It should be noted that in general the use of sustainable technologies (WMA and high RAP) had lower temperature differences than conventional mixtures (HMA and virgin blends). The cooling curve simulation model appears to be applicable to sustainable mixtures which do not appear to require special treatment or consideration

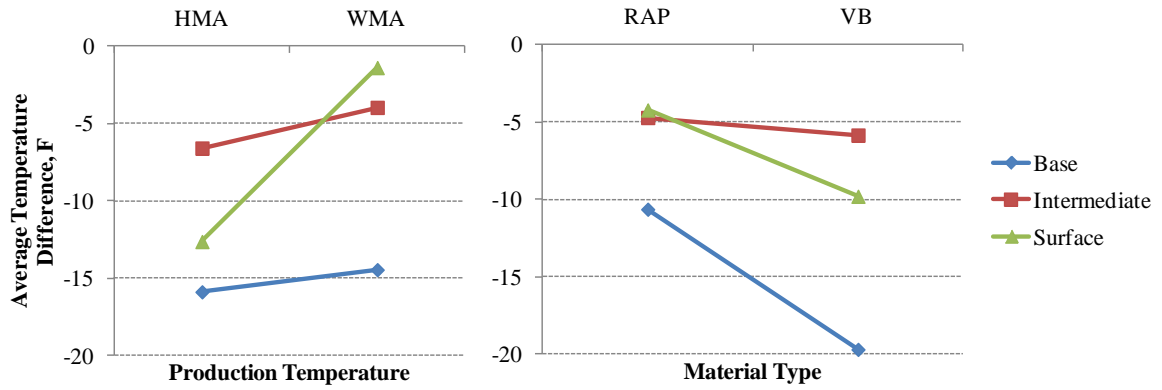


Figure 4-5 Interaction Plot for Temperature Difference – Pavement Lift.

The interaction between production temperature and the other factor levels is illustrated in Figure 4-6. Larger temperature differences were observed for HMA mixtures, but WMA mixtures seemed to vary more among factor levels. Overall, the difference in production temperature did not seem to affect the accuracy of the cooling curve simulation. The average differences were similar to those obtained in the original validation (within 10°C (18°F)).

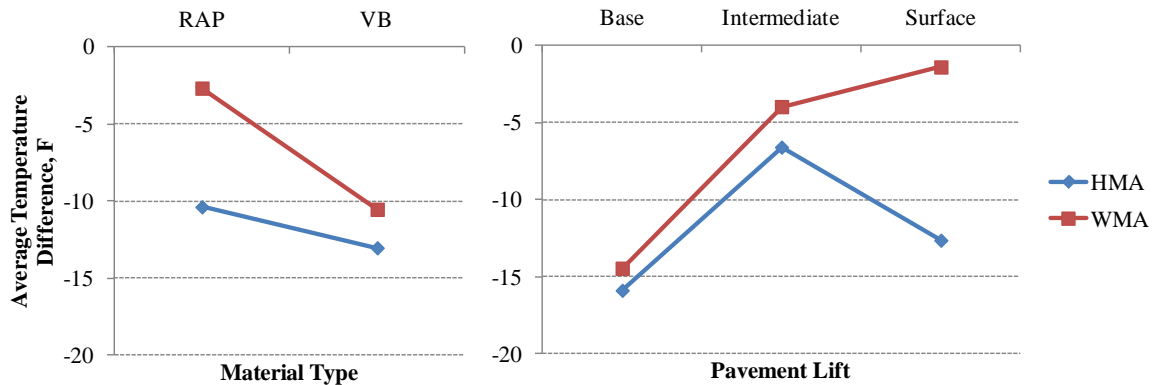


Figure 4-6 Interaction Plot for Temperature Difference – Production Temperature.

Figure 4-7 shows the interaction between material type and the other factor levels. It can be observed that high RAP mixtures also had average differences similar to those reported in the original validation. In both cases the average measured temperature is lower than the predicted

temperature, with the smaller differences obtained in the section produced with WMA technology.

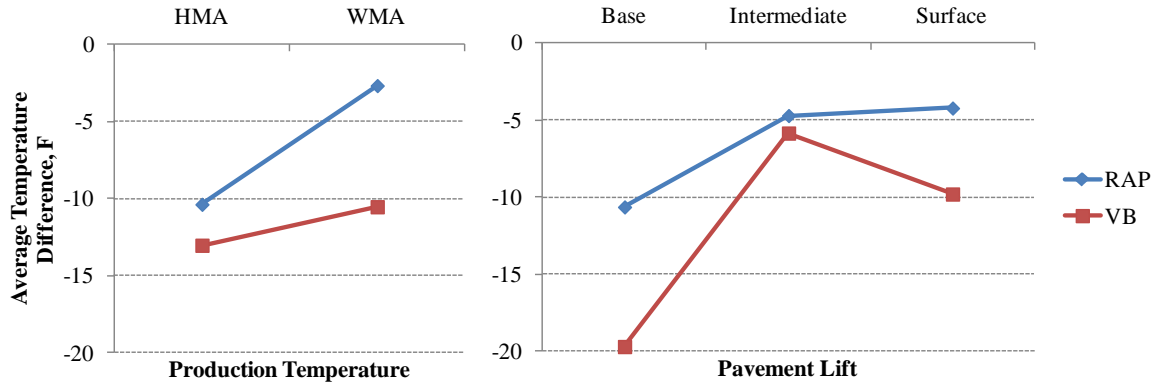


Figure 4-7 Interaction Plot for Temperature Difference – Material Type.

To evaluate the model applicability for PFC mixtures, the average temperature differences were calculated for the surface lifts in the control and PFC sections, as shown in Figure 4-8. A two sample t-test indicated that at a significance level of $\alpha = 0.05$, the average temperature differences of the mixtures are different (p-value = 0.005). However, the PFC mixture had a lower average temperature difference than the control, with 86.6% of the temperature differences within the acceptance limits. Although data for this particular mix type is limited, the model seems to accurately predict the cooling curve.

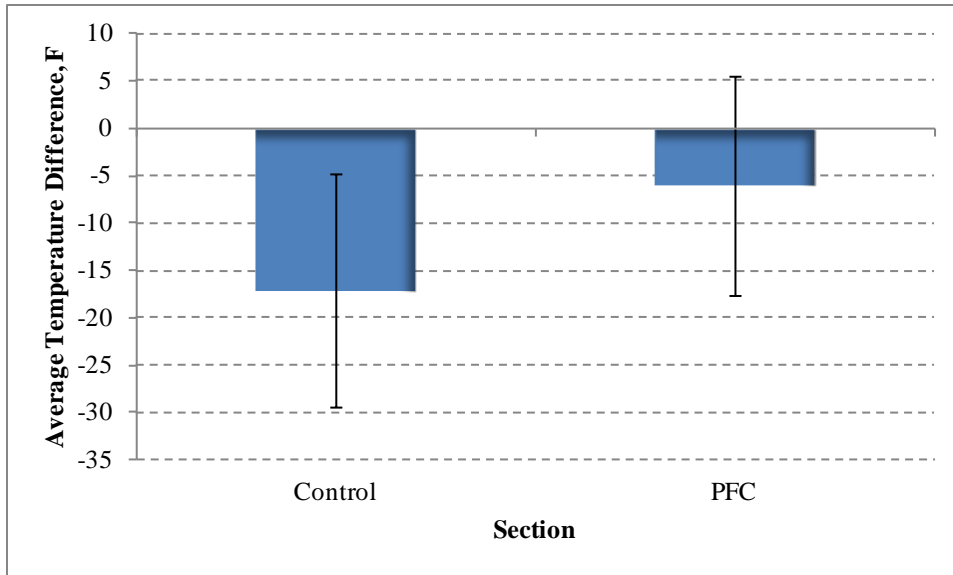


Figure 4-8 Average Temperature Differences for Control and PFC Mixtures.

In summary, although it was found that the different factors and their levels had a significant effect on the differences between the measured and predicted cooling curves, the simulation was more accurate for sustainable mixtures. Overall, there was no evidence that the difference between the measured and predicted cooling curves over the entire pavement structure exceeded the 18°F (10°C) tolerance established in the original validation study, and the existing model in MultiCool appears to be adequate to predict cooling curves for the sustainable mixtures included in this study.

IN-PLACE DENSITY

As mentioned previously, density measurements were taken in each section at four random locations along the inside and outside wheelpaths. The acceptance limits for in-place density set by the sponsors of the Group Experiment were between 91.5 and 96% of the maximum density.

Figures 4-9 through 4-11 show the average in-place density with standard deviations of each section by lift and the delivery temperature of the mixes. The PFC section is not shown in Figure 4-9 because the surface layer had a different density requirement (80 – 85% of the

maximum theoretical density). For the intermediate and base lifts, the PFC-Control section refers to the dense graded mixtures placed (same as the control). Although in three of the test sections mixtures were produced as warm mixes, all sections met the density requirements. It appears that the reductions in delivery temperature, ranging from 15 to 86°F, did not affect the compactability of the WMA mixtures significantly.

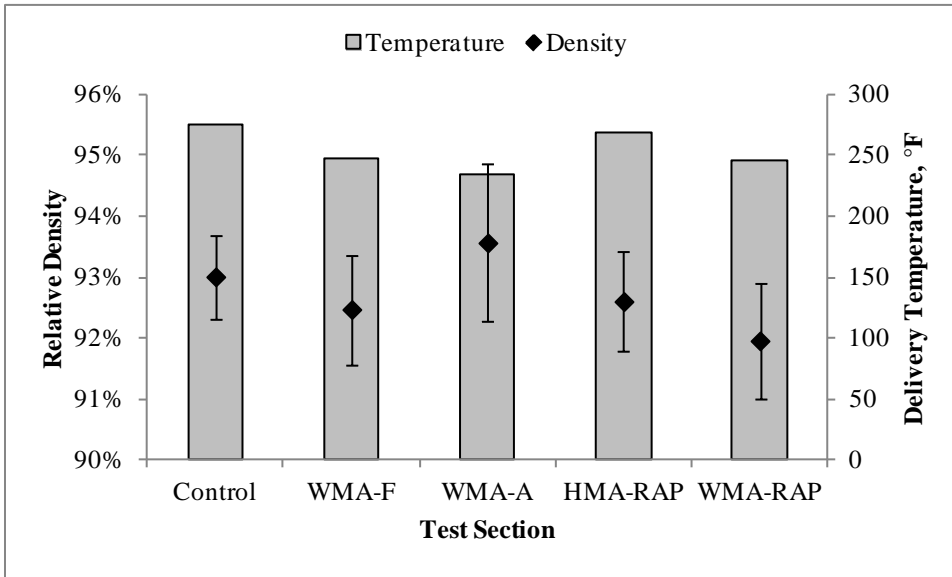


Figure 4-9 Average In-Place Density and Delivery Temperature – Surface Lift

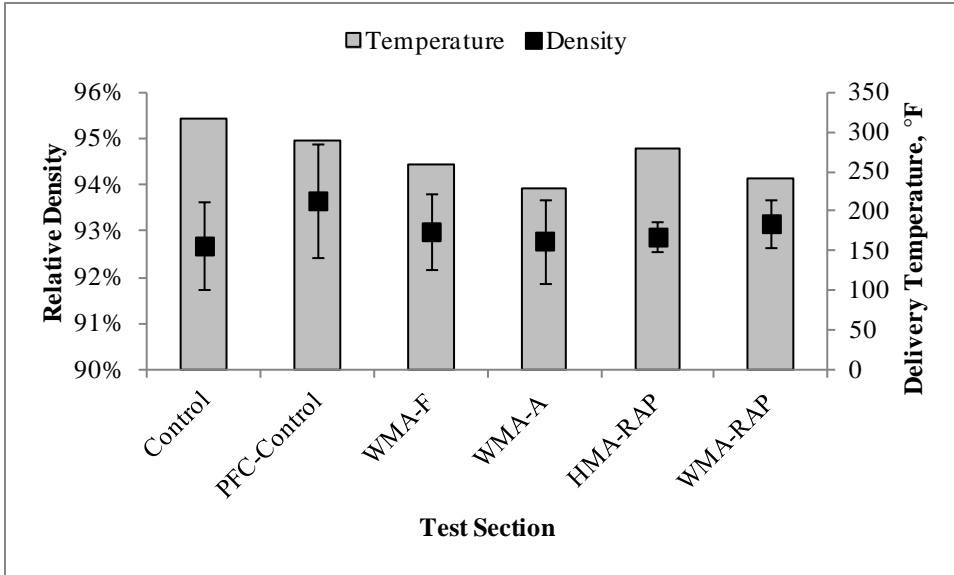


Figure 4-10 Average In-Place Density and Delivery Temperature – Intermediate Lift

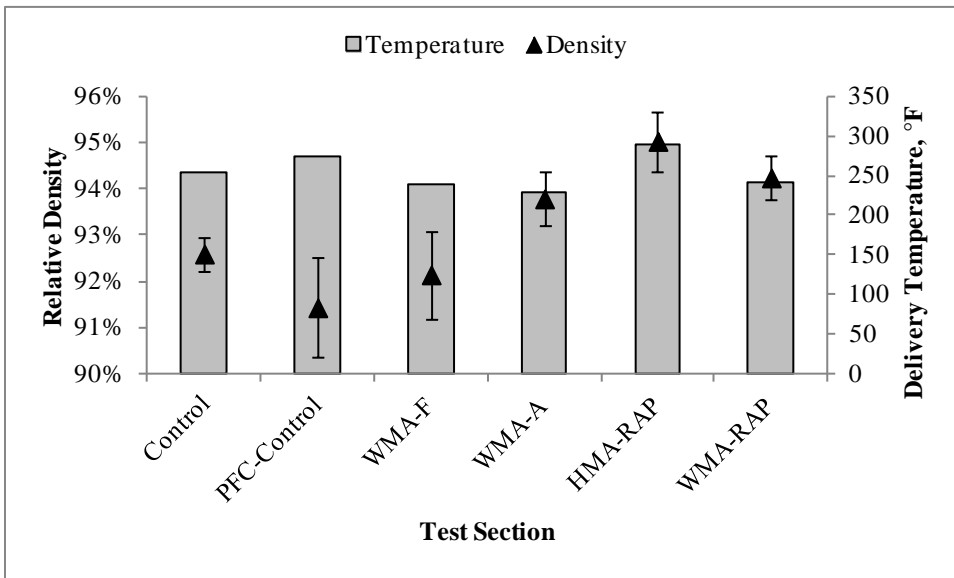


Figure 4-11 Average In-Place Density and Delivery Temperature – Base Lift

A direct statistical comparison could not be made among the sections because the environmental conditions and rolling patterns varied during placement and compaction of each section. This is evident by looking at the control and PFC-control sections in Figures 4-10 and 4-11, which used the same mixture and still had densities that varied as much as 1.2%. However, it can be noted that in general the control and high RAP mixtures exhibited less variability than the

WMA mixes, suggesting that compaction was more uniform throughout the asphalt concrete mat. Although this cannot be attributed to the use of WMA technology based on the information available, it could play a role in pavement performance and should not be dismissed.

SUMMARY

During construction of the IV research cycle, data collection efforts were focused on two main categories: mixture temperature during laydown and compaction, and in-place density. The objective was to determine whether sustainable mixtures had similar cooling rates than conventional dense-graded HMA mixes or if a different model would be required to simulate the mat temperatures during construction. In addition, density measurements were taken to ensure that all sections conformed to the requirements and that the use of sustainable technologies did not have a negative effect on compaction.

The results showed that the predicted cooling curves of the sustainable pavement sections were in good agreement with those measured in the field and that the existing model built into the MultiCool software can be used confidently with these materials. The in-place density measurements confirmed that all mixtures met the requirements established by the research group and that the reduction in production and delivery temperature in some of the mixtures did not affect their compactability.

CHAPTER 5

LABORATORY EVALUATION

An extensive laboratory evaluation was conducted using samples from plant produced mixes. Tests were performed on extracted binders as well as on mixture samples. The objective was to determine the effect of sustainable technologies on mix properties and performance and to compare the results with the field observations in the following chapters.

EFFECT OF SUSTAINABLE TECHNOLOGIES ON BINDER PROPERTIES

Binders from each section and pavement lift were recovered by the Rotovapor recovery method and tested to obtain their performance grades and parameters associated with pavement performance (rutting, fatigue cracking and thermal cracking). High RAP mixtures contain aged binder, which can make the binder blend stiffer and more susceptible to cracking. On the other hand, in WMA mixes the binder can contain additives and is subjected to lower production temperatures, so it may not age as much as HMA. Therefore, it is important to study how binder blends are affected by the use of sustainable technologies and how they influence pavement performance.

Performance Grade

The results for the critical temperatures and performance grades of all mixes are shown in Tables 5-1 through 5-3. In general, it was observed that the addition of RAP had a stiffening effect on the mixtures, increasing the high and low temperature grades compared to the control. The changes were less pronounced for high RAP mixtures produced as WMA. WMA mixes produced with

virgin aggregates were less affected, and only resulted in changes in the high temperature grade in some of the mixtures.

Table 5-1 Critical temperatures and performance grades – surface lift recovered binder

Property	Control	WMA-F	WMA-A	HMA-RAP	WMA-RAP
High Temperature, °C	81.7	82.0	80.3	87.8	83.8
Intermediate Temperature, °C	21.9	23.2	22.6	29.4	29.4
Low Temperature, °C	-24.7	-25.7	-25.7	-15.4	-17.7
Actual Grade	81.7 – 24.7	82.0 – 25.7	80.3 – 25.7	87.8 – 15.4	83.8 – 17.7
PG Grade	76 – 22	82 – 22	76 – 22	82 – 10	82 – 16

Table 5-2 Critical temperatures and performance grades – intermediate lift recovered binder

Property	Control	WMA-F	WMA-A	HMA-RAP	WMA-RAP
High Temperature, °C	85.1	86.6	82.5	95.0	88.7
Intermediate Temperature, °C	23.1	19.9	20.3	32.4	32.1
Low Temperature, °C	-25.1	-23.9	-25.1	-12.8	-14.1
Actual Grade	85.1 – 25.1	86.6 – 23.9	82.5 – 25.1	95.0 – 12.8	88.7 – 14.1
PG Grade	82 – 22	82 – 22	82 – 22	94 – 10	88 – 10

Table 5-3 Critical temperatures and performance grades – base lift recovered binder

Property	Control	WMA-F	WMA-A	HMA-RAP	WMA-RAP
High Temperature, °C	77.4	75.6	73.7	95.0	88.7
Intermediate Temperature, °C	24.1	20.5	21.8	32.4	32.1
Low Temperature, °C	-24.1	-25.1	-25.4	-12.8	-14.1
Actual Grade	77.4 – 24.1	75.6 – 25.1	73.7 – 25.4	95.0 – 12.8	88.7 – 14.1
PG Grade	76 – 22	70 – 22	70 – 22	94 – 10	88 – 10

Performance Parameters

Rutting

The $G^*/\sin\delta$ parameter obtained from DSR testing is an indicator of rutting potential and is part of the Superpave performance graded binder specification (AASHTO MP 1) to control rutting. Higher values of $G^*/\sin\delta$ correspond to binders with better rutting resistance. AASHTO MP 1 states that this parameter must have a minimum of 2.2 kPa. Figures 5-1 through 5-3 show the rutting parameter for binders recovered from each mixture at different temperatures, which were used to determine the true grade high critical temperature. Binders from the high RAP mixes met the minimum requirement at higher temperatures, which would make them more resistant to permanent deformation at high temperatures. Binders recovered from WMA mixes met the requirement at lower or similar temperatures than the control, meaning that they could experience more rutting. The results from the high RAP mixes used for intermediate and base lifts showed that the use of WMA technology lowered the temperature at which the requirement was met, but it still was higher than the control.

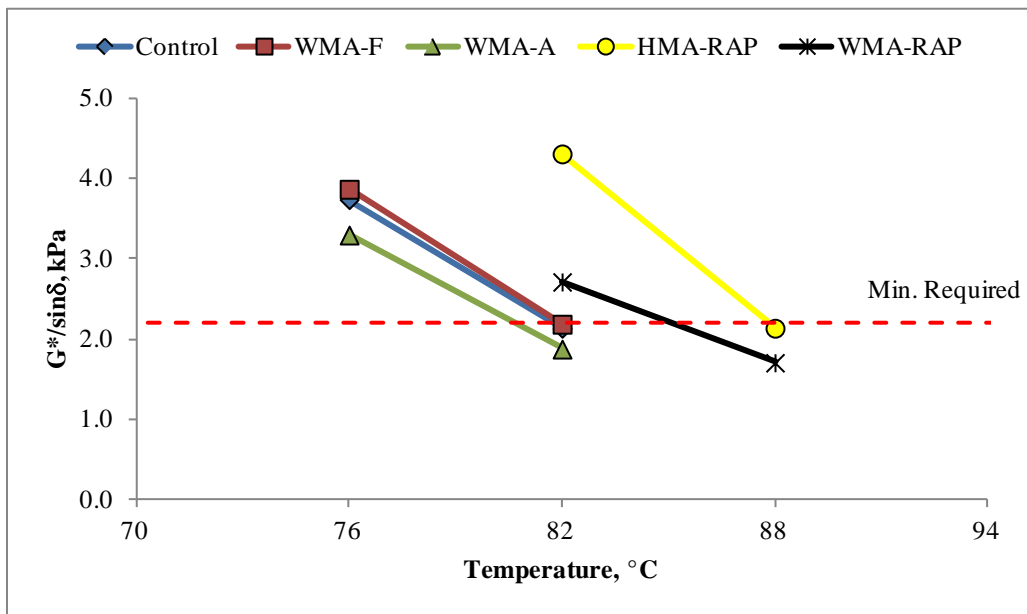


Figure 5-1 Rutting Parameter of Recovered Binders – Surface Lift.

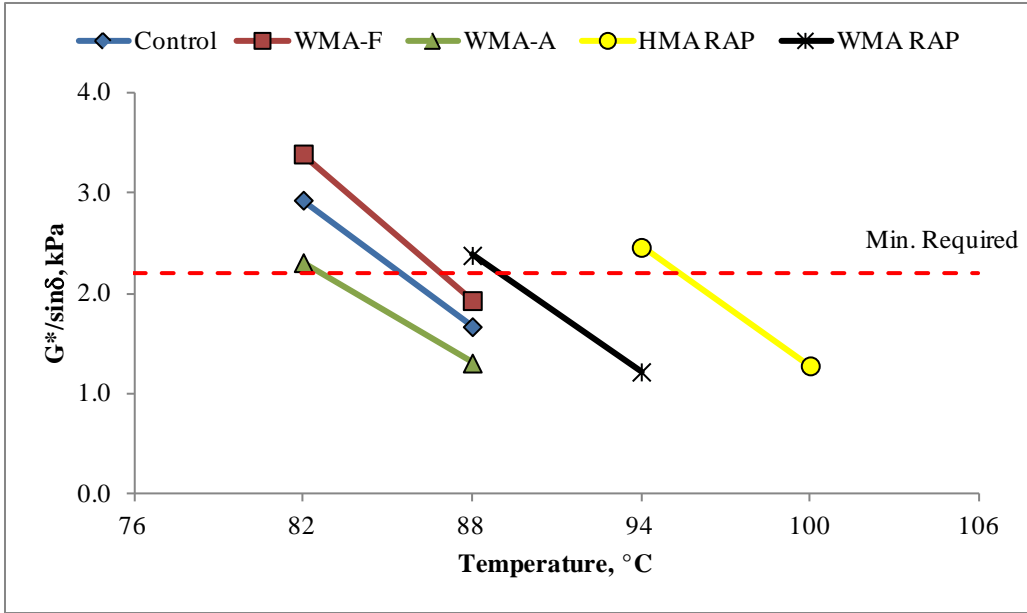


Figure 5-2 Rutting Parameter of Recovered Binders – Intermediate Lift.

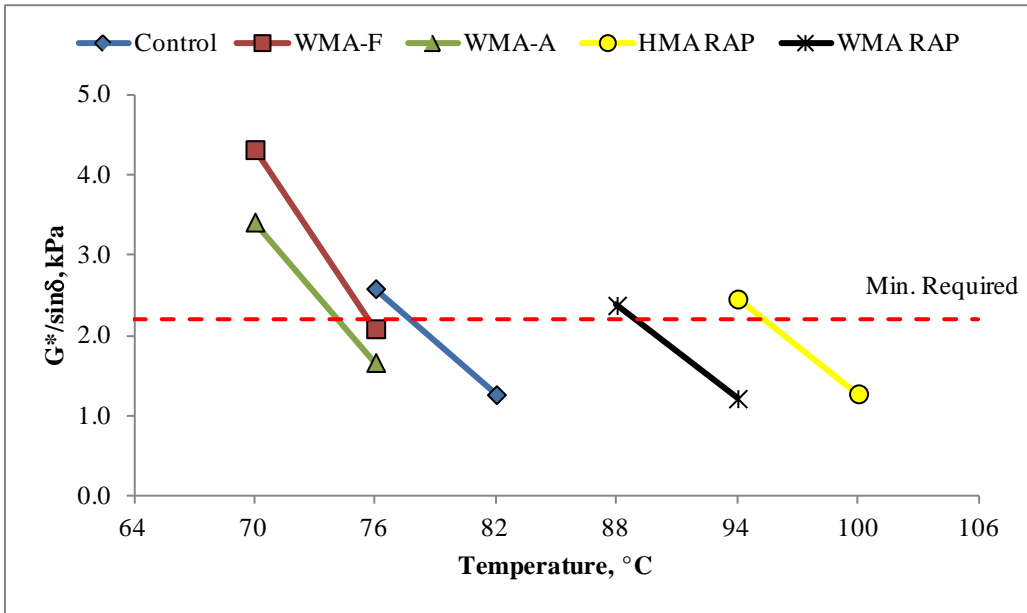


Figure 5-3 Rutting Parameter of Recovered Binders – Base Lift.

Fatigue Cracking

The fatigue parameter $G^*\sin\delta$ was obtained from DSR testing of PAV aged samples. The maximum value specified by AASHTO MP 1 is 5,000 kPa. Lower values of $G^*\sin\delta$ correspond to binders with better resistance to fatigue cracking. Figures 5-4 through 5-6 show the fatigue

parameter for all mixtures. As with the rutting parameters, binders recovered from high RAP mixes met the maximum $G^*\sin\delta$ requirement at higher temperatures, while binders recovered from WMA mixes met the requirement at lower or similar temperatures than the control. In this case, the high RAP mixes were not affected by the use of WMA technology and both met the requirement at the same temperature. The trends observed in Figures 5-4 through 5-6 suggest that at a given temperature, the high RAP extracted binders will have a higher $G^*\sin\delta$ than the control and virgin WMA binders, making them more susceptible to fatigue cracking.

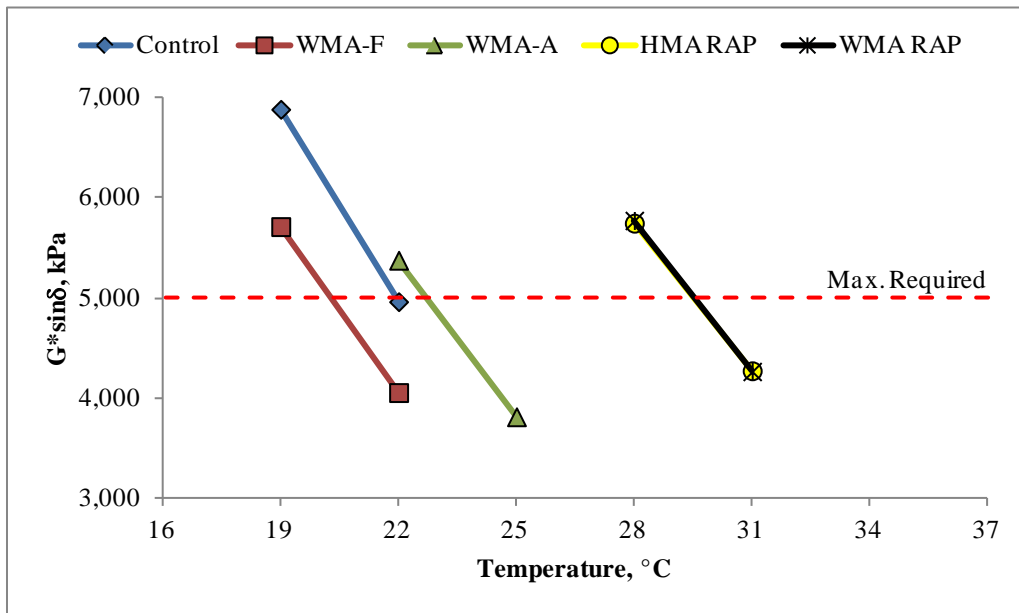


Figure 5-4 Fatigue Parameter of Recovered Binders – Surface Lift.

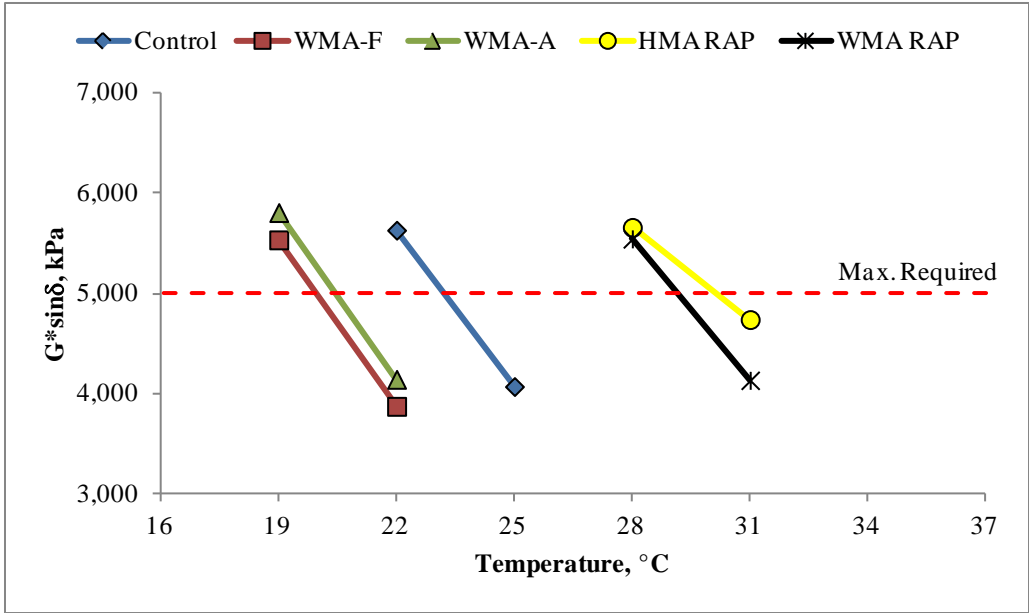


Figure 5-5 Fatigue Parameter of Recovered Binders – Intermediate Lift.

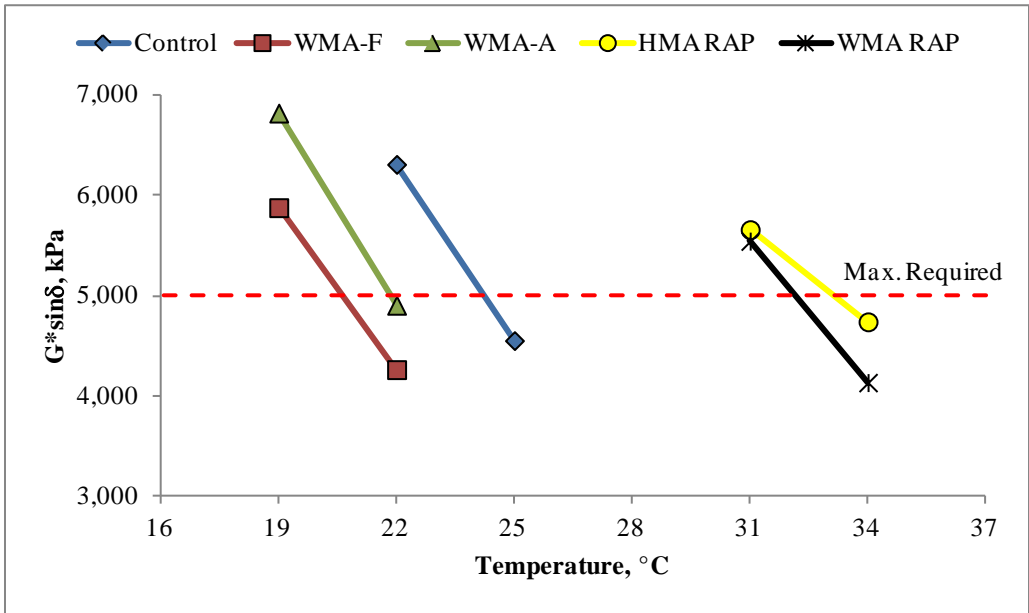


Figure 5-6 Fatigue Parameter of Recovered Binders – Base Lift.

Thermal Cracking

Susceptibility to thermal cracking was evaluated by means of the BBR test on RTFO and PAV aged samples. The parameters obtained were creep stiffness (S) and logarithmic creep rate (m) of the extracted binders. Creep stiffness is related to thermal stresses in an AC pavement due to

shrinking while the m-value is related to the ability of an AC pavement to relieve these stresses. Therefore, asphalt binders with minimum creep stiffness and maximum creep rate are desired to resist thermal cracking. AASHTO MP 1 specifies a maximum S of 300 MPa and a minimum m-value of 0.3.

Figures 5-7 through 5-9 show the thermal cracking parameters for all mixtures. The trends were similar to those for the rutting and fatigue cracking parameters. WMA mixtures appear to have the same ability to resist thermal cracking as the control (met the requirement at the same temperature), while high RAP mixes seemed to be more susceptible to thermal cracking (met the requirement at lower temperatures). Due to the limited amount of recovered material available, the low critical temperature of some of the high RAP binders were obtained by extrapolation. Since the samples were relatively close to the BBR criteria and would have passed at the next temperature increment, this approach was found to be acceptable.

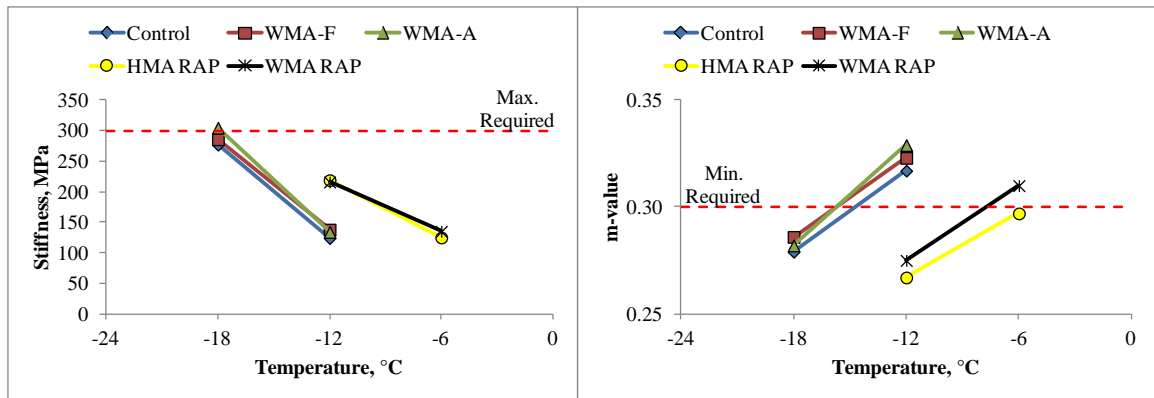


Figure 5-7 Thermal Cracking Parameters of Recovered Binders – Surface Lift.

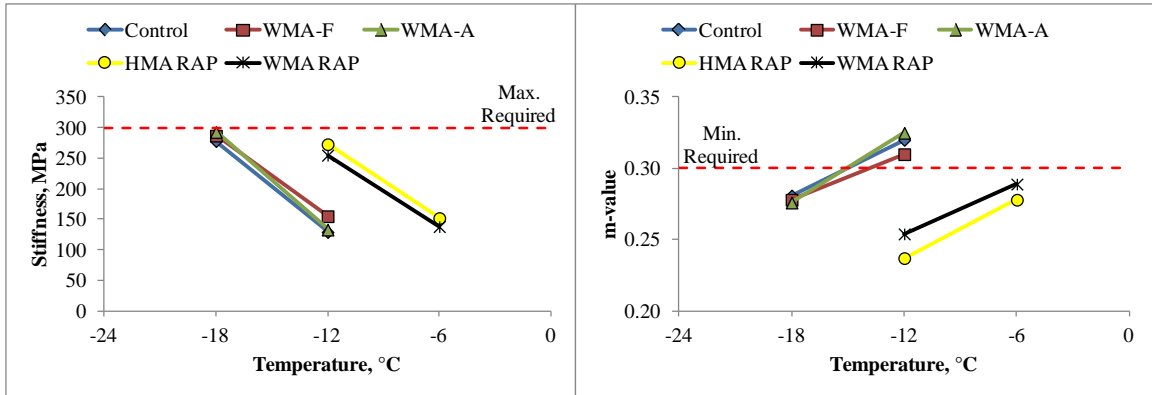


Figure 5-8 Thermal Cracking Parameters of Recovered Binders – Intermediate Lift.

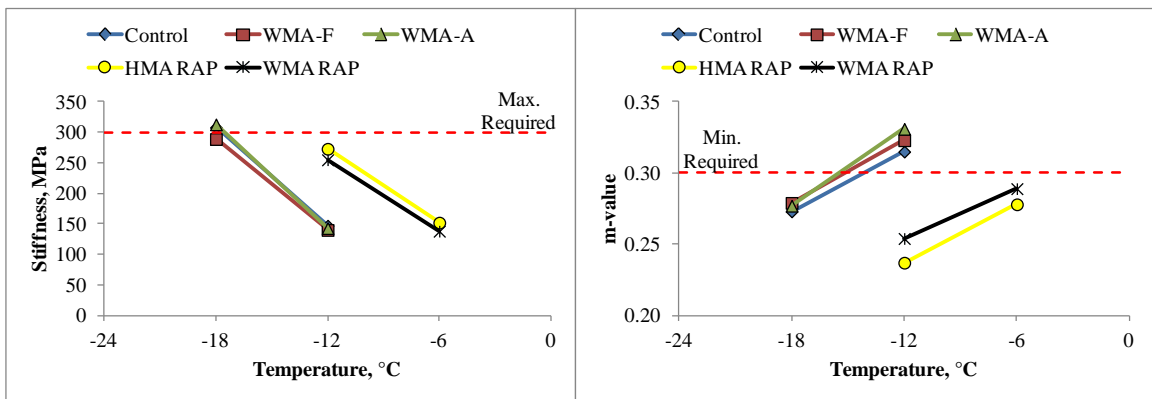


Figure 5-9 Thermal Cracking Parameters of Recovered Binders – Base Lift.

Overall, it was observed that the use of WMA technologies resulted in moderate changes to the extracted binder properties compared to the control and are expected to be more susceptible to rutting, have better resistance to fatigue cracking and perform similarly at low temperatures. On the other hand, the changes in binder properties appeared to be more pronounced for high RAP mixtures, making them more resistant to rutting but more prone to fatigue and thermal cracking.

EFFECT OF SUSTAINABLE TECHNOLOGIES ON MIXTURE PROPERTIES

Laboratory tests were also performed on plant-produced mixtures reheated and compacted in the laboratory. The tests were conducted to characterize the mixtures and evaluate their performance in a laboratory setting and to identify any effect resulting from the use of sustainable technologies. These results were also used to complement the field observations described in the following chapters.

Dynamic Modulus

The dynamic modulus (E^*) is a complex number that relates stress to strain for a linear viscoelastic material subjected to sinusoidal loading. The Mechanistic-Empirical Pavement Design Guide (MEPDG), developed under NCHRP Project 1-37A, uses the dynamic modulus to determine the temperature – and rate – dependent behavior of an asphalt concrete layer through the use of a master curve constructed at a reference temperature. Master curves are constructed based on the principle of time-temperature superposition; that is, the same modulus value of a material can be obtained either at low test temperatures and high frequencies (short loading times) or at high test temperatures but lower frequency (longer loading times).

Figures 5-10 through 5-12 show a comparison of the dynamic modulus of the control mix versus the dynamic modulus of the sustainable mixes obtained from the master curves for all pavement lifts in both confined and unconfined testing modes. The high RAP mixtures are not shown for the intermediate layer in Figure 5-11 because the same mix design was used for intermediate and base lifts, and therefore only samples from the base lifts were tested. If the dynamic moduli of the sustainable mixes are similar to the control (i.e. have similar master curves), the data in the figures should resemble the line of equality.

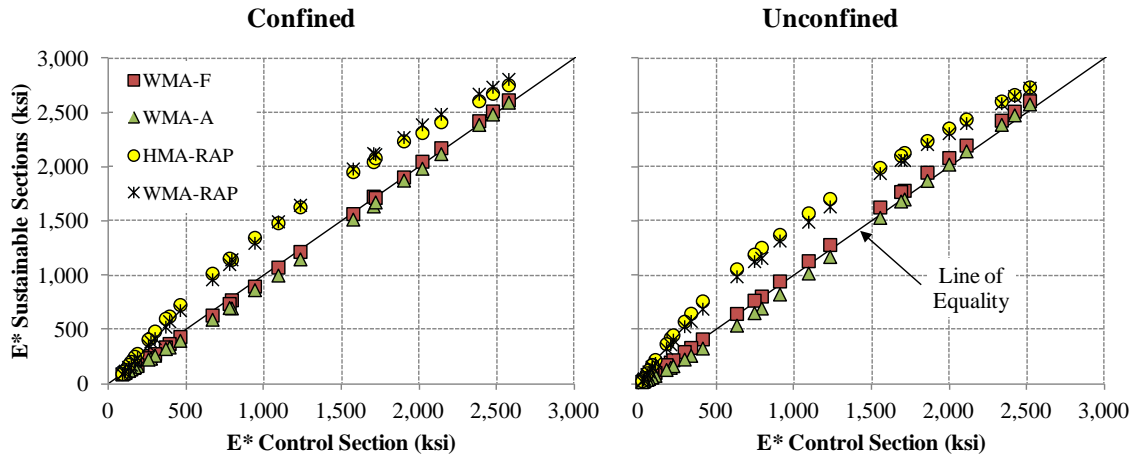


Figure 5-10 Dynamic Modulus Comparison for Surface Lift Mixtures.

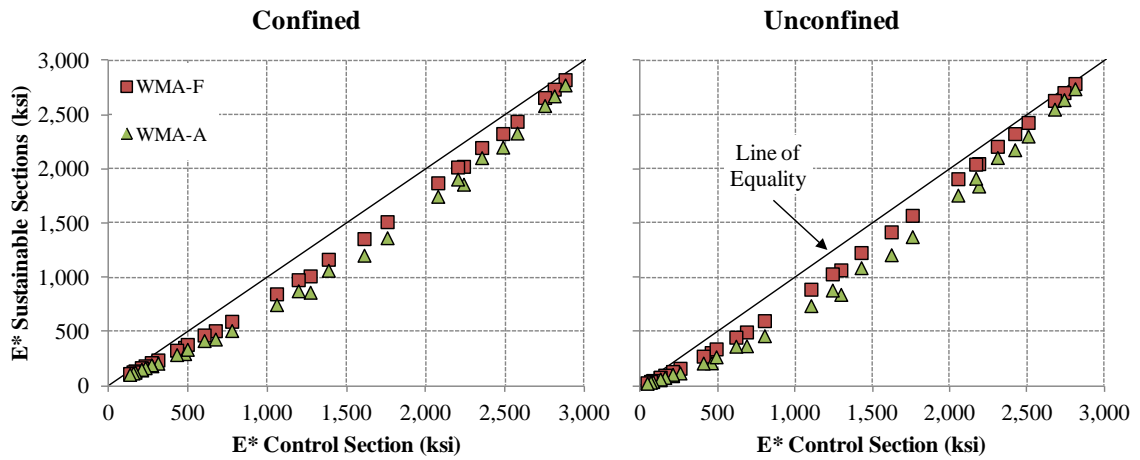


Figure 5-11 Dynamic Modulus Comparison for Intermediate Lift Mixtures.

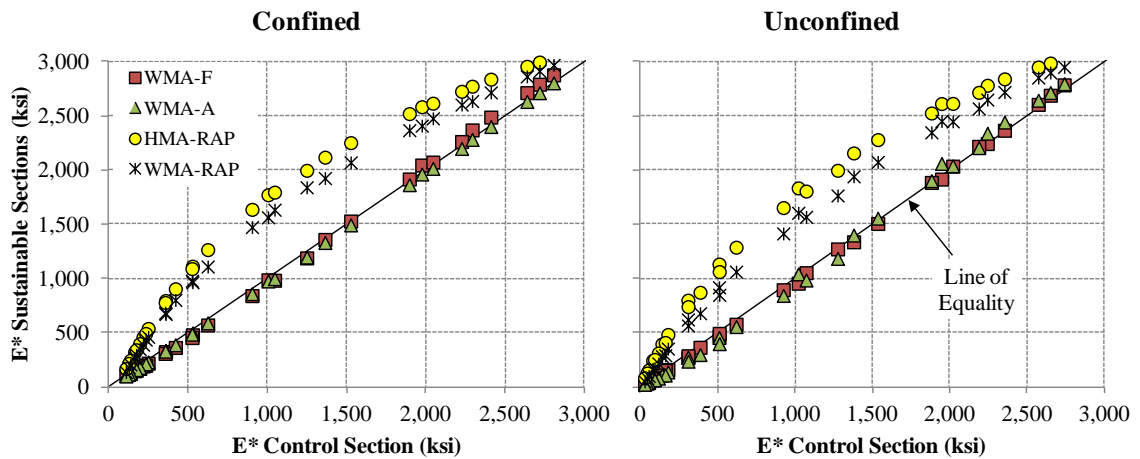


Figure 5-12 Dynamic Modulus Comparison for Base Lift Mixtures.

A regression analysis was performed to obtain linear equations for each data series. Intercepts close to zero and slopes close to one indicate that the data resemble the line of equality and the master curves of the sustainable mixes are similar to the control. It should be noted that these equations are intended to assess the similarity between the control and sustainable mixtures and not to predict E^* values. Table 5-4 shows the regression coefficients for all mixes. The general trend observed from these results is that WMA mixes produced with virgin materials tend to have lower E^* values, but overall are very similar to the control. High RAP mixes deviated more from the line of equality and had higher dynamic moduli than the control.

Figures 5-13 through 5-15 show the average E^* values for all mixtures obtained at a frequency of 10 Hz in a confined mode. Some researchers have recommended that a frequency of 10 Hz be used to represent highway speeds (98, 99). In general, statistical comparisons among the sections indicated that at 95% confidence level, at the 4 and 20°C temperatures there are no significant differences among the control and WMA sections, while the high RAP sections had statistically higher moduli. Because the high test temperature varied among the sections for the surface and base lifts, the same analysis could not be performed; however, the same trend was observed in terms of the high RAP sections having the highest results and the control and WMA mixes having similar values.

Table 5-4 Regression coefficients for master curve comparisons

Section vs. Control	Lift	Confined			Unconfined		
		Intercept	Slope	R ²	Intercept	Slope	R ²
WMA-F	Surface	-18.4	1.02	0.9996	-4.9	1.05	0.9999
	Intermediate	-90.1	0.97	0.9946	-112.3	1.00	0.9952
	Base	-51.0	1.04	0.9991	-26.1	1.02	0.9995
WMA-A	Surface	-33.3	1.00	0.9985	-50.8	1.03	0.9982
	Intermediate	-123.1	0.93	0.9868	-165.2	0.96	0.9835
	Base	-25.9	1.00	0.9998	-58.2	1.05	0.9981
HMA-RAP	Surface	141.5	1.09	0.9851	178.0	1.10	0.9796
	Intermediate	NA	NA	NA	NA	NA	NA
	Base	362.1	1.07	0.9549	355.3	1.10	0.9595
WMA-RAP	Surface	94.1	1.13	0.9888	138.6	1.10	0.9859
	Intermediate	NA	NA	NA	NA	NA	NA
	Base	273.1	1.05	0.9702	212.4	1.10	0.9789

NA = Not available. Test not performed on intermediate lift mix.

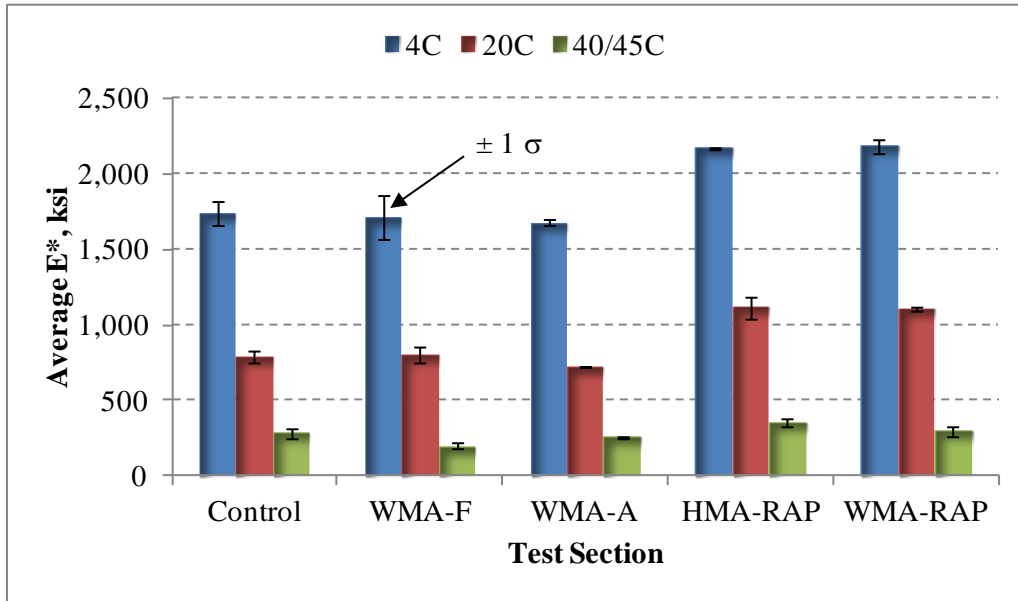


Figure 5-13 Dynamic Modulus at 10 Hz – Surface Lift.

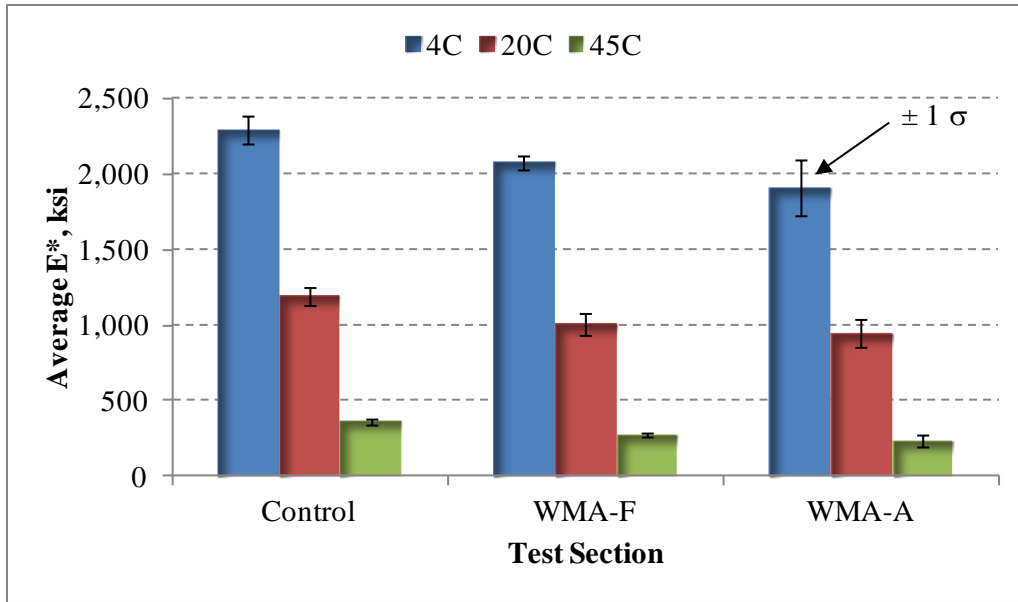


Figure 5-14 Dynamic Modulus at 10 Hz – Intermediate Lift.

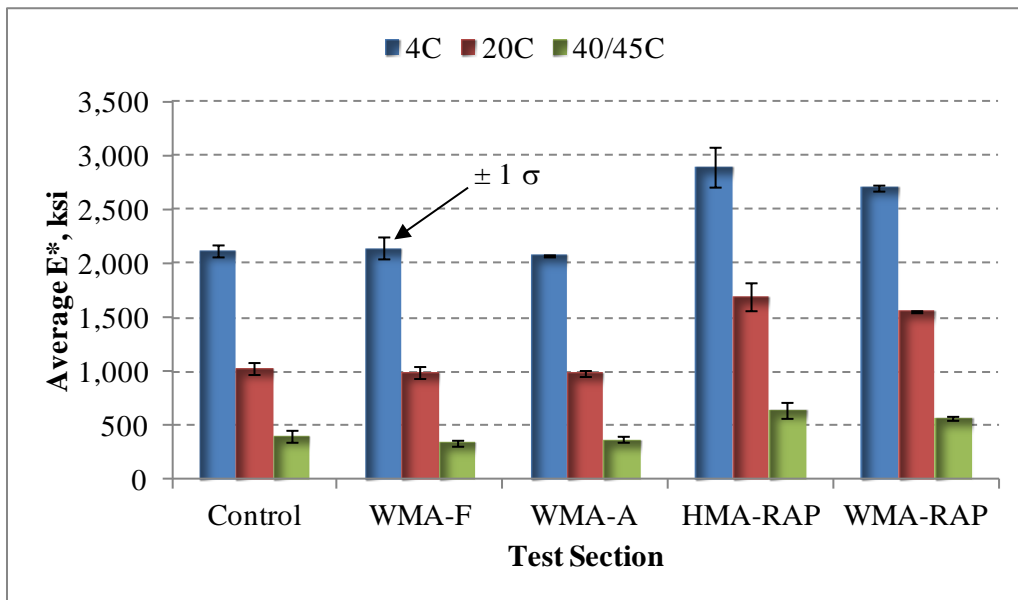


Figure 5-15 Dynamic Modulus at 10 Hz – Base Lift.

Asphalt Pavement Analyzer

Figure 5-16 shows the averages for manually and automatically measured rut depths for all surface mixes. In general, manual measurements were higher than automated ones, with the exception of the PFC mix. The open nature of the mixture may have caused the automated

measurement to be drastically higher than the manual. The manual result appears to be a more accurate representation of the mixture's rutting performance. These results showed that at a significance level of $\alpha = 0.05$ the PFC mix is significantly more resistant to rutting than all others, which is expected due to the stone-on-stone contact of the coarse aggregate. In addition, there was no evidence that the control and WMA mixes (WMA-F and WMA-A) were significantly different. The high RAP mixes had rut depths higher than the control, which contradicts the findings from the extracted binders.

Willis et al. (100) evaluated correlations between the APA test and field rutting performance for mixes placed at the NCAT Test Track. The authors concluded that the maximum acceptance criterion should be 5.5 mm, which correlated with a field rut depth of 10 mm. All mixtures in this study were below the proposed maximum limit.

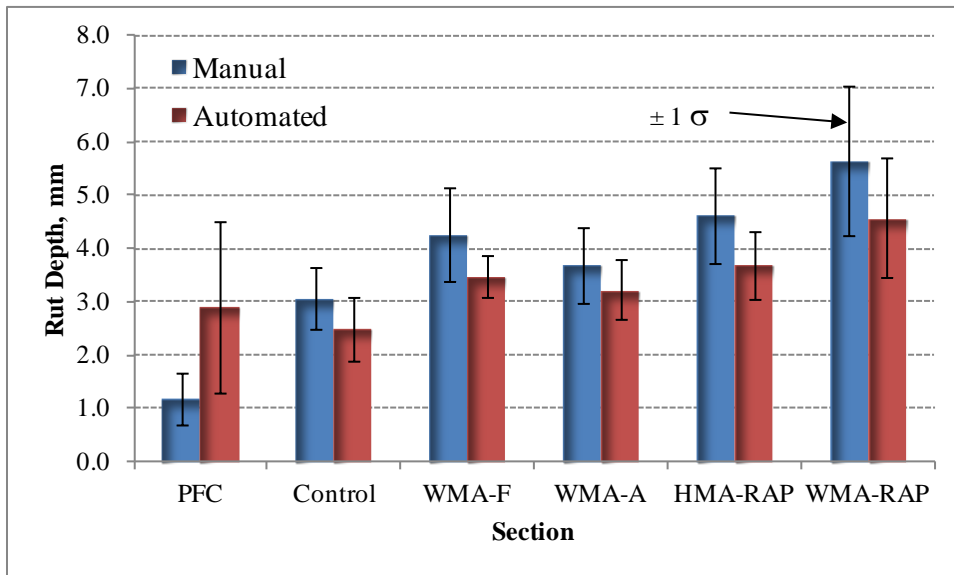


Figure 5-16 APA Rut Depths.

Several factors may be contributing to the discrepancies observed in Figure 5-16. Timm et al. (101) correlated results from APA testing and field measured rut depths using specimens compacted with the Superpave Gyrotory Compactor (SGC) and field cores. The authors found

that although the trends were correct, the correlation for the SGC specimens was poor. The data set for the field cores included fewer data points but had better correlation. Since this research only contains data from five sections, it is expected that the effect of SGC samples would produce inconsistencies.

One reason for the higher rut depths exhibited by high RAP mixes in laboratory tests compared to virgin mixes may be the effect of RAP on the effective binder (P_{be}). If the P_{be} decreases, the mixture has less binder available for binding aggregates together, resulting in higher rutting susceptibility (102, 103). Although the tests in this study were performed on the same plant produced mixes placed in the test sections, they were only conducted on surface mixes, which had the lowest P_{be} among sections.

Flow Number

Figure 5-17 summarizes the flow number results for all surface mixes, except the PFC mix, which was not tested by this method. The control mix specimens took the most number of cycles to reach tertiary flow, meaning that as with the APA results, they exhibited the highest rutting resistance. Only the differences observed between the control mix and all other mixes were statistically significant. It should be noted that all mixtures met the recommended minimum flow number for mixes designed for 3 to less than 10 million ESALs (53 for HMA and 30 for WMA) shown previously in Table 2-4. However, all mixtures were well below the recommended minimum criteria for mixes designed for 10 to less than 30 million ESALs (190 for HMA mixes and 105 for WMA mixes)

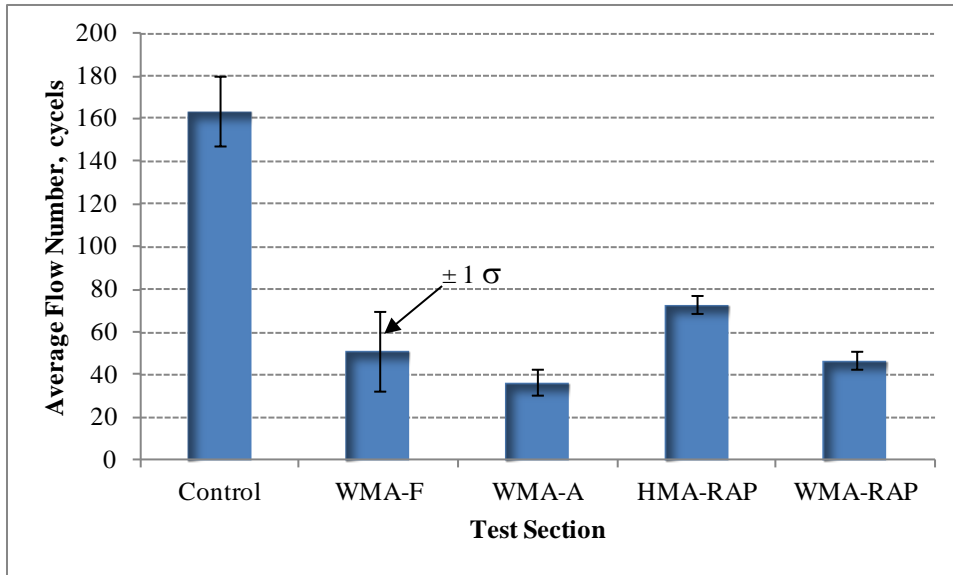


Figure 5-17 Flow Number Results.

Hamburg Wheel Tracking Device

The Hamburg Wheel Tracking Device was used to evaluate rutting and moisture susceptibility of the mixtures. Figure 5-18 illustrates an example of data obtained from the Hamburg device. The data recorded show the rutting progression with number of cycles. Two parameters were used to evaluate the mixtures: rutting rate and stripping inflection point. The rutting rate is the slope of the secondary consolidation tangent, while the stripping inflection point is the number of cycles at which the deformation of the sample is the result of moisture damage and not rutting alone.

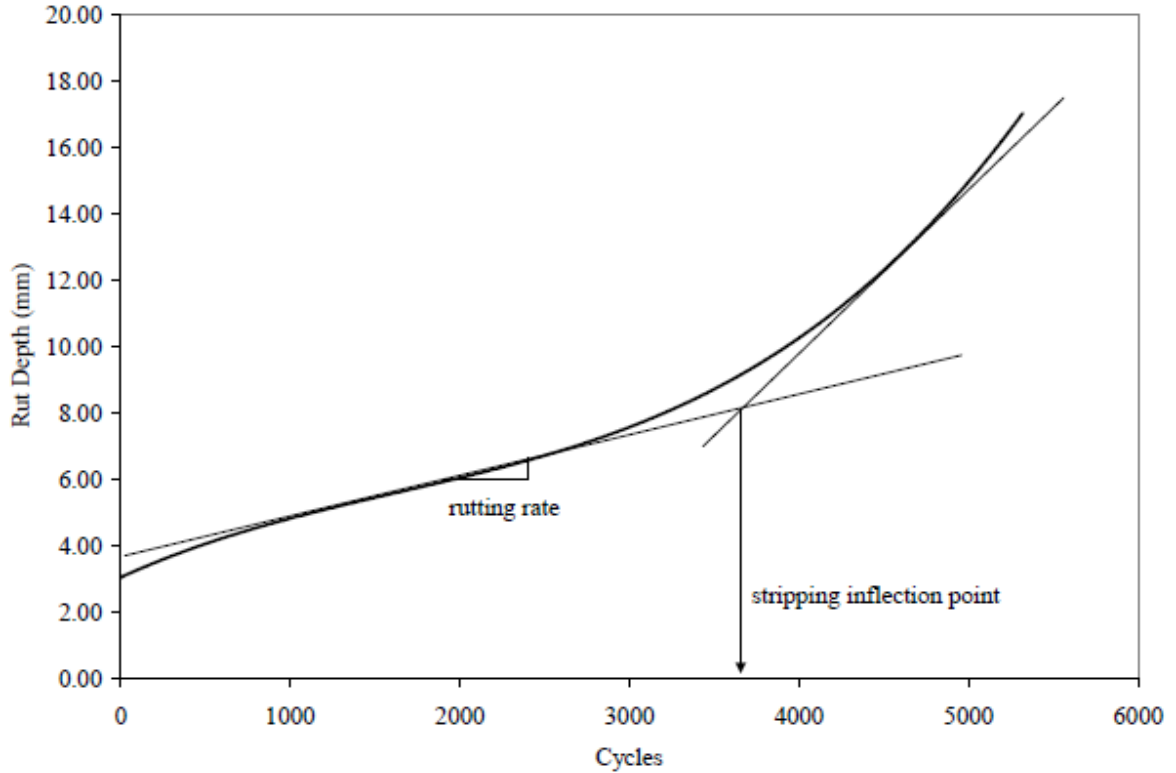


Figure 5-18 Example of Hamburg Data (104).

The rutting susceptibility results are shown in Figure 5-19. Lower rutting rates are indicative of better resistance to permanent deformation. The only significant difference at a significance level of $\alpha = 0.05$ was between the WMA-A and HMA-RAP sections (p -value = 0.0463). The general trend is that WMA mixes had higher rutting rates than the control, while high RAP mixes had lower rutting rates. In addition, WMA mixes exhibited higher variability than control and high RAP mixes. Unlike the APA and flow number tests, these results were more consistent with what would be expected (stiffer mixtures have higher rutting resistance), which was also reflected in the extracted binder tests. This suggests that the HWTD method may be more appropriate to evaluate rutting susceptibility of sustainable mixes in the lab.

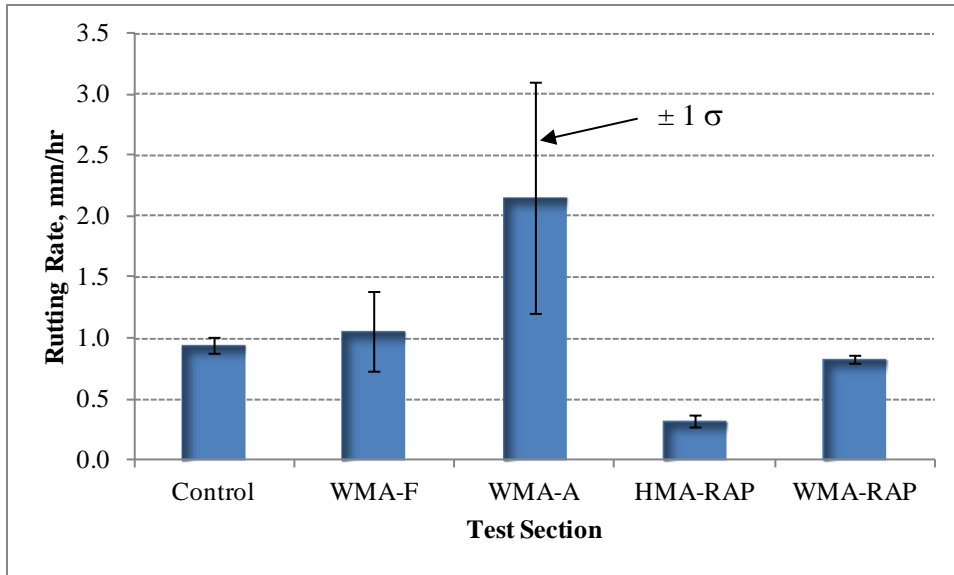


Figure 5-19 Hamburg Wheel Tracking Device Results for Rutting Susceptibility.

The moisture susceptibility results are given in Figure 5-20. Low stripping inflection points indicate low resistance to moisture damage. In general, stripping inflection points over 10,000 cycles represent good mixes. For the high RAP sections, the test concluded at 10,000 cycles without reaching a stripping inflection point (SIP). The WMA sections produced with virgin aggregates had stripping inflection points lower than the control, suggesting that they are more susceptible to moisture damage.

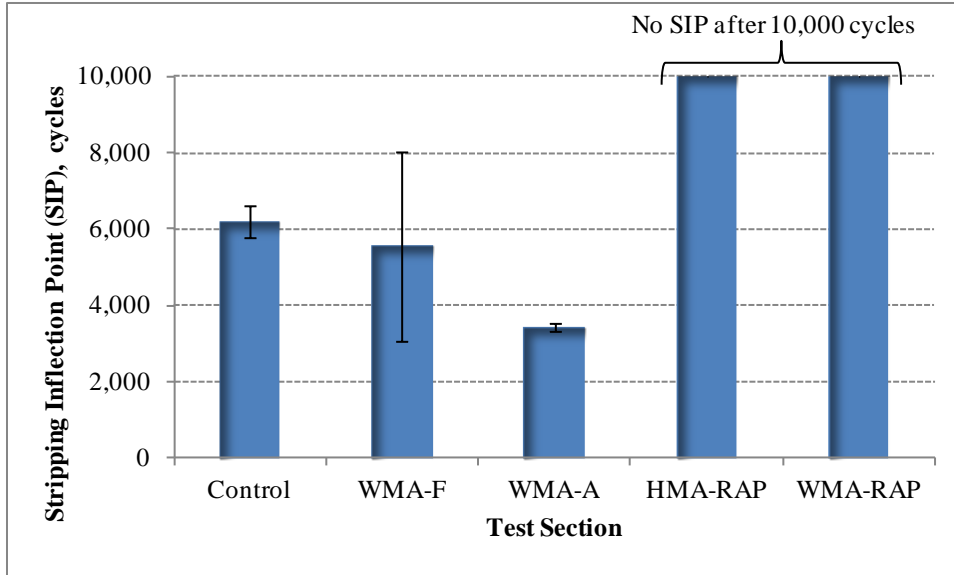


Figure 5-20 Hamburg Wheel Tracking Device Results for Moisture Susceptibility.

Tensile Strength Ratio

The tensile strength and TSR results are shown in Figure 5-21. In general, the tensile strengths (conditioned and unconditioned) of the WMA mixes were similar to the control at a significance level of $\alpha = 0.05$, while those of the high RAP mixes were higher. In addition, all but one of the individual tensile strengths exceeded 100 psi, which although is not required, is a desirable result. The TSR values appeared to be similar for all mixtures, meeting or exceeding the 0.8 requirement.

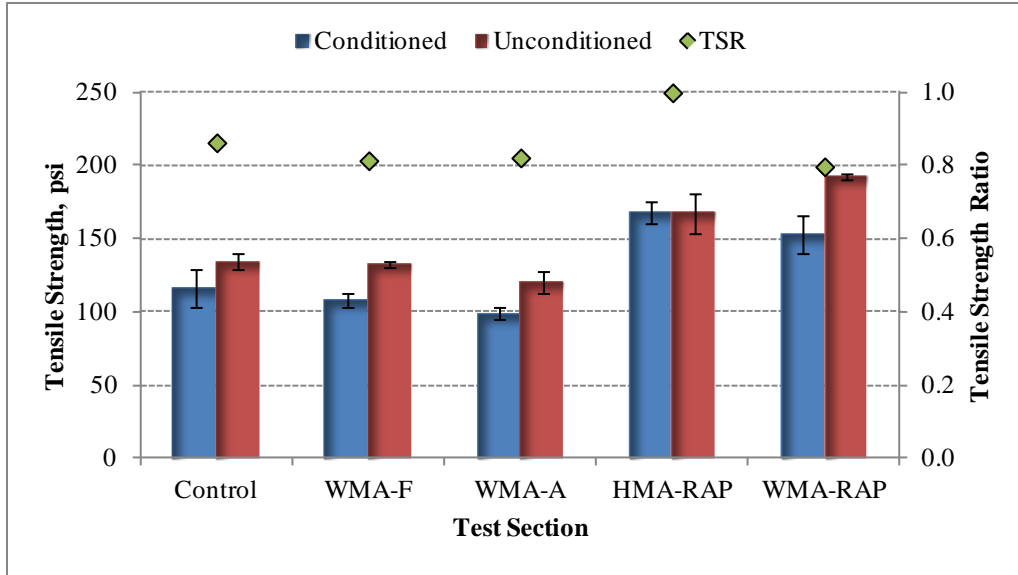


Figure 5-21 Tensile Strength Ratio Results.

Beam Flexural Fatigue

Figure 5-22 shows the number of cycles to failure of the mixtures at all strain levels. The statistical analysis indicated that at each strain level there was no significant difference among the mixtures, which could be due to the high variability of the samples. The results from this test were used to develop transfer functions, used to predict fatigue performance. One of the most common forms of fatigue transfer functions is shown in Equation 5.1:

$$N_f = K_1 \left(\frac{1}{\varepsilon} \right)^{K_2}$$

(5.1)

Where:

N_f = Number of load cycles to failure

ε = tensile strain at the outer fiber of the AC

K_1, K_2 = regression constants

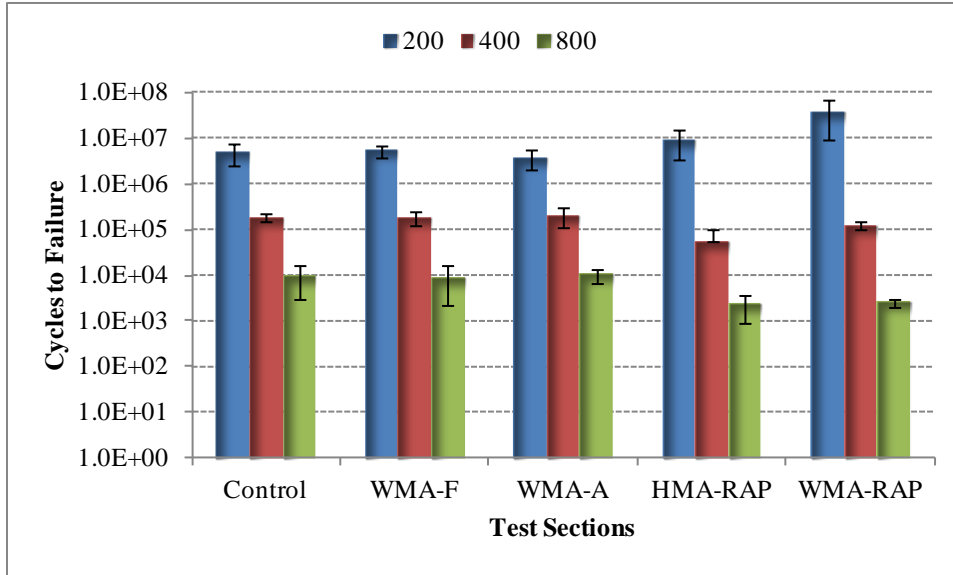


Figure 5-22 Flexural Beam Fatigue Results at All Strain Levels.

The regression constants for each mixture are shown in Table 5-5. To determine if there were any differences between the fatigue behavior of the control mix and the sustainable mixes, 95% confidence intervals (CI) were obtained for K_1 and K_2 . Overlapping CIs indicated that there was no statistical evidence that the coefficients were different. Figure 5-23 plots the 95% confidence intervals for all regression coefficients. It was found that the control and virgin WMA mixes had coefficients statistically similar. There was no statistical difference between the two high RAP mixtures, while only the HMA-RAP mix was considered similar to the control. The WMA-RAP mix had higher coefficients than the control, meaning that at low strain levels it is more resistant to fatigue cracking, while at higher strain levels it is expected to fail sooner.

Table 5-5 Regression coefficients for fatigue transfer functions

Section	K_1 (intercept)	K_2 (slope)	R^2
Control	1.18E+17	4.53	0.97
WMA-F	3.51E+17	4.71	0.98
WMA-A	1.50E+16	4.19	0.97
HMA-RAP	3.74E+20	6.02	0.93
WMA-RAP	2.65E+22	6.58	0.96

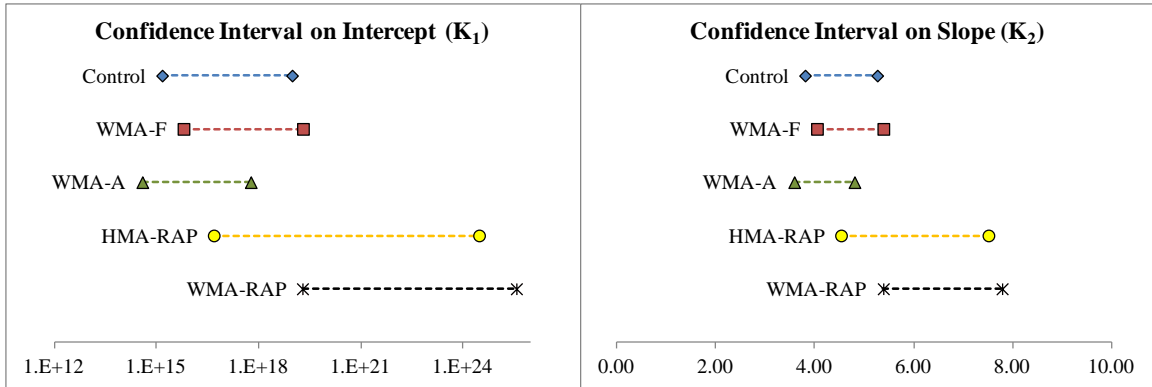


Figure 5-23 95% Confidence Intervals for Regression Coefficients.

The results from the beam fatigue test were also used to obtain the fatigue endurance limit (FEL), shown in Figure 5-24. Most mixtures had an endurance limit higher than the control, with the exception of the WMA-A mix. This means that those mixtures would be able to withstand strain levels higher than the control without accumulating fatigue damage. Because the FEL is calculated as a single value based on the set of nine samples tested for each mix, there is no variability associated with it and statistical comparisons cannot be made among the mixtures.

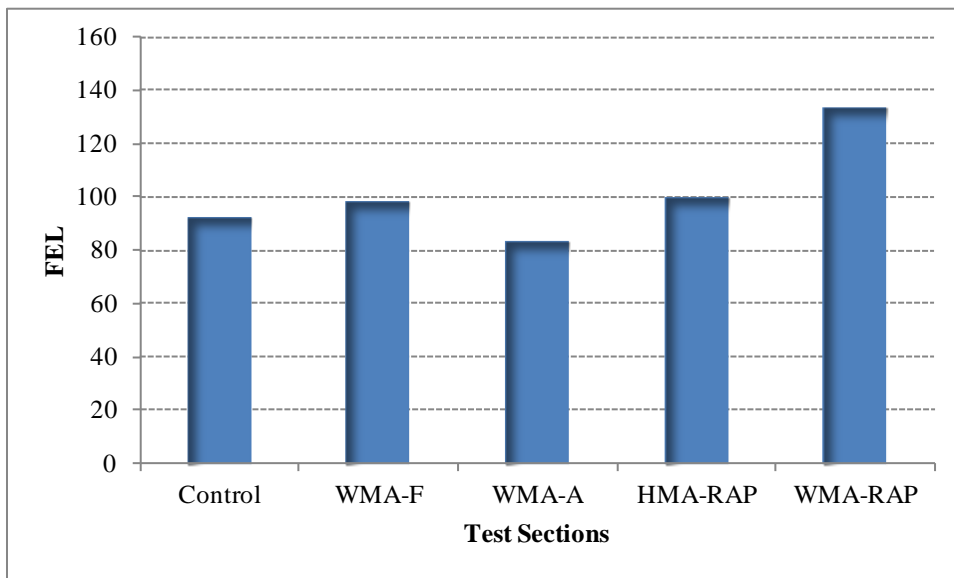


Figure 5-24 Fatigue Endurance Limit from Beam Fatigue Test.

Thermal Cracking Analysis

Figure 5-25 shows the thermal stress as a function of temperature for each surface mixture. The results indicated that at temperatures below 0°C, the high RAP mixtures develop thermal stresses at a higher rate than the control, while virgin WMA mixtures do it at a lower rate. Table 5-6 shows the creep stiffness at 50 seconds and the indirect tensile strength of the mixtures at -10°C. Mixtures with higher resistance to thermal cracking are characterized by low creep stiffness and high strength. While virgin WMA mixtures had lower stiffness than the control (were more flexible), they also had lower strengths. However, Tukey comparisons at a significance level of $\alpha = 0.05$ indicated that there was no statistical difference between the fracture strengths of the control and WMA mixes. Therefore, since they have similar strength and lower stiffness than the control, it can be concluded that the WMA mixtures had better resistance to low temperature cracking. On the other hand, high RAP mixtures exhibited higher creep stiffness and significantly lower strengths than the control, making them more susceptible to thermal cracking.

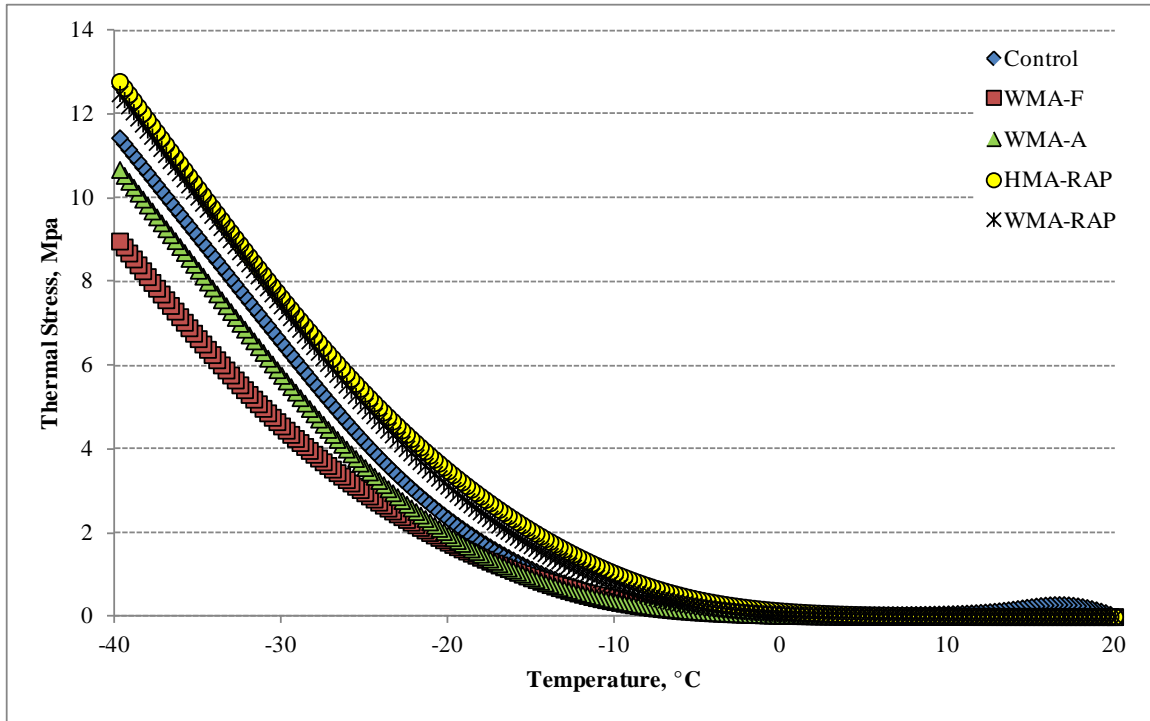


Figure 5-25 Thermal Stress versus Temperature.

Table 5-6 IDT Test results for GE surface mixes

Mixture	Stiffness (MPa)	Strength (MPa)	T _{crit} (°C)
Control	9.01E+03	4.71	-26.4
WMA-F	8.06E+03	4.48	-30.0
WMA-A	7.87E+03	4.46	-27.2
HMA-RAP	1.33E+04	4.10	-21.9
WMA-RAP	1.12E+04	4.06	-22.8

Table 5-6 also shows the critical temperatures of the surface mixes obtained from the IDT test. The critical temperature is the temperature at which the estimated thermal stress in a pavement due to contraction exceeds the tested indirect tensile strength of a mixture. Lower critical temperatures indicate higher resistance to thermal cracking. The results reiterate the findings from the stiffness and strength results, with virgin WMA mixes having similar or higher resistance to thermal cracking than the control, while high RAP mixes were more susceptible.

Critical temperatures are calculated as a single value for the entire set of samples, so statistical comparisons among mixtures cannot be performed.

Figure 5-26 shows the relationship between the critical temperatures obtained from the BBR and IDT tests. It can be observed that there is good correlation between both tests; however, the results from the IDT test on compacted samples are generally lower than those from the BBR test on extracted binders. The difference is more pronounced for the high RAP mixes, which contain not only aged binder, but also aggregate from RAP.

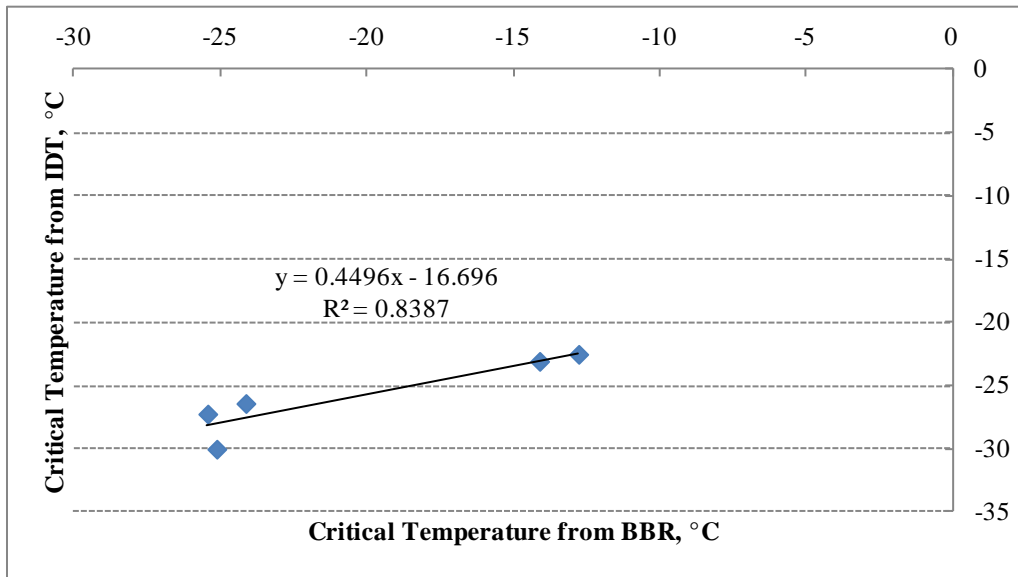


Figure 5-26 Relationship between Critical Temperatures from Binder and Mix Testing.

SUMMARY

Several tests were performed on extracted binders and plant produced mixture samples to evaluate the properties and laboratory performance of the different mixtures included in this study. Overall, it was found that the use of WMA technologies did not produce significant changes in mixture properties or performance. The main effect observed was the potential for higher permanent deformation compared to the control. High RAP mixes were stiffer than the control, which suggests higher susceptibility to cracking, but higher rutting resistance. However,

this was not reflected in some rutting tests or the flexural beam fatigue test. High RAP mixes were also more resistant to moisture damage than the control and WMA mixes.

Some inconsistencies were observed among different tests the evaluated rutting susceptibility, particularly the high susceptibility to permanent deformation of the high RAP mixes compared to the control and WMA mixes exhibited in the APA and flow number tests. These test results are compared to field measurements and further discussed in Chapter 7.

CHAPTER 6

ANALYSIS OF FIELD MEASURED PAVEMENT RESPONSES

As described in Chapter 3, response measurements (strain and pressure) were taken approximately once a week under live traffic loads and under different environmental conditions. Additionally, falling weight deflectometer (FWD) testing was performed several times per month to quantify the seasonal behavior of the pavement layer moduli. This information was used to develop relationships between the field measurements (responses and AC moduli) and pavement temperature. These relationships can be used to predict pavement performance and are discussed in the following sections.

AC Modulus – Temperature Relationships

AC modulus is a temperature-dependent property and plays an important role in the potential seasonal effects of rutting. While in the winter months the AC becomes very stiff and minimizes the rutting potential, during the summer months the stiffness decreases and rutting susceptibility increases. The modulus is also an important material property for use in M-E design methods, with particular emphasis on characterizing how it changes with temperature. Figure 6-1 illustrates the measured relationship between backcalculated AC modulus and mid-depth temperature. For each test section, the AC modulus measured at the outside wheelpath, where greater damage is expected to occur, was expressed as a function of mid-depth temperature using Equation 6-1.

$$E = \alpha_1 e^{\alpha_2 T}$$

(6-1)

where:

E = Backcalculated AC modulus, ksi

T = Mid-depth AC temperature, °F

α_1, α_2 = Regression coefficients

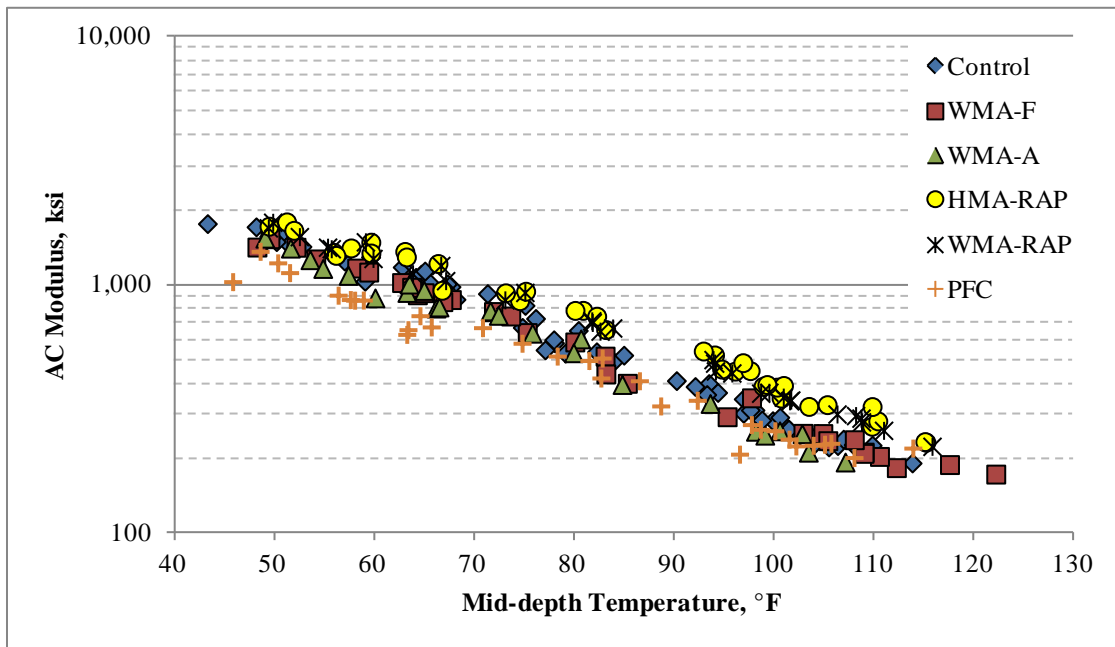


Figure 6-1 Relationship Between Backcalculated AC Modulus and Mid-depth Temperature.

Table 6-1 shows the results of the regression analysis for all sections. Each model showed good correlation between AC modulus and mid-depth temperature. To determine if the stiffness-temperature relationship was statistically similar among the sections, 95% confidence intervals (CI) were obtained for the intercepts (α_1) and slopes (α_2). If the intervals overlapped, it could be concluded that the differences in the regression coefficients were not statistically significant. Figure 6-2 illustrates the confidence intervals for all regression coefficients. At 95% confidence level, there was no evidence that the intercepts of high RAP sections were statistically different from the control. However, the intercepts of the WMA and PFC sections were significantly lower than the control, indicating that the modulus tended to be lower at all temperatures. The slopes of the high RAP sections were lower than that of the control section and virgin WMA sections, which means they were less influenced by temperature presumably due to

the presence of aged binder. The slope of the PFC section was also significantly lower than the control.

Table 6-1 Regression analysis for AC modulus as a function of mid-depth temperature

Section	α_1 (intercept)	α_2 (slope)	R ²
Control	9,051	-0.034	0.98
WMA-F	7,554	-0.033	0.98
WMA-A	8,217	-0.034	0.97
HMA-RAP	8,739	-0.031	0.97
WMA-RAP	8,629	-0.031	0.99
PFC	4,770	-0.029	0.92

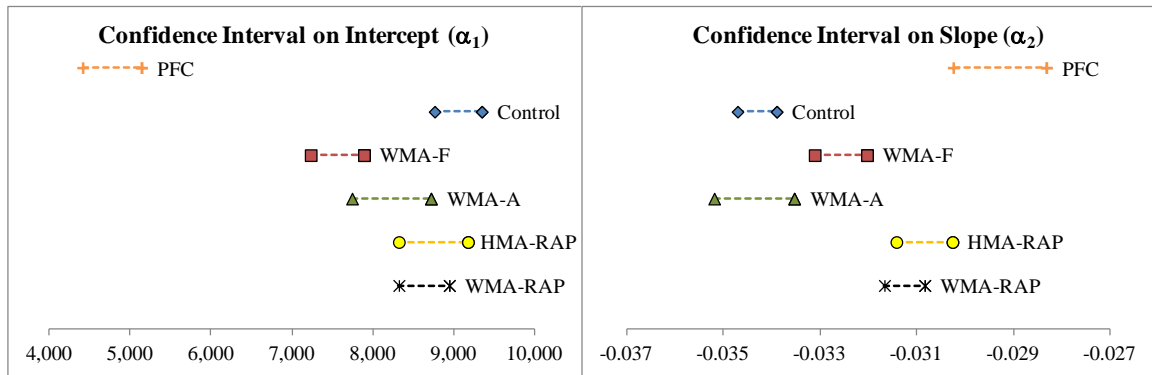


Figure 6-2 95% Confidence Intervals for Regression Coefficients – AC Modulus.

To fairly compare the different test sections, it was necessary to normalize the AC modulus to a reference temperature. Three values (50, 68 and 110°F) were used to include the range of temperatures at which testing was conducted. This was accomplished by dividing Equation 6-1 with a selected reference temperature (T_{ref}) by the same equation with measured temperature (T_{meas}) and solving for temperature normalized modulus (E_{Tref}), as shown in Equation 6-2.

$$E_{Tref} = E_{Tmeas} e^{\alpha_2(T_{ref} - T_{meas})}$$

(6-2)

where:

E_{Tref} = normalized AC modulus at reference temperature T_{ref} , ksi

$E_{T_{\text{meas}}}$ = measured AC modulus at temperature T_{meas} , ksi

T_{ref} = mid-depth reference temperature, 50, 68 or 110°F

T_{meas} = measured mid-depth temperature at time of test, °F

α_2 = section-specific regression coefficient from Table 6-1

The average AC moduli and standard deviations for each test section are presented in Figure 6-3. Tukey comparisons at a significance level of $\alpha=0.05$ were conducted for each reference temperature. In Figure 6-3, for each temperature series, letters were used to represent the statistical differences among test sections. Sections with the same letter are not significantly different. At 50°F, the two virgin warm mix sections (WMA-F and WMA-A) were not statistically different from each other (p-value = 0.9898), but all other sections were different among themselves (p-values < 0.0001). At 68°F, the differences among all sections were statistically significant; however, it should be noted that the magnitudes of the differences among virgin WMA sections and the control were not large. At 110°F, most differences among sections were statistically significant. The PFC and WMA-A sections were found to be similar (p-value = 0.1840), which was also the case between the control section and WMA-F (p-value = 0.8220). Although some statistically significant differences existed, the magnitudes of the moduli of all sections produced with virgin aggregates were within 10%, which may not be considered to have a practical impact.

The statistical significance can be attributed to the low coefficients of variation observed in the sections (under 15%) that caused relatively small differences in the data to be considered meaningful. From a practical perspective, the moduli of the control and virgin WMA sections may be considered similar at intermediate and high pavement temperatures. The same assumption can be made when comparing the two high RAP sections.

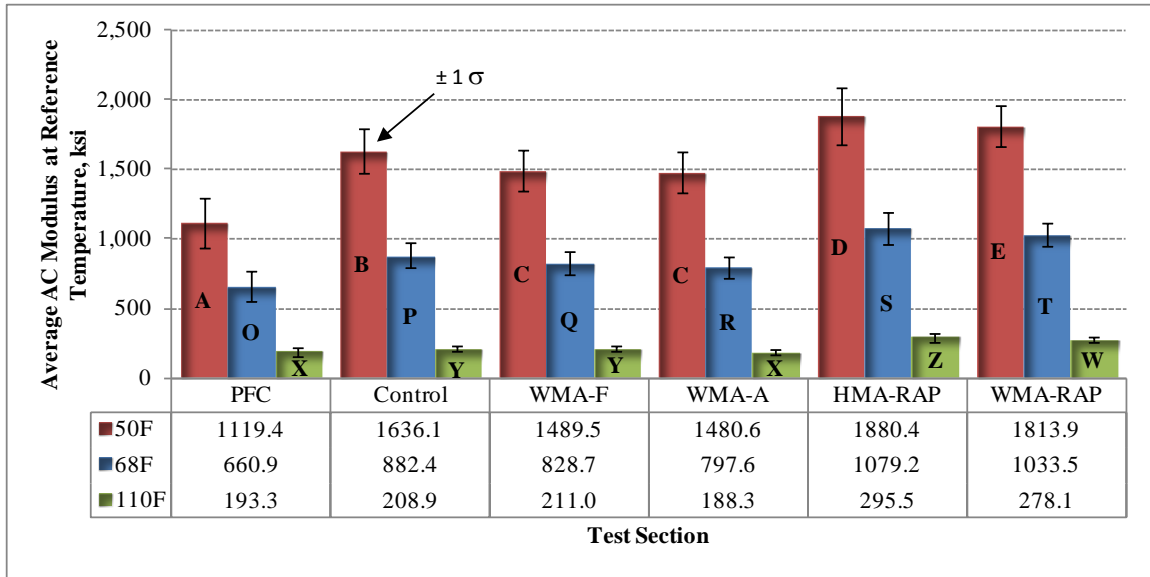


Figure 6-3 Temperature Normalized AC Modulus.

The temperature-normalized moduli over time plotted in Figure 6-4 show the same general trends observed in Figure 6-3. The results shown correspond to the intermediate reference temperature, but similar trends were observed at the low and high ends of the temperature range. The PFC section had higher variability over time, and the HMA-RAP section also exhibited erratic results, particularly in the second half of the analysis period.

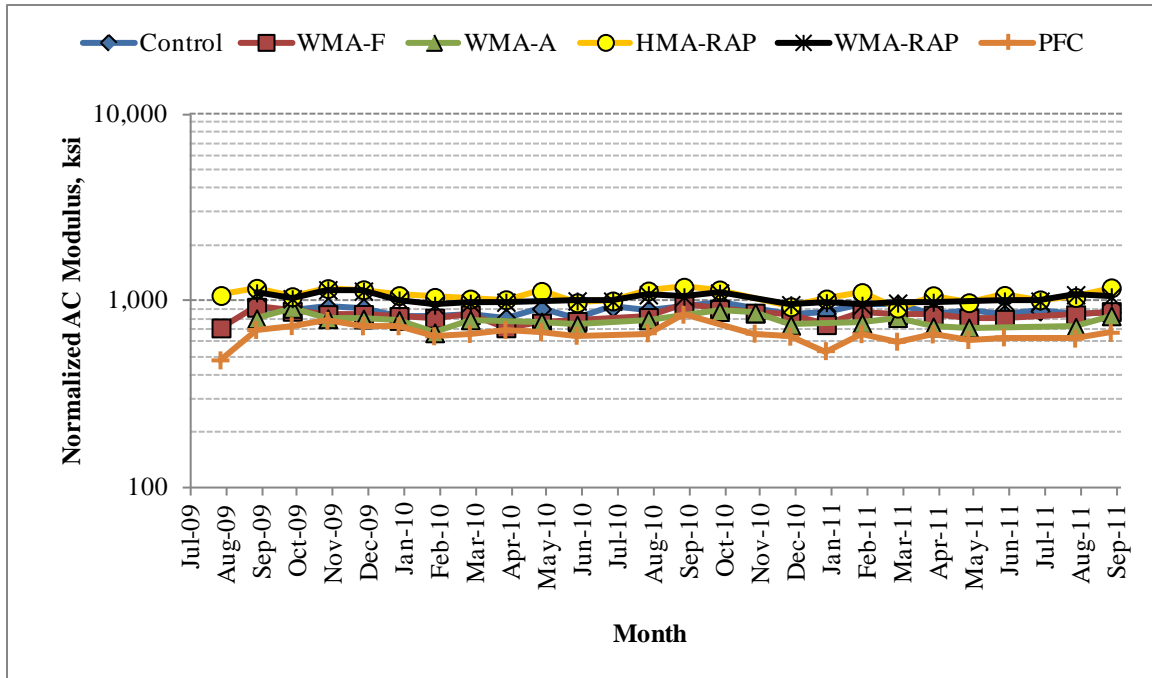


Figure 6-4 Average Monthly Normalized AC Moduli at 68°F.

An analysis of variance was performed to determine the effect of two factors (material type and production temperature) on AC modulus. Each factor had two levels; for material type the levels were virgin blends (VB) and high RAP mixtures (RAP), and for production temperature the levels were hot (HMA) and warm (WMA). The PFC section was excluded from this analysis because it did not contain information at all factor levels.

The results indicated that at all reference temperatures both factors are highly significant, as well as their interaction. Figure 6-5 illustrates the change in AC modulus for the factors production temperature (WMA vs HMA) and material type (RAP vs VB) at all reference temperatures. It can be observed that varying the material type produced a bigger change in AC modulus than varying the production temperature. Mixtures with high RAP content were stiffer than those produced with all virgin materials, especially at high mid-depth pavement temperatures. The AC moduli increased between 18 and 40% when RAP was used. On the other hand, for mixtures produced with WMA technology, the AC moduli decreased approximately 6%, regardless of pavement temperature.

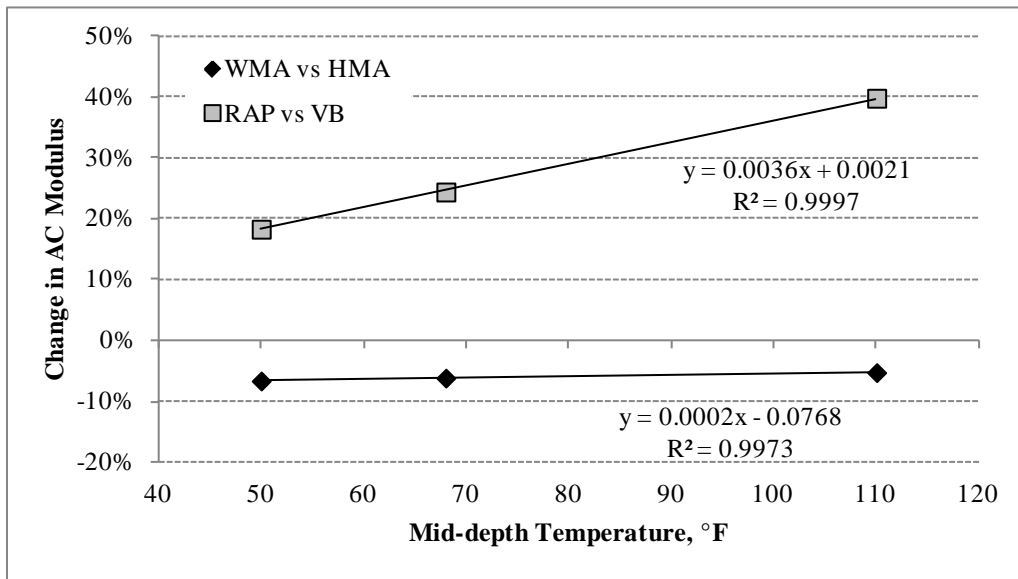


Figure 6-5 Variation in AC Modulus Across Factors.

Strain – Temperature Relationships

Dynamic pavement response measurements were taken to obtain horizontal longitudinal and transverse strain at the bottom of the AC layer. The tensile strains at the bottom of the AC layer are associated with fatigue (bottom-up) cracking in flexible pavements. Figure 6-6 shows that the steer axles produce similar strains in the longitudinal and transverse directions. This is expected because steer axles provide a more symmetrical pressure with similar dimensions on both the longitudinal and transverse directions. On the other hand, for single and tandem axles the contact area produced by dual tires has a smaller dimension in the longitudinal direction, inducing a greater strain. In addition, the influence areas on the pavement may overlap producing a combined effect. It was observed that these axle types tend to have longitudinal strains that are approximately 1.3 to 1.6 times higher than the transverse strains, which is consistent with previous findings by Priest and Timm (8). Only longitudinal strains were used for analysis because they represent the most severe condition.

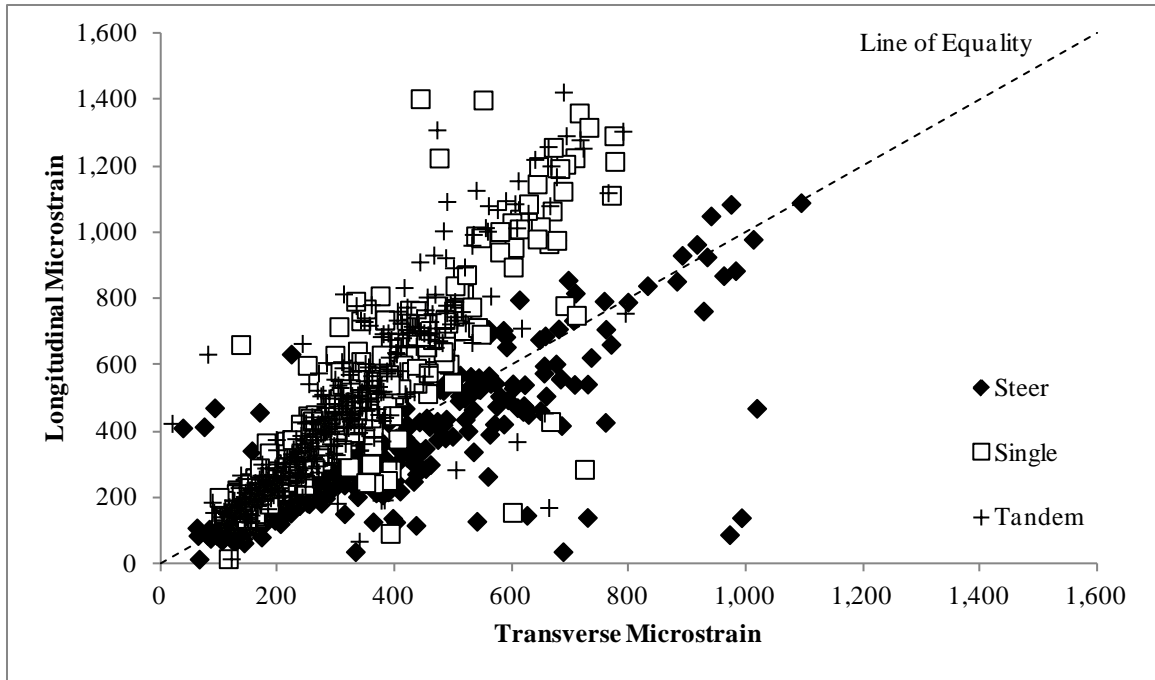


Figure 6-6 Relationship Between Longitudinal and Transverse Microstrain.

From Figure 6-6 it can be observed that there was some scatter in the measured data. This could be due to factors such as lateral distribution of wheel loads (wheel wander) or faulty gauges. To eliminate possible outliers, data were filtered prior to analysis. The criteria used discarded longitudinal strains that were higher than 2 times or lower than 1.5 times the transverse strain. This range includes typical longitudinal to transverse strain ratios observed in past Test Track cycles (8).

Figure 6-7 illustrates an example of the relationship between horizontal longitudinal microstrain and mid-depth pavement temperature for single axles. Since single axles exhibited the higher strains and represent the majority of axle passes on each section they are the only axle types considered in the analysis. However, similar trends were observed for all axle types.

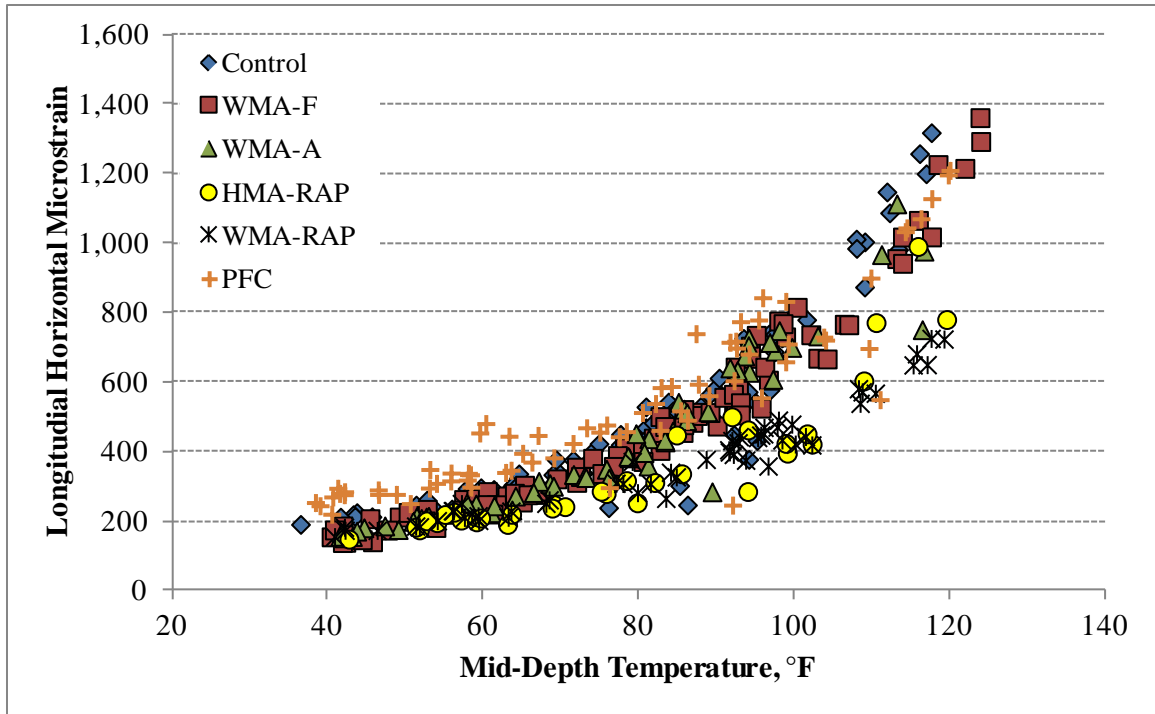


Figure 6-7 Relationship Between Horizontal Longitudinal Microstrain and Mid-depth Temperature – Single Axles.

As with AC modulus, pavement responses are also dependent on mid-depth temperature. In general, for all axle types the relationship between longitudinal horizontal microstrain and mid-depth temperature was characterized by:

$$\varepsilon = k_1 e^{k_2 T}$$

(6-3)

where:

ε = longitudinal horizontal microstrain

T = Mid-depth HMA temperature, °F

k_1, k_2 = Section-specific regression coefficients

Table 6-2 presents the results of the regression analysis for all test sections using a logarithmic scale and Figure 6-8 shows the 95% confidence intervals for all coefficients. All models showed good correlation between longitudinal strain and mid-depth temperature. In

general, the regression coefficients of the control and sustainable sections are statistically similar, with the exception of the PFC section, which had a higher intercept and lower slope. This means that strains tended to be higher than the control, especially at low pavement temperatures. At 95% confidence level, there was no evidence that the regression coefficients of the WMA sections were statistically different from the control. In the high RAP sections the strains were less influenced by temperature, but only the slope in the WMA-RAP was significantly lower than the control from a statistical perspective. The lower slopes are presumably due to the presence of stiffer binder. These results are consistent with the trends observed for AC modulus, which indicated that AC modulus was less temperature sensitive for the high RAP sections than the control.

Table 6-2 Regression analysis for longitudinal strain as a function of mid-depth temperature

Section	k_1 (intercept)	k_2 (slope)	R^2
Control	68.97	0.023	0.90
WMA-F	53.37	0.026	0.98
WMA-A	53.35	0.026	0.95
HMA-RAP	58.74	0.021	0.90
WMA-RAP	73.47	0.019	0.96
PFC	120.7	0.018	0.85

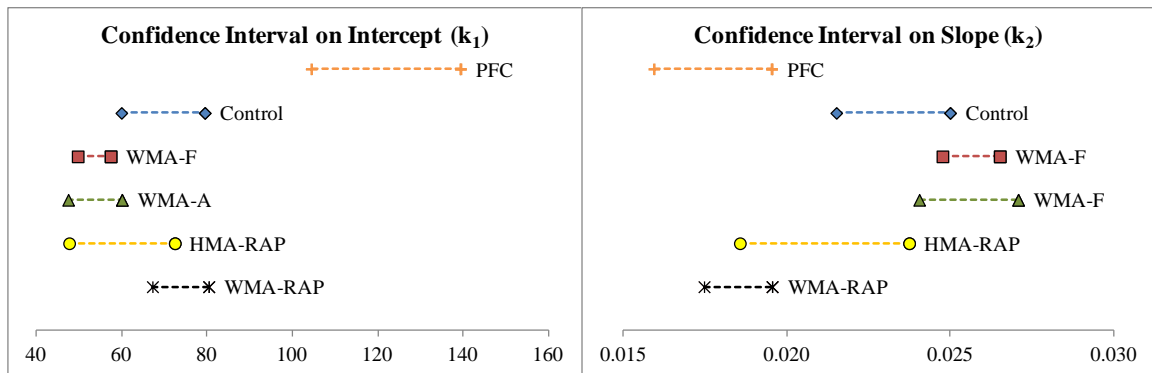


Figure 6-8 95% Confidence Intervals for Regression Coefficients – Longitudinal Strain.

The longitudinal strains were normalized to three reference temperatures following the same procedure used for AC modulus normalization. Additionally, because strains are also dependent on the thickness of the pavement layers, it was necessary to apply a correction to account for slight differences in as-built pavement thickness.

The correction factors were obtained based on theoretical relationships between layer thickness and longitudinal strain from layer elastic analysis. Each section was modeled using the software WESLEA for Windows, a computer application that uses linear elastic theory to calculate pavement responses due to specific loads. The layer moduli were estimated from FWD testing and the thicknesses were varied in half-inch increments from 5.5 to 8 inches for the AC layer and from 3 to 7.5 inches for the aggregate base layer. The structure was subjected to a 5,000 lb load and a tire pressure of 100 psi to simulate a single axle pass. The longitudinal strains were plotted against AC and aggregate base thickness and the data series were fitted using a power function as shown in Equation 6-4.

$$\varepsilon = aH^b$$

(6-4)

where:

ε = horizontal longitudinal microstrain

H = AC or aggregate base thickness, in

a, b = regression coefficients

The correction factor was found by dividing the right hand side of Equation 6-4 with reference thickness (H_{ref}) by the same term with measured thickness (H_{meas}).

$$CF = \frac{H_{ref}^b}{H_{meas}^b}$$

(6-5)

where:

H_{ref} = reference thickness (7 in for AC, 6 in for aggregate base)

H_{meas} = as-built thickness measured at the center of the gauge array, in

b = section-specific regression coefficient

Although differences during construction were subtle, this correction allowed for a more fair comparison of the test sections. Figure 6-9 illustrates the temperature-normalized and thickness-corrected longitudinal strains. The results from the statistical comparisons indicated that there were significant differences among some of the sections. For WMA virgin sections, the strains were lower than the control at low and intermediate temperatures, but similar at high temperatures. On the contrary, the strains of the PFC section were higher than the control at low and intermediate temperatures, and also similar at high temperatures. The high RAP sections exhibited lower strains than the control at all temperatures, as expected.

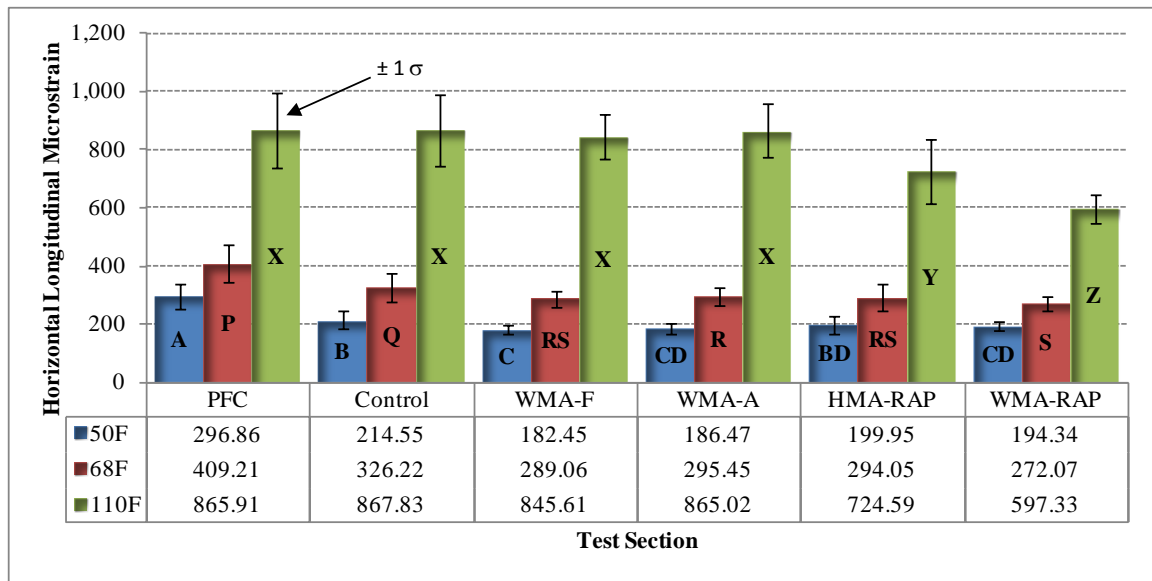


Figure 6-9 Temperature Normalized and Thickness Corrected Longitudinal Strains.

Figure 6-10 illustrates the temperature normalized and thickness corrected longitudinal strain over time at the intermediate reference temperature. It can be observed that the WMA and high RAP sections had lower variability over time than the control. The PFC section exhibited erratic results after the first year of operations, which could be indicative of damage. In the HMA-

RAP section, there were no longitudinal strains recorded after the first half of the analysis period, but enough measurements were obtained to capture a wide range of temperatures.

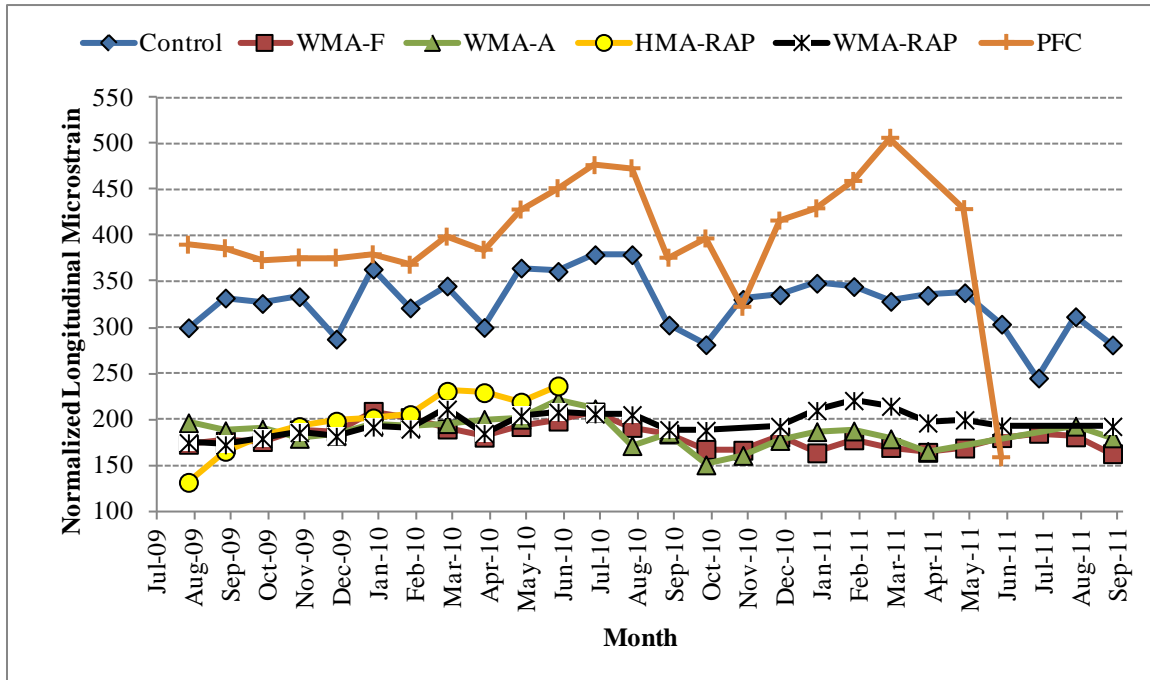


Figure 6-10 Average Monthly Thickness Corrected Longitudinal Strain Normalized at 68°F.

As with AC modulus, an analysis of variance was performed to determine the effect of material type and production temperature on longitudinal strain (excluding the PFC section). The results indicated that at the low reference temperature material type is not significant, at the intermediate temperature both factors are significant, and at the high temperature both factors and their interaction are significant. Figure 6-11 shows the change in longitudinal strain for both factors at all reference temperatures. It can be observed that WMA mixtures had strains approximately 10% lower than HMA mixtures. High RAP mixes had lower strains than virgin mixes, but the decrease in strain varied depending on pavement temperature, being only 1% lower at 50°F and up to 23% lower at 110°F.

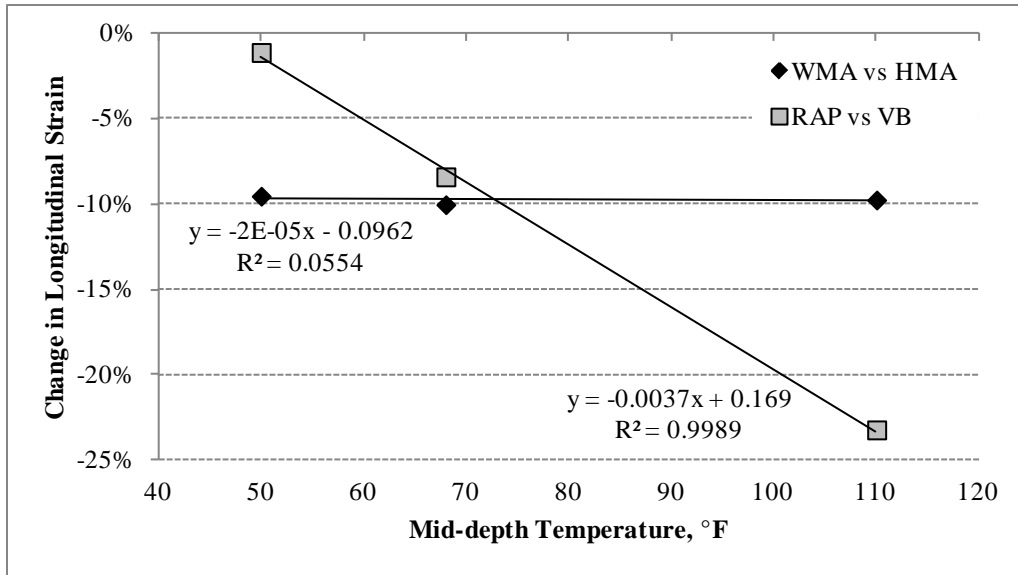


Figure 6-11 Variation in Longitudinal Strain Across Factors.

Pressure – Temperature Relationships

Permanent deformation can be related to the vertical pavement responses generated under moving wheel loads. Though traditional M-E transfer functions use vertical strain (*I05*), this response was not directly measured. Instead, vertical pressure measuring devices were used because of their robust nature and proven performance at the Test Track (*78, 100*). Pressures were measured at the top of the granular base and at the top of the subgrade for all sections.

Vertical pressures are also dependent on mid-depth pavement temperature, and follow a similar relationship to the one observed for horizontal strain, as shown in Figures 6-12 and 6-13.

The relationship between the variables was modeled by:

$$\sigma = k_1 e^{k_2 T}$$

(6-6)

where:

σ = vertical base or subgrade pressure, psi

T = Mid-depth AC temperature, °F

k_1, k_2 = Section-specific regression coefficients

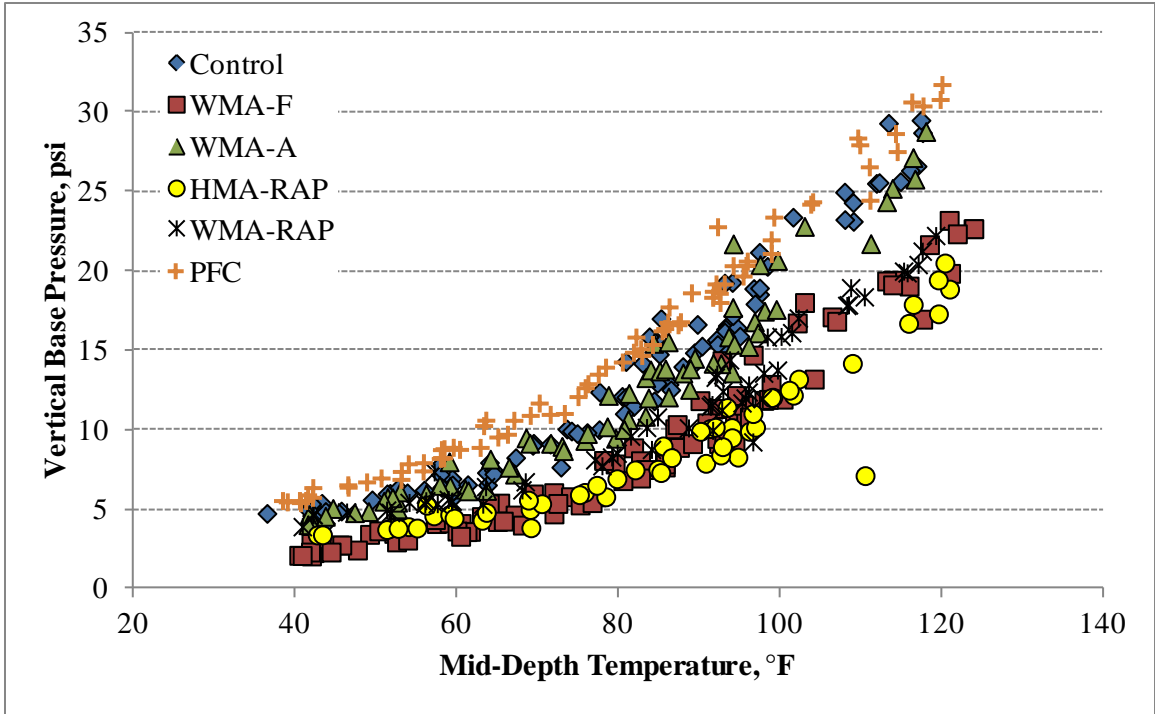


Figure 6-12 Relationship Between Vertical Base Pressure and Mid-depth Temperature – Single Axles.

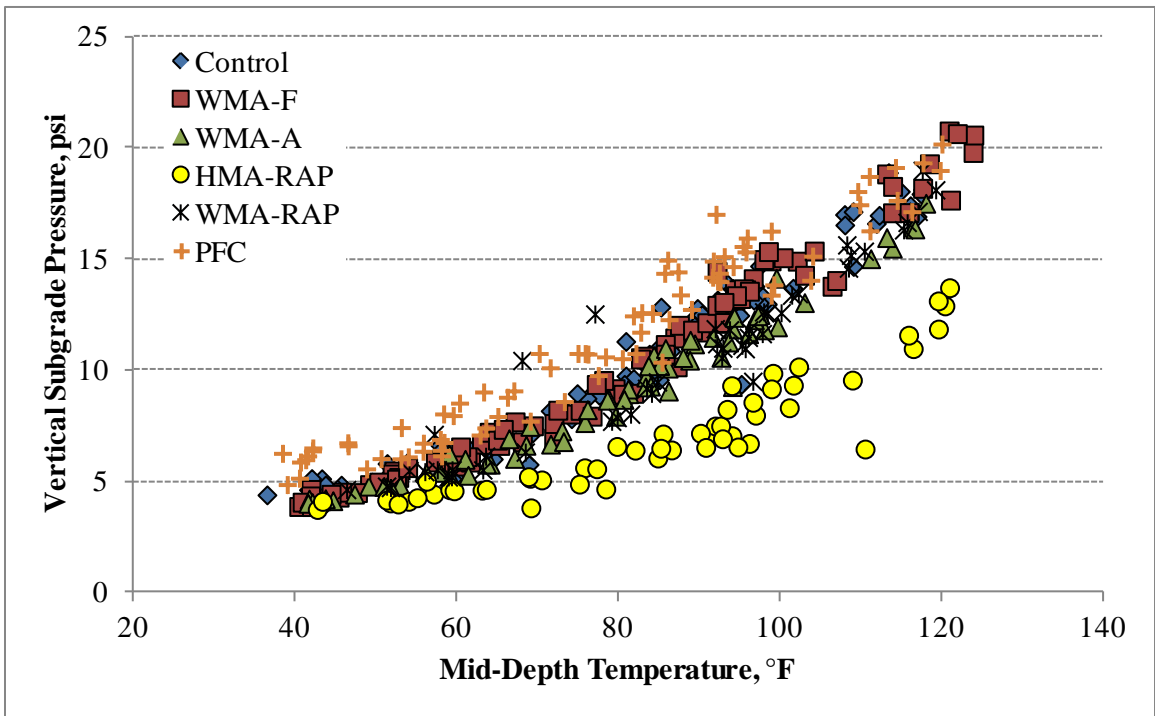


Figure 6-13 Relationship Between Vertical Subgrade Pressure and Mid-depth Temperature – Single Axles.

The results from the regression analysis are shown in Table 6-3. Most sections exhibited very good correlation, with R^2 values exceeding 0.90. The HMA-RAP section had a relatively lower R^2 value, due to higher variability in the data. 95% confidence intervals were obtained for the intercepts (k_1) and slopes (k_2) to identify differences in the stress-temperature relationship of the mixes and are shown in Figures 6-14 and 6-15. For base pressures, the control and WMA-A sections had intercepts and slopes statistically similar at 95% confidence level. Section WMA-F had a statistically lower intercept and a higher slope than the control, meaning that its vertical base pressures were lower at all temperatures. The high RAP sections also showed significant differences, with the HMA-RAP section having a lower intercept (lower pressures across all temperatures) and the WMA-RAP section having a lower slope (more sensitive to temperature changes) than the control. The PFC section had a higher intercept and lower slope than the control, which indicates higher pressures, especially at lower pavement temperatures.

For subgrade pressures, most sections had statistically similar intercepts and slopes to the control. The HMA-RAP section had a lower slope than the control, making it less susceptible to temperature changes, which was expected because the same trend was observed in the AC moduli results. The PFC section exhibited the same results observed for base pressure, with higher intercept and lower slope than the control.

Table 6-3 Regression analysis for vertical pressure as a function of mid-depth temperature

Section	Base			Subgrade		
	k_1	k_2	R^2	k_1	k_2	R^2
Control	1.595	0.025	0.96	1.935	0.020	0.96
WMA-F	0.711	0.029	0.97	1.826	0.020	0.98
WMA-A	1.475	0.025	0.97	1.725	0.020	0.98
HMA-RAP	1.145	0.023	0.92	1.753	0.016	0.89
WMA-RAP	1.611	0.022	0.96	1.903	0.019	0.93
PFC	2.241	0.023	0.99	2.801	0.017	0.93

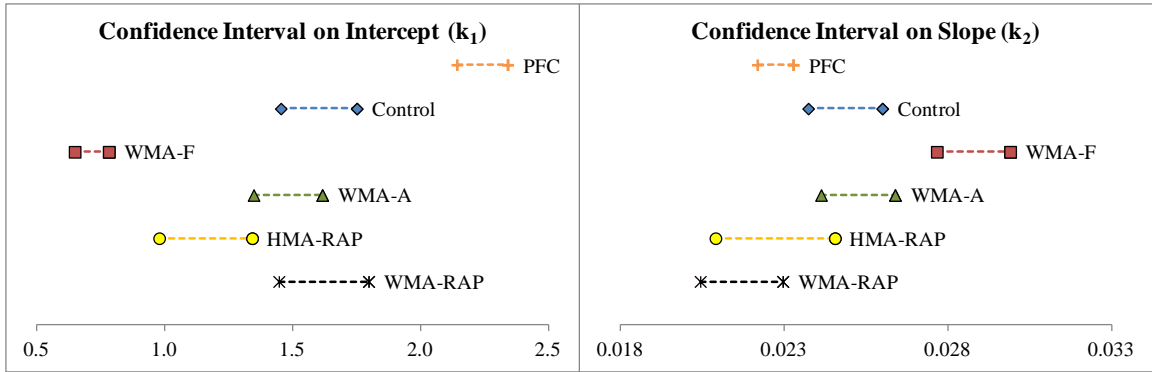


Figure 6-14 95% Confidence Intervals for Regression Coefficients – Base Pressure.

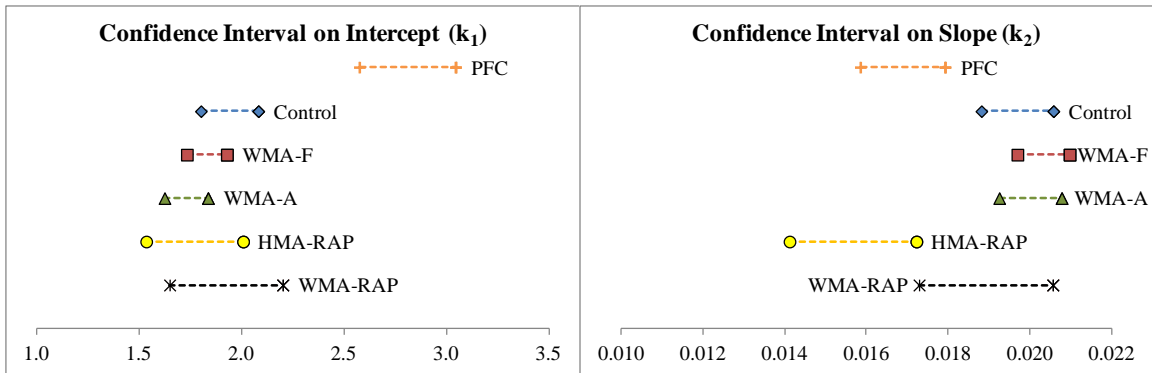


Figure 6-15 95% Confidence Intervals for Regression Coefficients – Subgrade Pressure.

The vertical pressures were normalized to three reference temperatures and corrected for pavement thickness following the same procedure used for longitudinal strains. Figures 6-16 and 6-17 illustrate the temperature-normalized and thickness-corrected pressures on top of the aggregate base and subgrade, respectively. The results from the statistical comparisons indicated that in general, the differences among sections were significant. For base pressure, the control section and WMA-A were similar at the high reference temperature. It was observed that the base pressures for section WMA-F were very low and even were below the subgrade pressures for that section. Normally, and theoretically, pressures at the asphalt concrete/aggregate base interface should exceed those at the aggregate base/subgrade interface. This suggests that there may have

been a problem with the instrumentation in that particular section and its base pressures were disregarded for the remainder of the analysis.

The subgrade pressures were also statistically different for most sections. Only the control and WMA-F sections were similar at the low reference temperature. However, the difference between the control and WMA sections did not exceed 10% at any of the reference temperatures. As expected, the HMA high RAP section, which had the highest AC modulus, consistently exhibited the lower pressures.

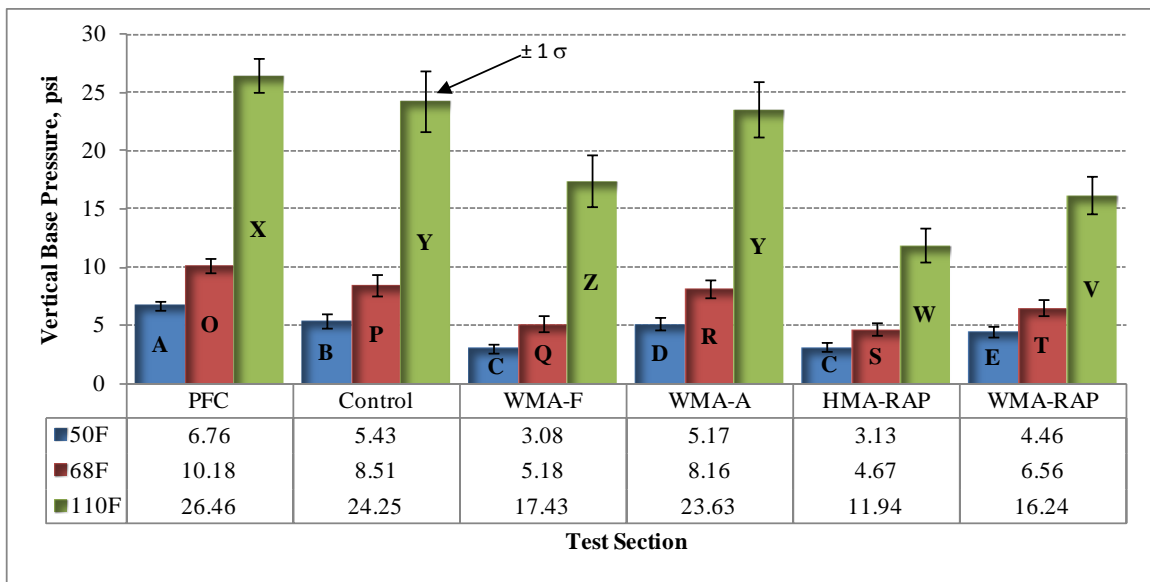


Figure 6-16 Temperature Normalized and Thickness Corrected Base Pressures.

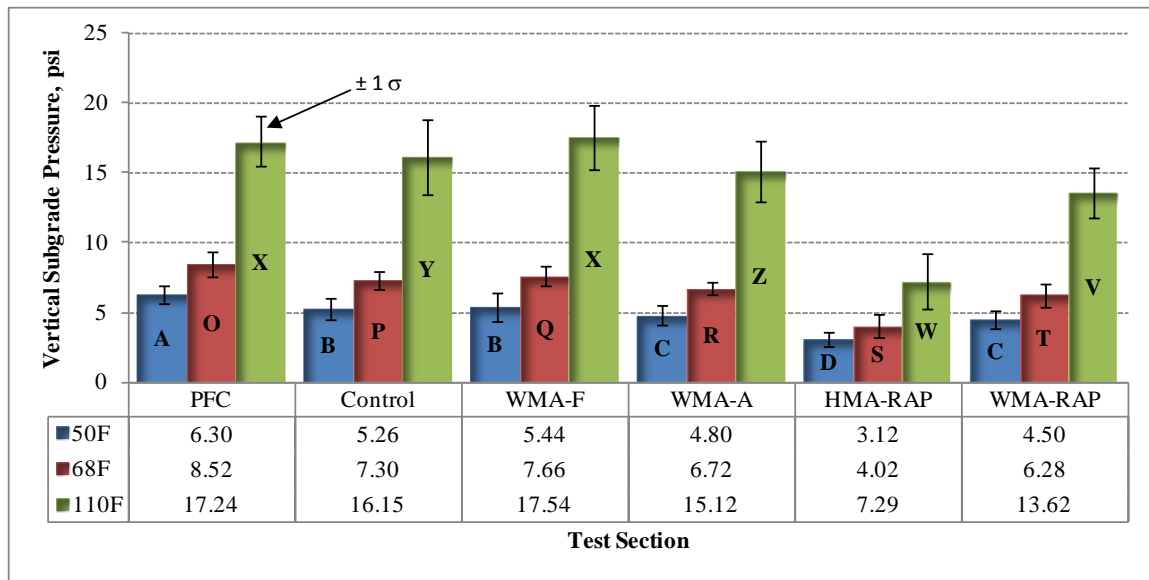


Figure 6-17 Temperature Normalized and Thickness Corrected Subgrade Pressures.

Figure 6-18 shows the results from the analysis of variance performed to determine the effect of material type and production temperature on vertical subgrade pressure. It was found that at all reference temperatures both factors and their interaction are significant. It can be observed that WMA mixtures had higher pressures than HMA mixtures, while high RAP mixes had lower pressures than virgin mixes. In both cases, the change in subgrade pressure increased with pavement temperature at similar rates, but the magnitude of the change was always higher when varying material type (27 to 36%) than when altering the production temperature (13 to 22%).

For vertical subgrade pressure, the change due to the use of WMA technologies did not remain constant with temperature, as it was observed for AC modulus and longitudinal strain. The magnitude of the pressure measurements is very low compared to modulus or microstrain, so the results are more sensitive to statistical significance. In addition, the differences observed between the HMA-RAP and WMA sections (virgin and high RAP) contributed to the presence of increased changes in pressure with temperature. When considering only the production temperature factor, it was found that the stiffer HMA-RAP section was less sensitive to pavement

temperature and provided better vertical stress distribution than the WMA sections. Nonetheless, the rate of change in pressure with mid-depth pavement temperature was low (0.15% per degree) and only increased 9% over the entire range of temperatures when WMA technologies were used.

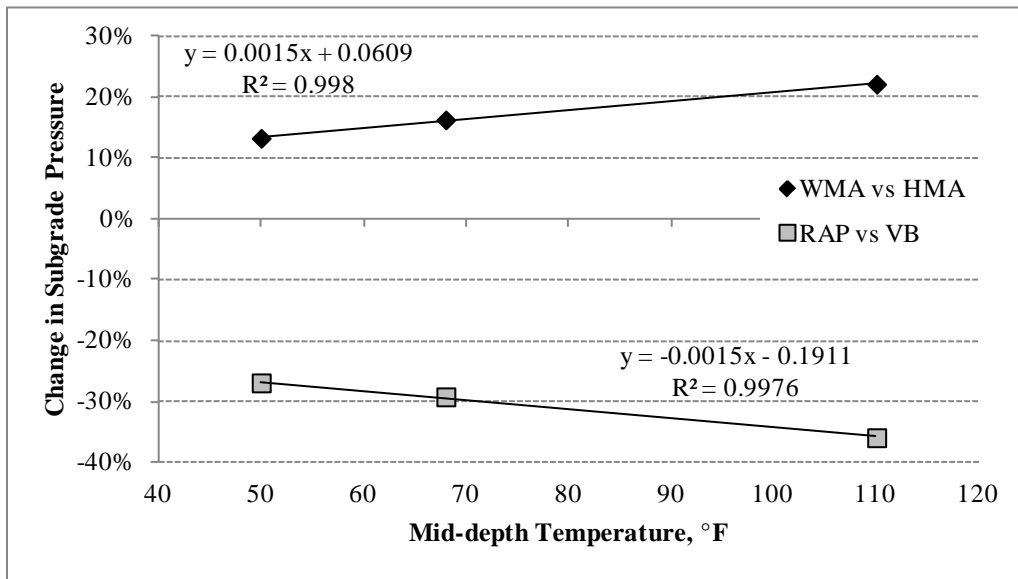


Figure 6-18 Variation in Vertical Subgrade Pressure Across Factors.

Significance of Differences

AC moduli and pavement responses were obtained at three reference temperatures and statistical comparisons were performed in the previous sections to determine if the use of sustainable technologies resulted in significant differences from the control section. However, it should be noted that although in some cases there were differences that were statistically significant, the magnitude of the change may not be of practical significance. Table 6-4 summarizes the differences observed in AC modulus, longitudinal strain and subgrade pressure for all sustainable sections compared to the control.

Table 6-4 Summary of differences in sustainable sections vs control

Sustainable section vs. Control	Reference Temperature		
	50°F	68°F	110°F
Change in AC Modulus			
WMA-F	-10%	-7%	2% *
WMA-A	-10%	-10%	-9% *
HMA-RAP	14% *	22%	43%
WMA-RAP	10%	16%	35%
PFC	-32%	-26%	-6% *
Change in Longitudinal Strain			
WMA-F	-15% *	-11%	-3%
WMA-A	-13%	-9%	0%
HMA-RAP	-7%	-10%	-17%
WMA-RAP	-9%	-17%	-31%
PFC	38%	25%	0%
Change in Subgrade Pressure			
WMA-F	3%	5%	9% *
WMA-A	-9%	-8%	-6%
HMA-RAP	-41%	-45%	-55%
WMA-RAP	-14%	-14%	-16%
PFC	20%	17%	7%

*Difference not statistically significant

To determine the practical significance of the differences, pavement responses were simulated using the software WESLEA. Simulations were performed for the design control section using the layer moduli obtained previously at each reference temperature. The control section was then modified to obtain the responses corresponding to two additional scenarios: a reduction in AC modulus of 10%, and a reduction in AC thickness of one-half inch (7 to 6.5 inches), which would represent the minimum variation that would be made in the AC layer.

It was found that at each reference temperature, reducing the AC modulus by 10% produced differences in strain and pressure that were lower than those obtained from reducing the AC thickness by one-half inch, as shown in Figures 6-19 and 6-20. Therefore, it was determined that a maximum difference of 10% in AC modulus can be considered not significant from a practical stand point. By the same principle, a reduction in thickness of one-half inch would increase the longitudinal strain and subgrade pressure by at least 10%, with the exception of

subgrade pressure at the high temperature. In general, it is reasonable to assume that a change in pavement response (strain or stress) of 10% or less does not present practical significance. It should be noted that these benchmark limits were established based on a control section with an asphalt layer thickness of 7 inches. In thinner pavements, a reduction of one-half inch AC would produce higher percentages of change in pavement responses, while in thicker pavements the change in responses would be lower. The limits set up in this assessment are meant to compare the test sections included in this study.

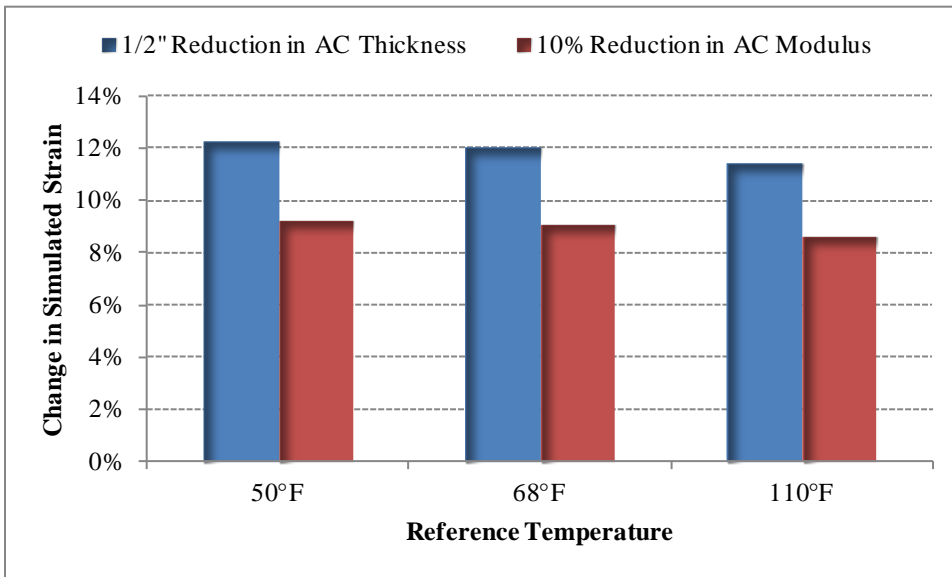


Figure 6-19 Change in Simulated Longitudinal Strain.

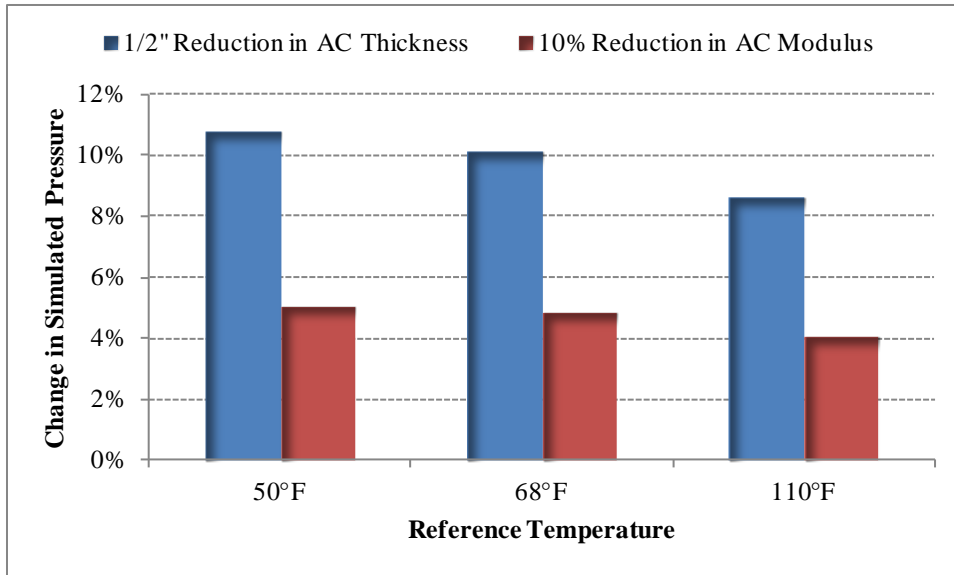


Figure 6-20 Change in Simulated Subgrade Pressure.

Figures 6-21 through 6-23 show the differences in AC modulus and pavement responses between the control and sustainable sections. It can be observed that the moduli of the virgin WMA sections can be considered similar to the control at all temperatures. High RAP sections tended to be stiffer than the control, especially as the pavement temperature increased, while the PFC section had lower modulus, but the difference was not significant at high temperatures.

For longitudinal strains, in general, virgin WMA sections are not significantly different from the control, with slightly higher differences at the low reference temperature. High RAP sections experienced lower strains that became more significant as temperature increased, while the PFC had higher strain than the control at low and intermediate temperatures but was similar at high temperatures. These results were consistent with the findings for AC modulus.

Finally, the vertical subgrade pressures of the virgin WMA sections were also similar to the control, and the vertical pressures of the high RAP sections were significantly lower, especially for the HMA-RAP section. The pressure in the PFC section was higher than the control, but was not significant at the high reference temperature. Once again, these results reflect the trends observed for the AC modulus and the relative stiffness of the sections.

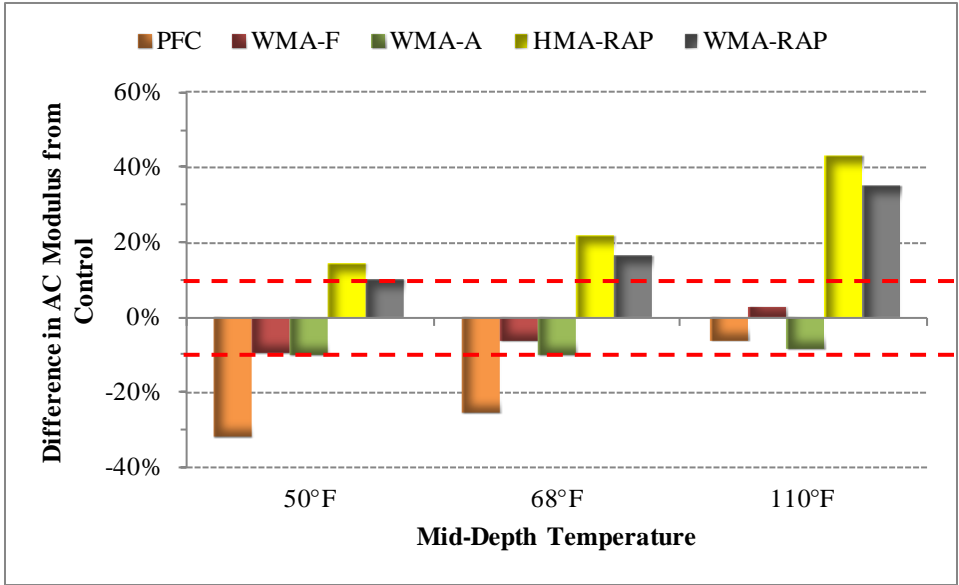


Figure 6-21 Difference in AC Modulus of Sustainable Sections Compared to the Control.

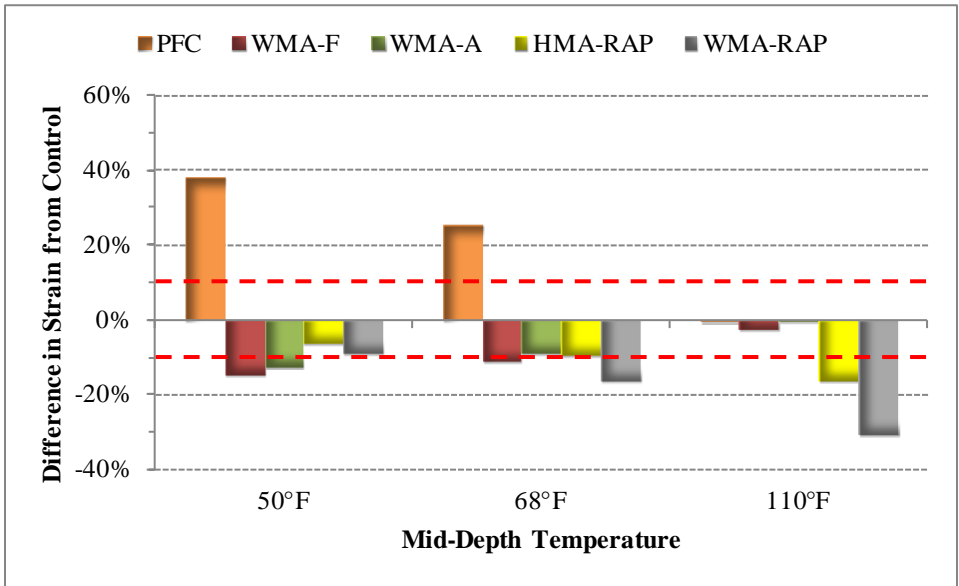


Figure 6-22 Difference in Longitudinal Strain of Sustainable Sections Compared to the Control.

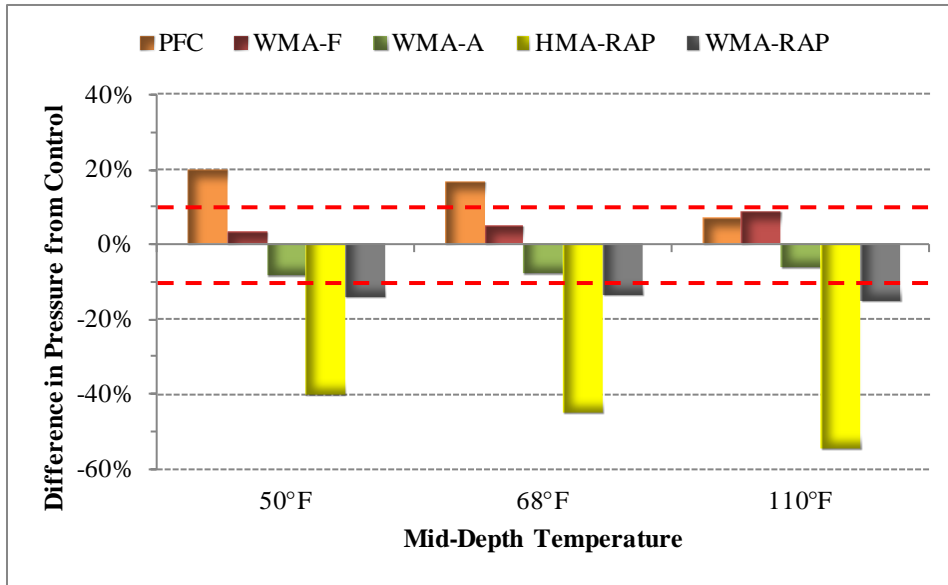


Figure 6-23 Difference in Subgrade Pressure of Sustainable Sections Compared to the Control.

SUMMARY

This chapter analyzed field measured responses of the test sections (strain and pressure) and related them to material properties (AC moduli). It was found that in general, virgin WMA sections had similar AC moduli as the control and the magnitude of their responses under traffic load was not affected significantly by the use of WMA technologies. High RAP sections were stiffer (had higher AC moduli) than the control, resulting in lower strains and pressures, especially at high temperatures. Finally, the PFC section was softer (had lower AC modulus) than the control at low and intermediate temperatures, and its responses were higher. However, at the high reference temperature no significant difference was observed between the PFC and control sections for moduli or responses.

When evaluating the influence of material type and production temperature, both factors were found to be significant, as well as their interaction. However, AC modulus and pavements responses were more affected by the use of high RAP contents than by changes in production temperature. In most cases, the change in modulus and responses due to the use of WMA

technologies remained constant at all pavement reference temperatures, but increased with pavement temperature for changes due to use of high RAP contents.

CHAPTER 7

OBSERVED FIELD PERFORMANCE

Test sections were monitored weekly to track field performance over time. Every Monday, trucking operations were suspended so that a number of tests could be conducted on the surface conditions of the pavement. This chapter summarizes the results for rutting, cracking, macrotexture and roughness.

RUTTING

The rutting progression of the test sections measured by the ALDOT method are shown in Figure 7-1. The smooth lines represent 3-date moving averages. It can be observed that early rutting accumulated rapidly and was similar for all the sections. As more ESALs were applied, the differences in performance became more accentuated. A Tukey's post ANOVA test was conducted for each test date to determine if there were statistical differences among the sections. It was found that the differences between the control and sustainable sections did not become significant until approximately 3.3 million ESALs had been applied, in May 2010.

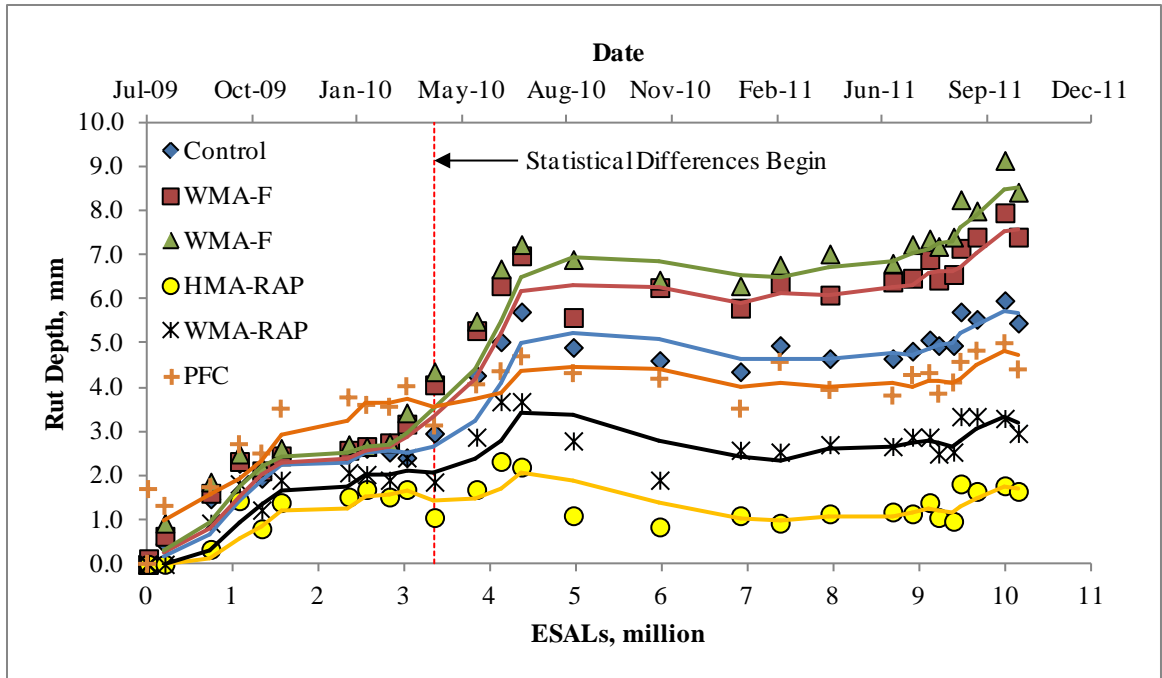


Figure 7-1 Rutting Progression of Test Sections.

The measurements corresponding to the last test date of the research cycle are represented in Figure 7-2. Tukey comparisons at 95% confidence level indicated that the virgin WMA sections had similar or higher rut depths than the control. Conversely, the two high RAP sections had the least rutting and were significantly lower than the control. The PFC section was not found to be statistically different from the control. Overall, the results were as expected because the WMA-F section exhibited higher pressures than the control while the high RAP mixes had lower pressures. Although section WMA-A had lower pressures than the control, it had relatively higher permanent deformation. This could be due to accumulated damage in the AC layer that has not yet manifested as cracking. Further monitoring and forensic analysis will be required to determine the cause. However, it is important to note that all sections performed very well, with rut depths under the 12.5 mm threshold.

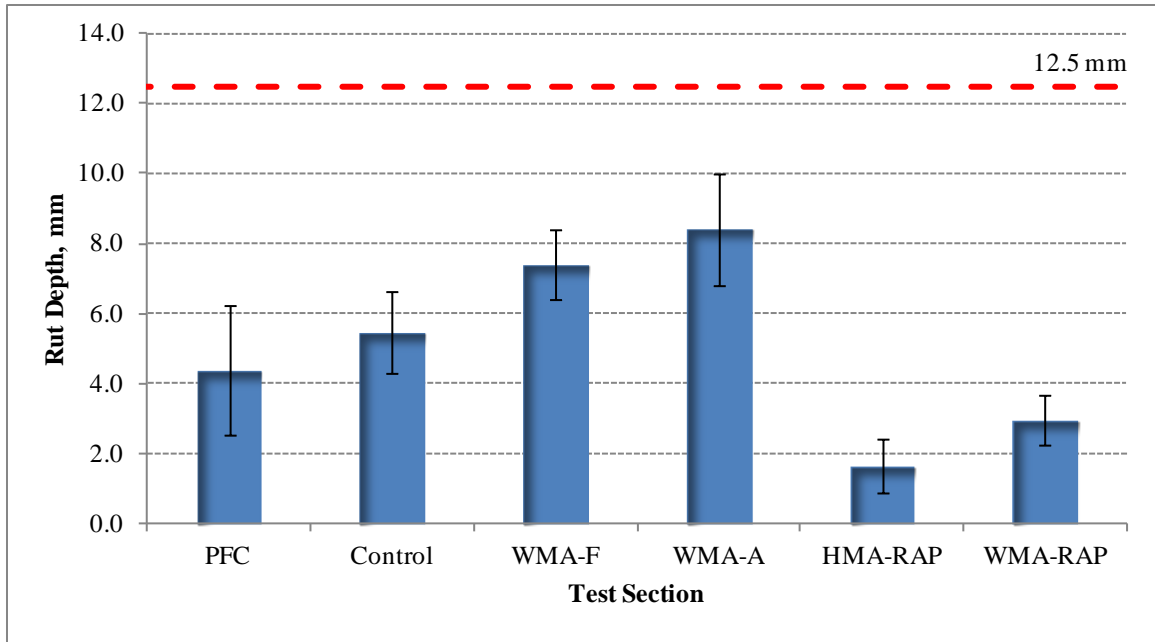


Figure 7-2 Final Rut Depths.

Table 7-1 shows the test sections ranked by rutting resistance according to each metric used in this study. It was observed that the rankings varied depending on the type of test performed. For laboratory tests, the general trend was that the control mix was among the most rutting resistant and high RAP mixes were among the most susceptible to permanent deformation. On the other hand, field measurements showed that the high RAP mixes were actually the most rutting resistant. Increased susceptibility of virgin WMA mixes compared to the control was shown in all laboratory tests as well as field measurements. The best match between field and laboratory rankings was observed for the Hamburg wheel tracking device method.

Table 7-1 Rutting resistance ranked by test method

Section	Rank			
	APA	Fn	Hamburg	Field
Control	2	1	3	4
WMA-F	4	3	4	5
WMA-A	3	5	5	6
HMA-RAP	5	2	1	1
WMA-RAP	6	4	2	2
PFC	1	NA	NA	3

Figure 7-3 plots the rutting parameter ($G^*/\sin\delta$) at 82°C versus the field measured rut depths on the last date of testing. It was observed that, as expected, binder stiffness was highly correlated to rutting potential. These results confirm the expected trend of mixes with stiffer binders having better rutting resistance. However, this experiment was designed so that pavement sections would have mixtures with similar virgin aggregates, gradations and volumetric properties. Variations in these factors may also affect rutting susceptibility without being identified in binder tests.

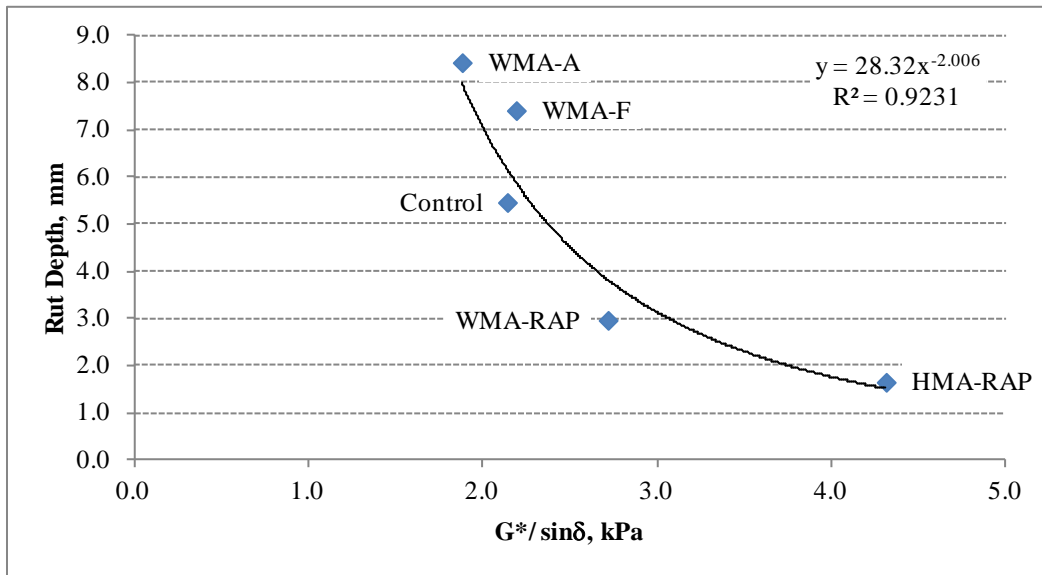


Figure 7-3 Effect of Binder Stiffness on Rutting Potential.

The measured rut depths from the last test date were plotted versus the base and subgrade pressures at 110°F, as shown in Figure 7-4. The trends are as expected, with greater pressures resulting in higher rut depths. Similar trends were observed at 50 and 68°F. Although only a few data points were included, the equations shown in Figure 7-4 provide a basis for a stress-based transfer function (i.e., correlation between pavement response and performance). Additional testing of full-scale sections using different materials and design parameters is required to develop a reliable transfer function.

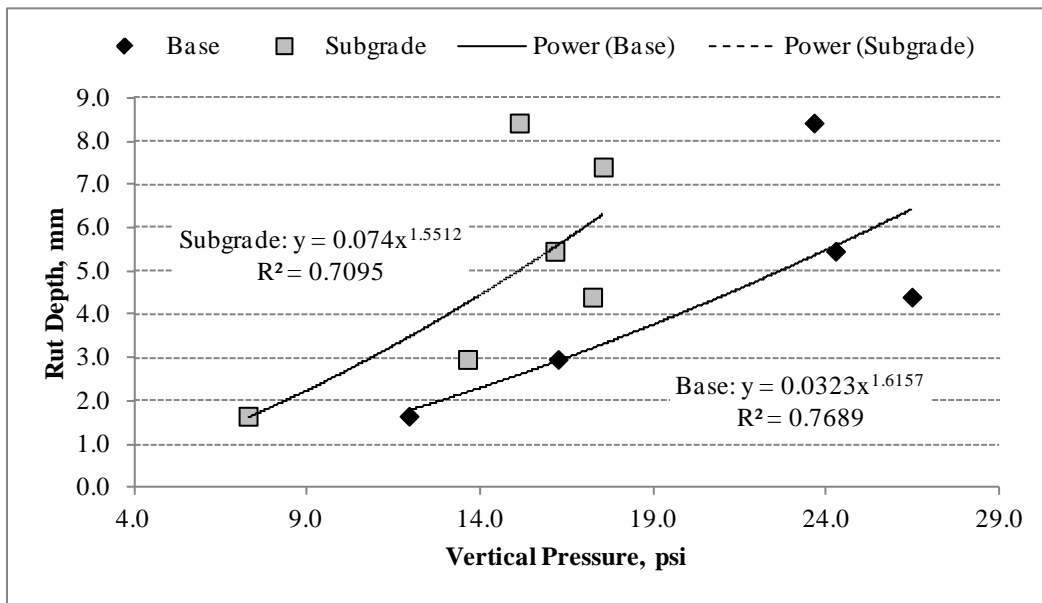


Figure 7-4 Relationship between Last Measured Rut Depth and Vertical Pressures at 110°F.

An analysis of variance was performed to determine the effect of two factors (material type and production temperature) on rut depth. Each factor had two levels; for material type the levels were virgin blends (VB) and high RAP mixtures (RAP), and for production temperature the levels were hot (HMA) and warm (WMA). The PFC section was excluded from this analysis because it did not contain information at all factor levels. The results indicated that both factors are highly significant, but not their interaction. In other words, the differences in rutting among

the levels of material type are independent from the levels of production temperature and vice versa. Figures 7-5 and 7-6 show the main effects plot and the interaction plot for the final rut depths, respectively.

Figure 7-5 shows that varying the material type produced a bigger change in rut depth than varying the production temperature. The points in the plot are the means of the rut depths at the various levels of each factor. The dashed lines correspond to the grand mean (the mean of all observations across factor levels). As expected, mixtures with high RAP content and mixtures produced at higher temperatures were more resistant to permanent deformation. The interaction plot presented in Figure 7-6 shows how the use of high RAP contents produced a reduction in rut depths of approximately the same magnitude for warm and hot mixes. Conversely, the use of WMA technologies increased the rut depths by approximately the same amount, regardless of whether the mixtures contained high RAP or not.

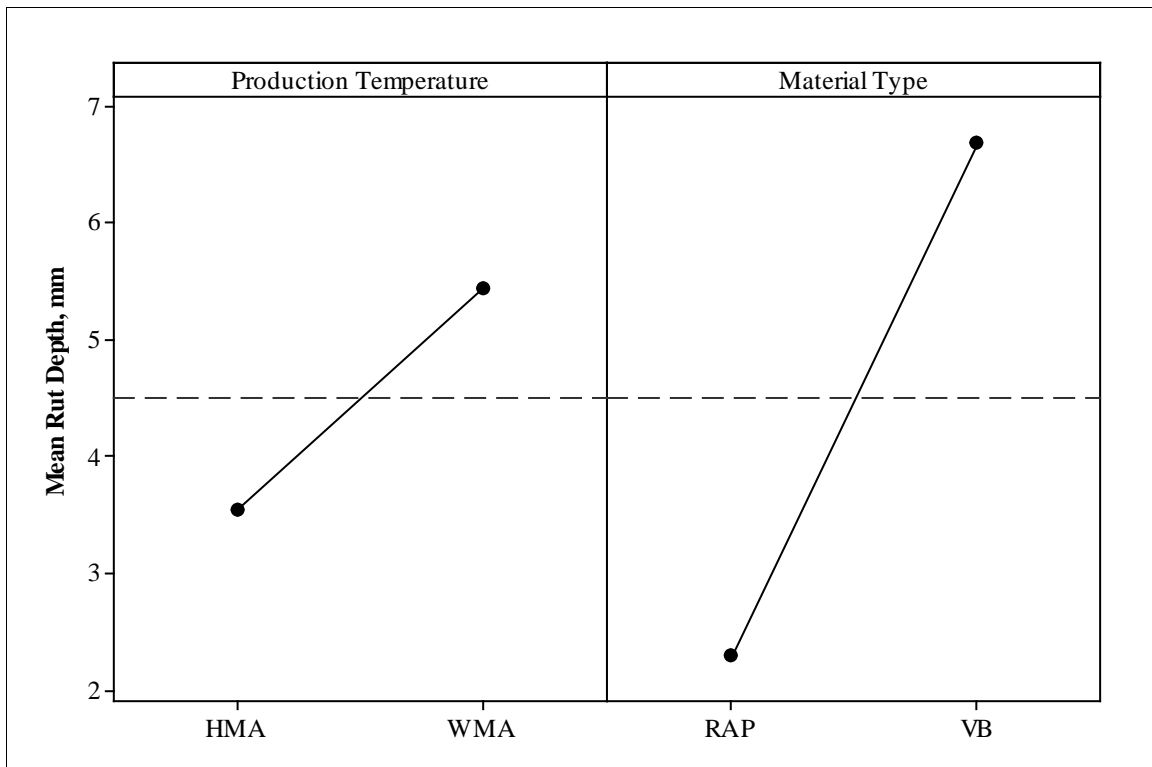


Figure 7-5 Main Effects Plot for Rut Depth.

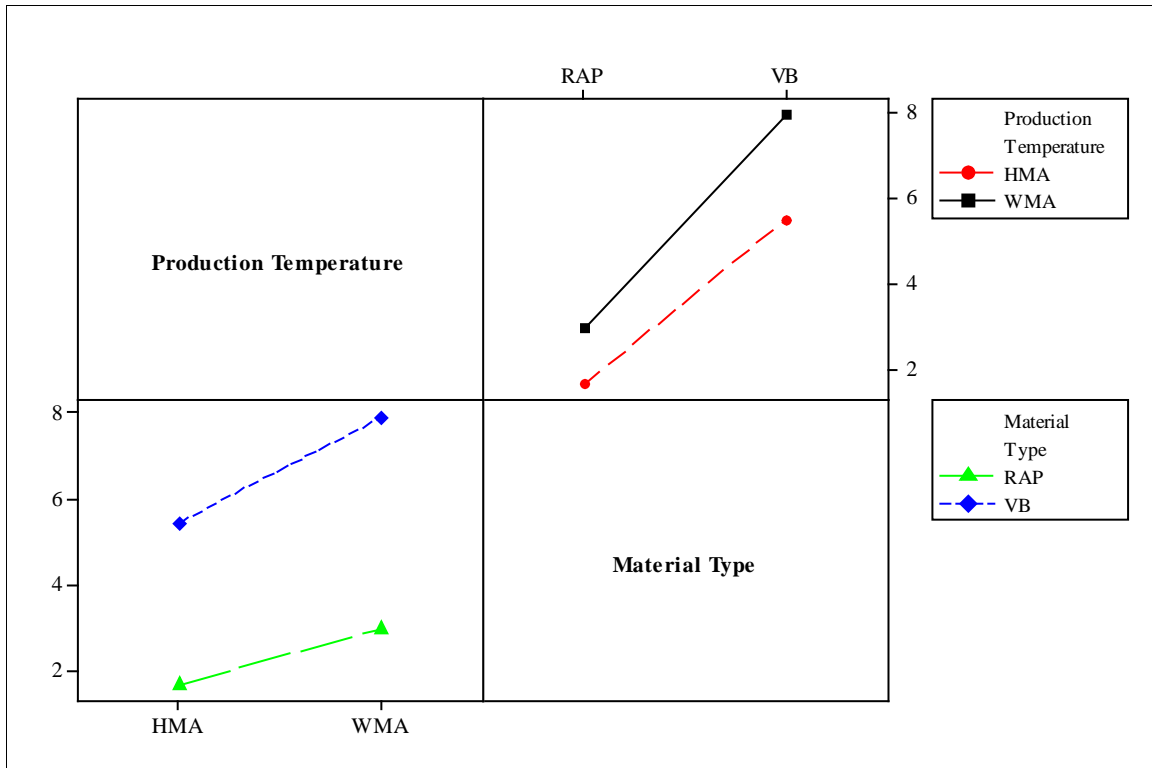


Figure 7-6 Interaction Plot for Rut Depth.

CRACKING

At the conclusion of the research cycle, no cracking had been observed in any of the test sections. Not having a measure of cracking does not allow for a direct field comparison of sustainable sections against the control. However, the susceptibility to fatigue damage can still be assessed using other data from laboratory and field observations. The transfer functions developed in Chapter 5 were used to estimate field performance based on the estimated strains at 68°F:

$$N_f = K_1 \left(\frac{1}{\varepsilon_{68}} \right)^{K_2}$$

(7.1)

Where:

N_f = Number of load cycles to failure

ε_{68} = estimated field strain at 68°F

K_1, K_2 = section-specific regression constants

Table 7-2 provides the variables for each fatigue transfer function (from Chapter 5), the field strain at 68°F (from Chapter 6) and the estimated cycles until failure at the field strain. It also contains the number of cycles until failure as a percentage of the control section. The results indicate that the WMA and high RAP sections are expected have better fatigue performance than the control at 68°F due to their lower strain level and corresponding fatigue transfer functions. It should be noted that the PFC section had the same base mixture as the control and only the field strain level was changed in the analysis. Therefore, based on the higher strain observed in the field, this section is expected to withstand approximately 36% of the load cycles from the control section. However, further monitoring of field performance is needed to support these findings.

Table 7-2 Predicted cycles to failure at 68°F

Section	K_1	K_2	ϵ_{68}	$N_f @ \epsilon_{68}$	N_f % of control
Control	1.18E+17	4.53	326	479,287	100
WMA-F	3.51E+17	4.71	289	880,300	184
WMA-A	1.50E+16	4.19	295	658,193	137
HMA-RAP	3.74E+20	6.02	294	519,085	108
WMA-RAP	2.65E+22	6.58	272	2,462,588	514
PFC	1.18E+17	4.53	409	171,591	36

MACROTEXTURE

Previous research at the NCAT Test Track suggests that surface macrotexture is related to pavement durability. The mean texture depth (MTD) increases as raveling occurs and aggregate particles are dislodged from the mat, leaving exposed surface voids in their place (106). Figure 7-7 shows the change in macrotexture over the duration of the research cycle. For dense graded sections, the change in macrotexture with traffic can be approximated by a linear equation. The regression coefficients from the linear regressions are shown in Table 7-3. It can be observed that the rate of change in MTD with traffic is similar for all sections. Hypothesis tests performed on the slopes confirmed that at 95% confidence level, there was no statistical difference between the sustainable sections and the control. In the PFC section, the MTD decreased over the first half of

the research cycle likely due to aggregate seating, and then remained constant at a value of approximately 1.2 mm.

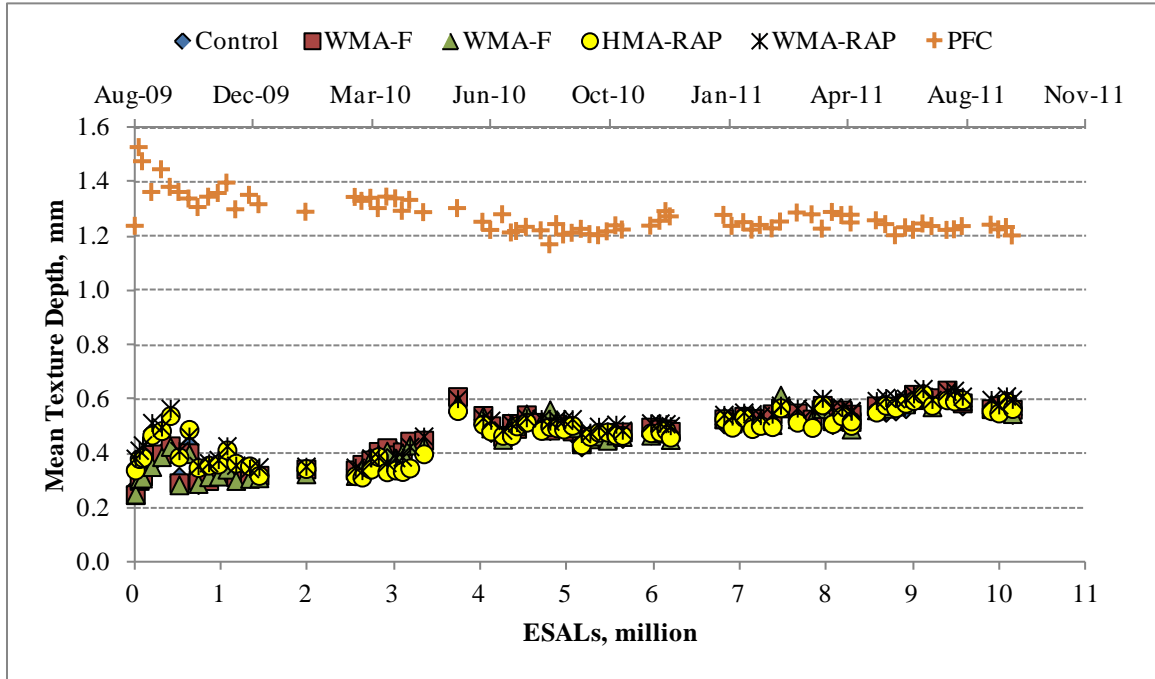


Figure 7-7 Change in Macrotexture over Time.

Table 7-3 Regression analysis for dense graded sections

Section	Intercept	Slope	R ²
Control	0.34	0.026	0.80
WMA-F	0.33	0.028	0.81
WMA-A	0.32	0.028	0.79
HMA-RAP	0.36	0.022	0.63
WMA-RAP	0.39	0.023	0.68

ROUGHNESS

In the MEPDG, the International Roughness Index (IRI) is used as a measure of the overall smoothness of the pavement and is dependent on various pavement distresses and design, site, and climatic parameters. Figure 7-8 shows the field measured IRI for all test sections over time and with traffic. Overall, the IRI remained constant over the analysis period, indicating that ride

quality was not significantly affected. The WMA-A section appeared to have the greatest rate of increase in IRI, which was expected because it exhibited the highest amount of rutting (the only surface distress observed in the test sections). The higher variability observed in the PFC section could be due to the open nature of the wearing course. All sections maintained IRI values well below the maximum threshold of 170 in/mile recommended by the FHWA (107).

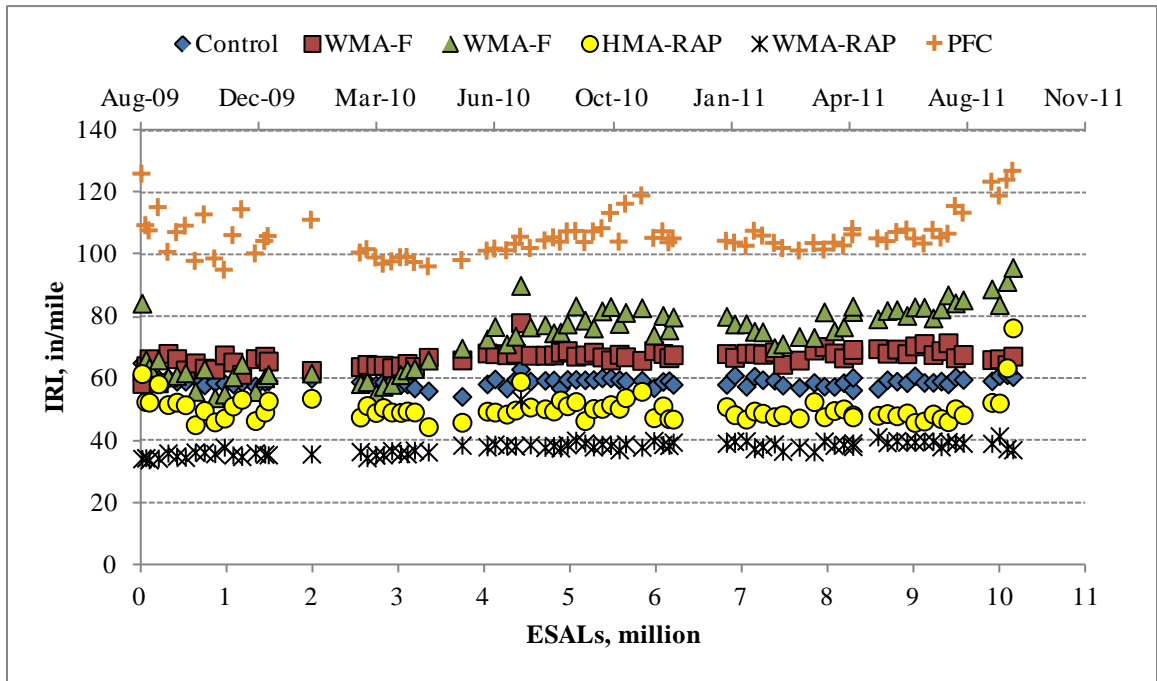


Figure 7-8 Change in IRI over Time.

SUMMARY

Upon completion of the research cycle, all sections had exhibited very good field performance. Although some differences were found between the control and sustainable sections, rut depths were under the recommended maximum of 12.5 mm after 10 million ESAL. Laboratory assessment of rutting performance using the APA and flow number tests correlated poorly with field results, while the Hamburg wheel tracking device and extracted binder tests appeared to be

more accurate. Rutting was influenced by both the production temperature of the mixtures and the material type; however, greater changes in rut depth occurred due to inclusion of high RAP than to the use of WMA technologies. Permanent deformation was also related to the vertical pressures at the top of the aggregate base and subgrade layers, suggesting that stress-based transfer functions could be developed, but more testing of full-scale sections is needed to develop a reliable equation.

Although no cracking was observed in any of the sections, laboratory test results and field strain measurements were used to estimate the fatigue performance of the sections. All sustainable sections are expected have better resistance to fatigue cracking than the control, but further monitoring of field performance is needed to support these findings.

Changes in surface macrotexture over time, which could be used as an indicator of raveling, were similar for all sections. In addition, the IRI of the test sections remained nearly constant over the analysis period and was below the maximum recommended value.

In general, the results obtained indicate that it is possible to build and operate sustainable pavement sections while maintaining performance standards similar or better than those of conventional asphalt pavement sections.

CHAPTER 8

STRUCTURAL CAPACITY OF PFCs

While PFC mixtures have been used for their safety and environmental benefits (previously discussed in Chapter 2), limited research has been performed to quantify their structural contribution to the pavement structure. In practice, state DOTs range from equating PFCs to dense graded mixtures to giving them no structural value (59). Properly characterizing the structural capacity of PFCs is important to ensure better pavement performance prediction and more effective designs.

FIELD MEASURED RESPONSES

To compare the structural behavior of PFC and dense graded mixtures, two test sections were constructed at the NCAT Test Track. These sections have been discussed in Chapter 3. The only difference between the two was that the control section had a dense graded surface lift, while the PFC section had a porous mix. Therefore, the differences observed in field measured responses and field performance can be attributed to the change in surface lift.

This analysis was conducted at a reference temperature of 68°F (20°C), the same temperature used to perform flexural beam fatigue testing. While at low temperatures the main concern is thermal cracking, a non load-related distress; at high temperatures pavements are more sensitive to permanent deformation. Field measurements indicated that the PFC section did not perform significantly different from the control in terms of rutting. Therefore, the analysis focused on the fatigue behavior of the PFC mixture.

Figure 8-1 shows the difference in AC modulus and longitudinal strain between the control and PFC sections at a reference temperature of 68°F. It can be observed that using a PFC mixture in the surface lift instead of a dense graded mix caused a reduction in backcalculated AC modulus of 26%. Consequently, this reduction in AC modulus resulted in an increase in the measured horizontal longitudinal strain of 25%. In both cases, the differences were statistically significant at a significance level of $\alpha=0.05$.

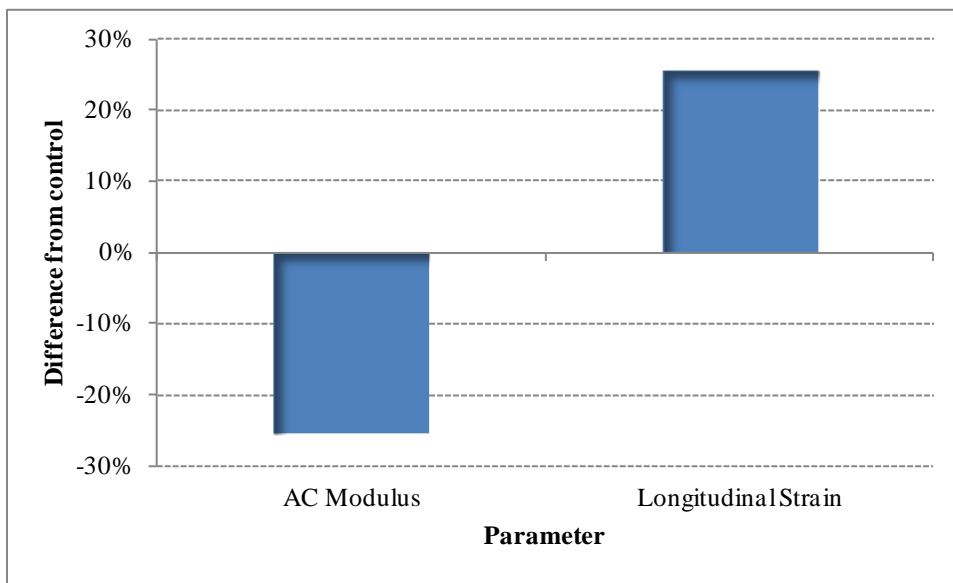


Figure 8-1 Difference in Measured Parameters at 68°F.

ESTIMATING THE IN-PLACE MODULUS OF PFCs

The measured reduction in AC modulus corresponds to the entire AC layer. To quantify the in-place modulus of the PFC mixture, the moduli of the individual lifts and their effect on the overall AC modulus of the sections was evaluated using Odemark's method, also known as the method of equivalent thicknesses. The principle of this method is to transform a system consisting of layers with different moduli into an equivalent system where all layers have the same modulus (108).

The effective modulus of the control section was calculated from dynamic modulus data at 68°F and 10 Hz to simulate highway speeds using equation 8-1:

$$E_{effective} = \left[\frac{C_2(C_1 h_1^3 \sqrt{E_1} + h_2^3 \sqrt{E_2} + h_3^3 \sqrt{E_3})}{h_1 + h_2 + h_3} \right]^3$$

(8-1)

where:

E_1, E_2, E_3 = dynamic modulus of surface, intermediate and base lifts, respectively (psi)

h_1, h_2, h_3 = thickness of the surface, intermediate and base lifts, respectively (in)

C_1, C_2 = correction factors

Since in the PFC section E_1 is unknown, the modulus of the PFC lift was obtained by giving $E_{effective}$ a value 26% lower than the effective modulus calculated for the control section, as measured in the field, and solving for E_1 . Table 8-1 shows the dynamic modulus data from laboratory testing and the calculated effective moduli.

Table 8-1 Dynamic and effective moduli data

Section	Measured Dynamic Modulus (psi)			$E_{effective}$ (psi)
	E_1	E_2	E_3	
Control	722,191	1,216,093	1,009,801	1,034,125
PFC	Unknown			770,422

To achieve a difference in effective modulus of 26% like the one obtained for the backcalculated AC moduli of the control and PFC sections, the modulus of the PFC lift would have to be approximately 35,000 psi, a value comparable to that used for aggregate base materials. A previous study (109) conducted at the Test Track based on deflection data and direct strain measurements estimated a structural coefficient for PFC of 0.15, which is consistent with this result.

To validate the results, a single axle pass was modeled in each of the sections using the software WESLEA. Each section consisted of three layers (asphalt concrete, granular base and subgrade), having the same thicknesses and moduli for both sections, with the exception of the AC layer. Table 8-2 shows the structural information used to model the longitudinal strains of both sections under a single axle pass. The results indicated that the simulated longitudinal strains in the PFC section were 27% higher than the control, 2% more than the difference obtained from direct measurements under live traffic loads. In general, the results are in good agreement with the field measurements and it would be appropriate to assign the PFC layer a modulus similar to a granular base. However, this value is based on limited data from two sections and further research is warranted to fully validate this finding.

Table 8-2 Software inputs – structural information

Inputs	Layer 1	Layer 2	Layer 3
Material Type	Asphalt Concrete	Granular Base	Subgrade
Layer Modulus, psi	Control: 1,034,125 PFC: 770, 422	2,032	26,672
Poisson's Ratio	0.35	0.40	0.45
Thickness, in	7.0	6.0	999

EFFECT OF THICKNESS RATIO ON MODULUS REDUCTION

The 26% reduction observed in the effective AC modulus corresponds to the particular pavement structures included in this study. However, the difference in moduli between sections with dense graded wearing surfaces and sections with PFCs depends on the ratio of the PFC lift thickness to the total AC layer thickness. As the ratio approaches zero (e.g., less PFC relative to the rest of the AC cross section), the effective modulus is less affected by the presence of the PFC material and the reduction in modulus is less significant.

To illustrate this, the effective modulus of a PFC section was calculated using dynamic modulus data for the dense graded lifts, the estimated PFC modulus obtained in the previous

section, and different combinations of layer thicknesses that resulted in a range of ratios of PFC thickness to total AC thickness (H_{PFC}/H_T). Since PFCs are used as surface layers, it is unlikely that their thickness would exceed one third of the total thickness, so only a range of 0 to 0.33 was used. The resulting effective moduli (E_{PFC}) were compared to the effective moduli of a control section ($E_{control}$) having the same structure as the PFC section (same layer thickness combination) but with a dense graded mixture in the surface lift. Figure 8-2 plots the reduction in AC modulus ($E_{PFC}/E_{control}$) for a range of thickness ratios. Although most data points were calculated using Odemark's method, they appear to follow the expected trend from measured values.

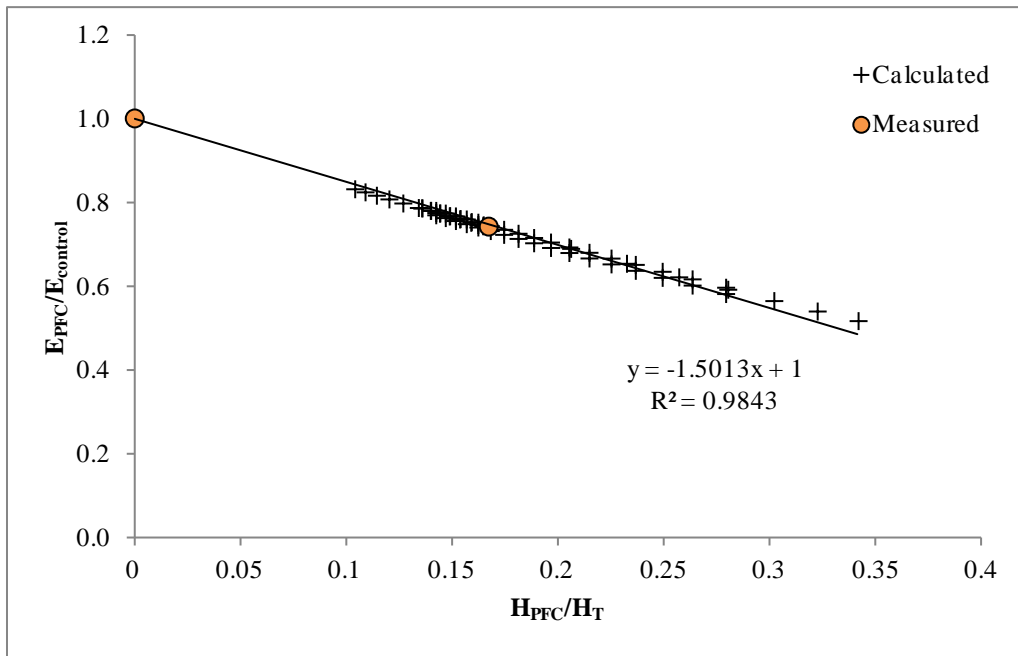


Figure 8-2 Effect of Thickness Ratio on Modulus Reduction.

EFFECT OF THICKNESS RATIO ON STRAIN

As the effective AC modulus changes with varying thickness ratios, the horizontal longitudinal strain at the bottom of the AC layer is also expected to change. The same pavement sections used to construct Figure 8-2 were entered into the software WESLEA to simulate a single axle pass and model the longitudinal strains for sections with dense graded and PFC surface lifts. Figure

8-3 shows the relationship between thickness ratio and the change in longitudinal strain. As expected, the strain of PFC sections relative to the control ($\epsilon_{PFC}/\epsilon_{control}$) increases with increasing thickness ratio.

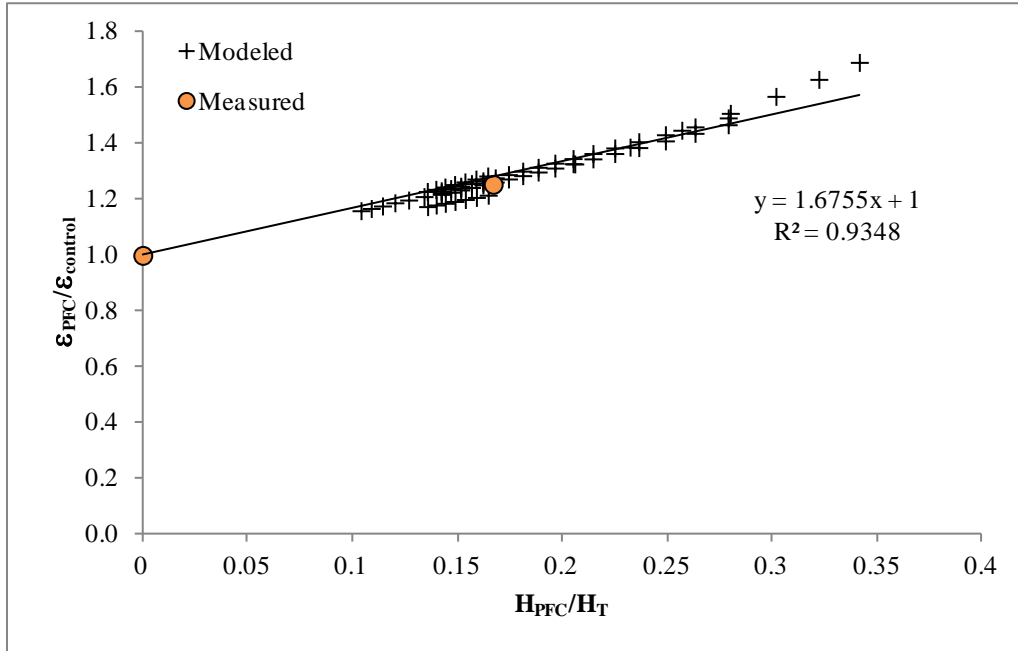


Figure 8-3 Effect of Thickness Ratio on Longitudinal Strain.

SUMMARY

For the sections included in this study, it appears that the structural capacity of PFC mixtures is significantly lower than that of a dense graded material, and their elastic moduli can be similar to the values used for aggregate base materials. However, the effect of the presence of a PFC surface lift in the overall modulus of the AC layer and consequently in the horizontal longitudinal strains at the bottom of the AC depends on the ratio between the PFC and total AC layer thicknesses. More research on full-scale sections is needed to support these conclusions. In addition, the test sections did not exhibit any surface cracking at the conclusion of the research cycle. Further monitoring is also needed to better evaluate the structural capacity of the PFC section compared to the control.

CHAPTER 9

CONCLUSIONS AND RECOMMENDATIONS

SUMMARY

The increasing use of sustainable pavement technologies and the transition of many state agencies from an empirical pavement design method to a mechanistic-empirical approach have prompted the need to evaluate the physical and structural characteristics of these sustainable pavements. By doing so, performance prediction can be improved, thus allowing for more efficient designs. In this study, five sustainable pavement test sections were included: two warm mix asphalt sections (one foam-based and one additive-based), two high RAP sections (one produced as a hot mix and one produced as a warm mix) and one section containing a porous friction course. All of these were compared to a control section of the same thickness consisting of dense-graded materials and produced as a hot mix.

This research included laboratory testing of plant-produced mixtures and field measurements of full-scale instrumented test sections at the NCAT Test Track. Laboratory tests were conducted to obtain physical characteristics of the recovered binders and mixtures and to evaluate the performance of the mixes under a controlled environment. Field data were used to characterize the seasonal behavior of the pavement layer moduli and to compare the pavement responses of the different sections under live traffic loads. Finally, field performance was monitored on a regular basis throughout the experiment.

CONCLUSIONS

Based on the results obtained in this research, the following conclusions can be made regarding the sustainable pavement technologies included in this dissertation:

- In the construction phase, the cooling rates during laydown and compaction of sustainable mixtures are similar to those of conventional mixtures and can be predicted using the same model. In addition, all sections were successful in achieving their respective in-place density requirements, suggesting that compactability should not be a concern when using sustainable pavement technologies.
- The dynamic modulus (E^*), a property central to the mechanistic-empirical design method, was found to be statistically similar for the control and virgin WMA mixtures. On the other hand, the dynamic modulus of high RAP mixes was significantly higher than the control due to the presence of aged RAP binder.
- Tests performed on the recovered binders of the mixtures also showed increased moduli for high RAP mixes and no significant effect on WMA mix moduli. The results also suggested that high RAP mixes may be more resistant to permanent deformation, but more susceptible to fatigue and thermal cracking than the control. WMA mixes may be more susceptible to rutting, have better resistance to fatigue cracking and perform similarly at low temperatures.
- Tests conducted on compacted samples showed the same trend for thermal cracking as the binder tests. However, some results from rutting and fatigue tests contradicted the findings from the binder tests, ranking the high RAP mixes higher in susceptibility to permanent deformation and cracking than the control. Moisture susceptibility was not a concern for any of the mixes.

- The AC modulus-temperature relationship was not affected by the use of WMA technologies in virgin mixes. The modulus of high RAP and PFC mixes was less sensitive to changes in pavement temperature.
- Virgin WMA sections had lower AC moduli than the control. Although the differences were statistically significant due to low variability in the sections, the magnitudes of the moduli of all sections produced with virgin aggregates were within 10%, which may not be considered to have a practical impact. High RAP mixes exhibited the highest AC moduli overall, while the PFC section had the lowest.
- The pavement responses (strain and stress) were not affected significantly by the use of WMA technologies. High RAP sections had lower responses than the control, especially at high temperatures, while the PFC section had higher responses at low and intermediate temperatures but was similar to the control at high temperatures.
- The factors of material type and production temperature and their interaction significantly affected the AC modulus, longitudinal strain and vertical stress of the sections. However, the use of high RAP had a greater impact than the reduction in production temperature.
- All sections had performed well at the conclusion of the research cycle. Although some differences were found between the control and sustainable sections, rut depths were under the recommended maximum of 12.5 mm after 10 million ESAL. No cracking was observed in any of the sections, and changes in surface macrotexture over time, an indicator of raveling, were similar for all sections. Finally, the IRI of the test sections remained nearly constant over the analysis period and was below the maximum recommended value. These results indicate that it is possible to build and operate sustainable pavement sections while maintaining performance standards similar or better than those of conventional asphalt pavement sections.

- Laboratory assessment of rutting performance using the APA and flow number tests correlated poorly with field results, while the Hamburg wheel tracking device and extracted binder tests appeared to be more accurate. Good correlation was found between field rut depths and the vertical pressures at the top of the aggregate base and subgrade layers.
- The structural capacity of PFC mixtures was found to be significantly lower than that of a dense graded material, and their elastic modulus was similar to the values used for aggregate base materials. However, the overall effect of PFC on pavement responses related to performance depends on the ratio between the PFC and total AC layer thicknesses.

RECOMMENDATIONS

It is recommended that additional traffic be applied to the sections already in place. Further monitoring, data collection and future forensic analysis are recommended to validate the findings from this research. To evaluate the fatigue potential of the sections and validate the results obtained so far in this investigation, it is important to continue to application of traffic until there is a measurable amount of distress.

Caution must be taken when evaluating the performance of sustainable mixes in the laboratory, as the results may differ from actual field performance. Binder testing on recovered samples appeared to be an accurate representation of field performance when other variables (gradation, volumetrics and pavement structure) are kept constant.

Limited data from the sustainable sections included in this study suggest that it may be possible to develop stress-based transfer functions. Inclusion of more sections containing different materials and pavement structures is warranted to develop a reliable function.

More research on full-scale sections is needed to support the conclusions regarding the structural capacity of PFCs. It is recommended that sections containing different ratios of PFC to total AC layer be included in future investigations.

REFERENCES

1. Chappat, M. *The Environmental Road of the Future: Life Cycle Analysis*. Colas Group, 2003.
2. Asphalt Paving Association of Iowa. *The Iowa Asphalt Report, The Green Issue*. 2008.
3. Cervarich, M. B. Six Asphalt Production Facts You Should Share. *Better Roads*, Vol. 74, 2004.
4. Hansen, K., and D. Newcomb. *RAP Usage Survey*. National Asphalt Pavement Association, Lanham, Maryland, August 2007.
5. Copeland, A. *Reclaimed Asphalt Pavement in Asphalt Mixtures: State of the Practice*. Report No. FHWA-HRT-11-021, Federal Highway Administration, McLean, Virginia, 2011.
6. Kandhal, P. S., and R. B. Mallick. *Open-Graded Asphalt Friction Course: State of the Practice*. NCAT Report 98-07, National Center for Asphalt Technology, Auburn University, 1998.
7. Mallick, R. B., P. S. Kandhal, L. A. Cooley and D. E. Watson. *Design, Construction and Performance of New-Generation Open-Graded Friction Courses*. NCAT Report 00-01, National Center for Asphalt Technology, Auburn University, 2000.
8. Priest, A. L. and D. H. Timm. *Methodology and Calibration of Fatigue Transfer Functions for Mechanistic-Empirical Flexible Pavement Design*. NCAT Report 06-03, National Center for Asphalt Technology, Auburn University, 2006.
9. Newcomb, D. *Mechanistic-Empirical Pavement Design – Where are we headed?* *HMAT Magazine*, September/October 2004, pp. 31-36.
10. Crawford, G. *National Update of MEPDG Activities*. Presented at the 88th Transportation Research Board Annual Meeting, Washington D. C., 2009.

11. Bonaquist, R. *Mix Design Practices for Warm Mix Asphalt*. NCHRP Report 691, Transportation Research Board of the National Academies, Washington D.C., 2010.
12. Anderson, R.M., G. Baumgardner, R. May and G. Reinke. *Engineering Properties, Emissions, and Field Performance of Warm Mix Asphalt Technologies*. NCHRP 9-47 Interim Report, Transportation Research Board of the National Academies, 2008.
13. D'Angelo, J., E. Harm, J. Bartoszek, G. Baumgardner, M. Corrigan, J. Cowser, T. Harman, M. Jamshidi, W. Jones, D. Newcomb, B. Prowell, R. Sines, and B. Yeaton. *Warm-Mix Asphalt: European Practice*. International Technology Scanning Program, Federal Highway Administration, December 2007.
14. Prowell, B. D. and G. C. Hurley. *Warm-Mix Asphalt: Best Practices*. National Asphalt Pavement Association, December 2007.
15. Mallick, R. B., J. Bergendhal and M. Pakula. *A Laboratory Study on CO2 Emission Reductions Through the Use of Warm Mix Asphalt*. Presented at the 88th Transportation Research Board Annual Meeting, Washington D. C., 2009.
16. Middleton, B. and R.W. Forfylow. *An Evaluation of Warm Mix Asphalt Produced with the Double Barrel Green Process*. Presented at the 7th International Conference on Managing Pavement Assets (ICMPA), Calgary, 2008.
17. Davidson, J.K. and R. Pedlow. *Reducing Paving Emissions Using Warm Mix Technology*. Proceedings of the Fifty-Second Conference of the Canadian Technical Asphalt Association, Ontario, 2007.
18. Austerman, A., W. Mogawer and R. Bonaquist. *Evaluating the Effects of Warm Mix Asphalt Technology Additive Dosages on the Workability and Durability of Asphalt Mixtures Containing Recycled Asphalt Pavement*. Paper No. 09-1279 Presented at the 88th Transportation Research Board Annual Meeting, Washington D. C., 2009.

19. Croteau, J. and B. Tessier. *Warm Mix Asphalt Paving Technologies: a Road Builder's Perspective*. Presented at the Annual Conference of the Transportation Association of Canada, Toronto, September 2008.
20. Kristjánisdóttir, O., S. T. Muench, L. Michael, and G. Burke. *Assessing Potential for Warm-Mix Asphalt Technology Adoption*. Journal of the Transportation Research Board, No. 2040, National Academies, Washington, D.C., 2007, pp. 91–99.
21. Crews, E. *Extended Season Paving in New York City Using Evotherm™ Warm Mix Asphalt*. Mead Westvaco Asphalt Innovations, South Carolina, December 2008.
22. Kuennen, T. *Warm mix keeps asphalt workable after long haul to California coast*. Asphalt Innovations.
23. Mallick, R. B., P. S. Kandhal, and R. L. Bradbury. *Using Warm-Mix Asphalt Technology to Incorporate High Percentage of Reclaimed Asphalt Pavement Material in Asphalt Mixtures*. Journal of the Transportation Research Board, No. 2051, National Academies, Washington, D.C., 2008, pp. 71–79.
24. Tao, M. and R. B. Mallick. *An Evaluation of the Effects of Warm Mix Asphalt Additives on Workability and Mechanical Properties of Reclaimed Asphalt Pavement (RAP) Material*. Paper No. 09-3503 Presented at the 88th Transportation Research Board Annual Meeting, Washington D. C., 2009.
25. Newcomb, D. *An Introduction to Warm Mix Asphalt*. National Asphalt Pavement Association, 2007.
26. Kristjánisdóttir, O., S. Muench, L. Michael, and G. Burke. *Assessing Potential for Warm-Mix Asphalt Technology Adoption*. Journal of the Transportation Research Board, No. 2040, National Academies, Washington, D.C., 2007, pp. 91–99.
27. Prowell, B. D, G. C. Hurley and E. Crews. *Field Performance of Warm-Mix Asphalt at National Center for Asphalt Technology Test Track*. Journal of the Transportation Research Board, No. 1998, National Academies, Washington, D.C., 2007, pp. 96–102.

28. Hurley, G. C. and B. D. Prowell. *Evaluation of Aspha-Min Zeolite for Use in Warm Mix Asphalt*. NCAT Report 05-04, National Center for Asphalt Technology, Auburn University, 2005.
29. Hurley, G. C. and B. D. Prowell. *Evaluation of Sasobit for Use in Warm Mix Asphalt*. NCAT Report 05-06, National Center for Asphalt Technology, Auburn University, 2005.
30. Xiao, F., S. N. Amirkhanian and B. J. Putman. *Evaluation of Rutting Resistance in Warm-Mix Asphalts Containing Moist Aggregates*. Journal of the Transportation Research Board, No. 2180, National Academies, Washington, D.C., 2010, pp. 75–84.
31. Xiao, F., J. Jordan and S. Amirkhanian. *Laboratory Investigation of Moisture Damage in Warm Mix Asphalt Containing Moist Aggregate*. Paper No. 09-2904 Presented at the 88th Transportation Research Board Annual Meeting, Washington D. C., 2009.
32. Kvasnak, A., R. West, J. Moore, J. Nelson, P. Turner and N. Tran. *Case Study of Warm Mix Asphalt Moisture Susceptibility in Birmingham*. Paper No. 09-3703 Presented at the 88th Transportation Research Board Annual Meeting, Washington D. C., 2009.
33. Wasiuddin, N. M., M. M. Zaman and E. A. O’Rear. *Effect of Sasobit and Aspha-Min on Wettability and Adhesion Between Asphalt Binders and Aggregates*. Journal of the Transportation Research Board, No. 2051, National Academies, Washington, D.C., 2008, pp. 80–89.
34. Hodo, W. D., A. Kvasnak and E. R. Brown. *Investigation of Foamed Asphalt (Warm Mix Asphalt) with High Reclaimed Asphalt Pavement (RAP) Content for Sustainment and Rehabilitation of Asphalt Pavement*. Paper No. 09-3789 Presented at the 88th Transportation Research Board Annual Meeting, Washington D. C., 2009.
35. National Asphalt Pavement Association. *Black and Green. Sustainable Asphalt, Now and Tomorrow*. Special Report 200. Lanham, Maryland, September 2009.
36. Copeland, A. *Reclaimed Asphalt Pavement in Asphalt Mixtures: State of the Practice*. Report No. FHWA-HRT-11-021, Federal Highway Administration, McLean, Virginia, 2011.

37. Federal Highway Administration. *High Reclaimed Asphalt Pavement Use*. FHWA Publication No. FHWA-HRT-11-057, Federal Highway Administration, McLean, Virginia, 2011.
38. Kandhal, P. and Mallick, R.B. *Pavement Recycling Guidelines for State and Local Governments—Participant's Reference Book*, Report No. FHWA-SA-98-042, Federal Highway Administration, Washington, DC, 1997.
39. McDaniel, R. and T. Nantung. *Designing Superpave Mixes with Locally Reclaimed Asphalt Pavement: North Central States Jointly Fund Study*. TR News, No. 239, National Academies, Washington, D.C., 2005, pp. 28–30.
40. National Technology Development, LLC. *Quantify the Energy and Environmental Effects of Using Recycled Asphalt and Recycled Concrete for Pavement Construction*. Phase I Final Report. Report No. C-08-02, NYS Department of Transportation, 2009.
41. Al-Qadi, I.L., M. Elseifi, and S.H. Carpenter. *Reclaimed Asphalt Pavement – A Literature Review*. Research Report FHWA-ICT-07-001, Illinois Center for Transportation, Urbana, Illinois, 2007.
42. Kandhal, P. and K. Foo. *Designing Recycled Hot Mix Asphalt Mixtures Using Superpave Technology*. NCAT Report 96-05, National Center for Asphalt Technology, Auburn University, 1997.
43. McDaniel, R., H. Soleymani, R.M. Anderson, P. Turner and R. Peterson. *Recommended Use of Reclaimed Asphalt Pavement in the Superpave Mix Design Method*. NCHRP Web Document 30, National Cooperative Highway Research Program, 2000.
44. Huang, B., G. Li, D. Vukosavljevic, X. Shu, X., and B. K. Egan. *Laboratory Investigation of Mixing Hot-Mix Asphalt with Reclaimed Asphalt Pavement*. Journal of the Transportation Research Board, No. 1929, National Academies, Washington, D.C., 2005, pp. 37–45.

45. Solaimanian, M. and M. Tahmoressi. *Variability Analysis of Hot-Mix Asphalt Concrete Containing High Percentage of Reclaimed Asphalt Pavement*. Journal of the Transportation Research Board, No. 1543, National Academies, Washington, D.C., 1996, pp. 89–96.
46. F. Zhou, G. Das, T. Scullion, and S. Hu. *RAP Stockpile Management and Processing in Texas: State of the Practice and Proposed Guidelines*. Report 0-6092-1, Texas Transportation Institute, College Station, Texas, 2010.
47. National Cooperative Highway Research Program. *NCHRP Program Synthesis of Highway Practice No. 54: Recycling Materials for Highways*, Transportation Research Board, Washington, DC, 1978.
48. Epps, J.A., Little, D.N., Holmgreen, R.J., and Terrel, R.L. *Guidelines for Recycling Pavement Materials*, NCHRP Report No. 224, Transportation Research Board, Washington, DC, 1980.
49. Sullivan, J. *Pavement Recycling Executive Summary and Report*, Report No. FHWA-SA-95-060, Federal Highway Administration, Washington, DC, 1996.
50. McDaniel, R. and R.M. Anderson. *Recommended Use of Reclaimed Asphalt Pavement in the Superpave Mix Design Method: Guidelines*, Research Results Digest No. 253, National Cooperative Highway Research Program, Washington, DC, 2001.
51. McDaniel, R. and R.M. Anderson. *Recommended Use of Reclaimed Asphalt Pavement in the Superpave Mix Design Method: Technician's Manual*, NCHRP Report No. 452, Transportation Research Board, Washington, DC, 2001.
52. Li X., T.R. Clyne, and M.O. Marasteanu. *Recycled Asphalt Pavement (RAP) Effects on Binder and Mixture Quality*. Report No. MN/RC – 2005-02, Minnesota Department of Transportation, July, 2004.
53. Daniel, J.S., and A. Lachance. *Mechanistic and Volumetric Properties of Asphalt Mixtures with Recycled Asphalt Pavement*. Journal of the Transportation Research Board, No. 1929, National Academies, Washington, D.C., 2005, pp. 28–36.

54. Huang, B., Z. Zhang and W. Kinger. *Fatigue Crack Characteristics of HMA Mixtures Containing RAP*. Proceedings, 5th International RILEM Conference on Cracking in Pavements, Limoges, France, 2004.
55. West, R., A. Kvasnak, N. Tran, B. Powell and P. Turner. *Testing of Moderate and High Reclaimed Asphalt Pavement Content Mixes*. Journal of the Transportation Research Board, No. 2126, National Academies, Washington, D.C., 2009, pp. 100–108.
56. National Center for Asphalt Technology. *LTPP Data Shows RAP Mixes Perform as Well as Virgin Mixes*. Asphalt Technology News, Volume 21, Number 2, National Center for Asphalt Technology, Auburn, AL, 2009.
57. Hong, F. D. Chen and M. Mikhail. *Long-Term Performance Evaluation of Recycled Asphalt Pavement Results from Texas*. Journal of the Transportation Research Board, No. 2180, National Academies, Washington, D.C., 2010, pp. 58–66.
58. Roberts, F.L., P.S. Kandhal, E.R. Brown, D.Y. Lee, and T.W. Kennedy. *Hot Mix Asphalt Materials, Mixture Design, and Construction*. NAPA Education Foundation, Lanham, MD, Second Edition, 1996.
59. Cooley, L.A., J.W. Brumfield, R.B. Mallick, W.S. Mogawer, M. Partl, L. Poulikakos and G. Hicks. *Construction and Maintenance Practices for Permeable Friction Courses*. National Cooperative Highway Research Program Report 640, National Research Council, Washington, D.C., 2009.
60. Kandhal, P. and R. Mallick. *Open-Graded Asphalt Friction Course: State of the Practice*. NCAT Report 98-07, National Center for Asphalt Technology, Auburn University, 1998.
61. Kandhal, P. *Design, Construction, and Maintenance of Open-Graded Asphalt Friction Courses*. Information Series 115. National Asphalt Pavement Association, Lanham, MD, 2002.

62. Smit, A.d.F and B. Waller, *Sound Pressure and Intensity Evaluations of Low Noise Pavement Structures with Open Graded Asphalt Mixtures*. NCAT Report 07-02, National Center for Asphalt Technology, Auburn University, 2007.
63. Kandhal, P. *Asphalt Pavements Mitigate Tire/Pavement Noise*. Hot Mix Asphalt Technology, March-April, 2004, pp. 22-31.
64. Asphalt Pavement Alliance. www.quietpavement.com. Last accessed November, 2011.
65. Birgisson, B., R. Roque, A. Varadhan, T. Thai and L. Jaiswal. *Evaluation of Thick Open Graded and Bonded Friction Courses for Florida*. University of Florida, Gainesville, FL, 2006.
66. Berbee, R., G. Rijs, R. de Brouwer, and L. van Velzen. *Characterization and Treatment of Runoff from Highways in the Netherlands Paved with Impervious and Pervious Asphalt*. Water Environment Research, 71(2), 1999.
67. Barrett, Michael. *Stormwater Quality Benefits of a Porous Asphalt Overlay*. Center for Transportation Research. Report No. FHWA/TX-07/0-4605-2, Austin, Texas, 2006.
68. Mallick, R., P. Kandhal, A. Cooley and D. Watson. *Design, Construction, and Performance of New-Generation Open-Graded Friction Courses*. NCAT Report 00-01, National Center for Asphalt Technology, Auburn University, 2000.
69. Huber, G. *Performance Survey on Open-Graded Friction Course Mixes*. Synthesis of Highway Practice 284. Transportation Research Board, National Research Council, Washington, D.C., 2000.
70. Van Der Zwan, J.T., T. Goeman, H.J.A.J. Gruis, J.H. Swart, and R.H. Oldenburger. *Porous Asphalt Wearing Courses in the Netherlands: State of the Art Review*. Journal of the Transportation Research Board, No. 1265, National Academies, Washington, D.C., 1990, pp. 95–110.

71. Van Heystraeten, G. and C. Moraux. *Ten Years' Experience of Porous Asphalt in Belgium*. Journal of the Transportation Research Board, No. 1265, National Academies, Washington, D.C., 1990, pp. 34–40.
72. Bolzan, P. E., J. C. Nicholls, G. A. Huber. *Searching for Superior Performing Porous Asphalt Wearing Courses*. Presented at the 80th Transportation Research Board Annual Meeting, Washington D. C., 2001.
73. Alvarez, A.E., A. Epps Martin, C.K. Estakhri, J.W. Button, G.J. Glover and S.H. Hung. *Synthesis of Current Practice on the Design, Construction, and Maintenance of Porous Friction Courses*. Report 0-5262-1, Texas Transportation Institute, College Station, Texas, 2006.
74. Federal Highway Administration. *Open-Graded Friction Courses FHWA Mix Design Method*. Technical Advisory T 5040.31. Federal Highway Administration, U.S. Department of Transportation, Washington D.C., 1990.
75. Watson, D.E., K.A. Moore, K. Williams and A.L. Cooley. *Refinement of New-Generation Open-Graded Friction Course Mix Design*. Journal of the Transportation Research Board, No. 1832, National Academies, Washington, D.C., 2003, pp. 78–85.
76. Tolman, F. and F. van Gorkum. *A Model for the Mechanical Durability of Porous Asphalt*. European Conference on Porous Asphalt, Madrid, 1997.
77. Fortes, R.M. and J.V. Merighi. *Open-graded HMA Considering the Stone-on-Stone Contact*. Proceedings of the International Conference on Design and Construction of Long Lasting Asphalt Pavements, Auburn, Alabama, June 2004.
78. Timm, D. *Design, Construction and Instrumentation of the 2006 Test Track Structural Study*. NCAT Report 09-01, National Center for Asphalt Technology, Auburn University, 2009.
79. ALDOT-350-87. *In-Place Bituminous Plant Mix Density Measurements*. Alabama Department of Transportation Testing Manual, 2005.

80. AASHTO T164. Standard Method of Test for Quantitative Extraction of Asphalt Binder from Hot Mix Asphalt (HMA). American Association of State Highway Transportation Officials, 2008.
81. ASTM D5404/D5404M-11. Standard Practice for Recovery of Asphalt from Solution Using the Rotary Evaporator. American Society for Testing and Materials, 2011.
82. AASHTO M320-05. Standard Specification for Performance-Graded Asphalt Binders. American Association of State Highway Transportation Officials, 2005.
83. AASHTO PP1. Standard Practice for Accelerated Aging of Asphalt Binder Using a Pressurized Aging Vessel (PAV). American Association of State Highway Transportation Officials, 2009.
84. AASHTO TP 79. Standard Method of Test for Determining the Dynamic Modulus and Flow Number for Hot Mix Asphalt (HMA) Using the Asphalt Mixture Performance Tester (AMPT). American Association of State Highway Transportation Officials, 2009.
85. Virtual Superpave Laboratory. Publication Number ED-001, CD-ROM. National Asphalt Pavement Association.
86. AASHTO TP 63. Standard Method of Test for Determining the Rutting Susceptibility of Hot Mix Asphalt (HMA) Using the Asphalt Pavement Analyzer (APA). American Association of State Highway Transportation Officials, 2007.
87. Biligiri, K. P., K. E. Kaloush, M. S. Mamlouk and M. W. Witczak. *Rational Modeling of Tertiary Flow for Asphalt Mixtures*. Journal of the Transportation Research Board, No. 2001, National Academies, Washington, D.C., 2007, pp. 63-72.
88. AASHTO T324. Standard Method of Test for Hamburg Wheel-Track Testing of Compacted Hot Mix Asphalt (HMA). American Association of State Highway Transportation Officials, 2004.

89. AASHTO T283. Standard Method of Test for Resistance of Compacted Hot Mix Asphalt (HMA) to Moisture-Induced Damage. American Association of State Highway Transportation Officials, 2007.
90. AASHTO T321. Standard Method of Test for Determining the Fatigue Life of Compacted Hot Mix Asphalt (HMA) Subjected to Repeated Flexural Bending. American Association of State Highway Transportation Officials, 2007.
91. AASHTO T322. Standard Method of Test for Determining the Creep Compliance and Strength of Hot Mix Asphalt (HMA) Using the Indirect Tensile Test Device. American Association of State Highway Transportation Officials, 2007.
92. Hot Mix Asphalt for Seniors and Graduate Students. Publication Number FHWA-IF-04-014, CD-ROM. Federal Highway Administration, 2004.
93. Willis, J.R. and D. Timm. *Field-Based Strain Thresholds for Flexible Perpetual Pavement Design*. NCAT Report 09-09, National Center for Asphalt Technology, Auburn University, 2009.
94. Chang, C., Y. Chang and J. Chen. *Effect of Mixture Characteristics on Cooling Rate of Asphalt Pavements*. Journal of Transportation Engineering, Vol. 135, No. 5, 2009, pp. 297-304.
95. White, S., G. Heiman, G. Huber, R. Besant, and A. Bergan. *Initial Cooling of Pavements and the Development of Pavement Cooling Charts*. Canadian Journal of Civil Engineering, Vol. 17, No. 1, 1990, pp. 94-101.
96. Chadbourn, B. A., D. E. Newcomb, V. R. Voller, R. A. De Sombre, J. A. Luoma and D. H. Timm. *An Asphalt Paving Tool for Adverse Conditions*. Report MN/RC-1998-18, Minnesota Department of Transportation, 1998.
97. Timm, D. H., V. R. Voller, E. Lee and J. Harvey. *Calcool: A multi-layer Asphalt Pavement Cooling Tool for Temperature Prediction During Construction*. The International Journal of Pavement Engineering, Vol. 2, 2001, pp. 169-185.

98. Bonaquist, R. F., W. Stump III, and D. W. Christensen. *Simple Performance Tester for Superpave Mix Design: First-Article Development and Evaluation*. NCHRP Report 513, Transportation Research Board of the National Academies, Washington, D.C., 2003.
99. Witczak, M. W., K. Kaloush, T. Peillinen, M. El-Basyouny, and H. Von Quintus. *Simple Performance Test for Superpave Mix Design*. NCHRP Report 465, Transportation Research Board of the National Academies, Washington, D.C., 2002.
100. Willis R., D. Timm, R. West, B. Powell, M. Robbins, A. Taylor, A. Smit, N. Tran, M. Heitzman and A. Bianchini. *Phase III NCAT Test Track Findings*. NCAT Report 09-08, National Center for Asphalt Technology, Auburn University, 2009.
101. Timm D., R. West, A. Priest, B. Powell, I. Selvaraj, J. Zhang, and R. Brown. *Phase II NCAT Test Track Results*. NCAT Report 06-05, National Center for Asphalt Technology, Auburn University, 2006.
102. Apeageyi, A., B. Diefenderfer and S. Diefenderfer. *Rutting Resistance of Asphalt Concrete Mixtures Containing Recycled Asphalt Pavement*. Paper No. 11-1840 Presented at the 90th Transportation Research Board Annual Meeting, Washington D. C., 2011.
103. Daniel, J.S. and A. Lachance. *Mechanistic and Volumetric Properties of Asphalt Mixtures with Recycled Asphalt Pavement*, Journal of the Transportation Research Board, No. 1929, National Academies, Washington, D.C., 2005, pp. 28–36.
104. Hurley, G. and B. Prowell. *Evaluation of Potential Processes for Use in Warm Mix Asphalt Mixes*. Journal of the Association of Asphalt Paving Technologists, Vol. 75, 2006, pp. 41 – 85.
105. Applied Research Associates. *Guide for Mechanistic–Empirical Design of New and Rehabilitated Pavement Structures*. NCHRP, Transportation Research Board of the National Academies, Washington, D.C., 2004.
106. Powell, R.B. *Predicting Field Performance on the NCAT Pavement Test Track*. Dissertation, Auburn University, 2006.

107. Federal Highway Administration. *Pavement Health Track Remaining Service Life (RLS) Forecasting Models, Technical Information. Guidance on Setting Key Parameters.*
<http://www.fhwa.dot.gov/pavement/healthtrack/pubs/technical/pht06.cfm>. Accessed April, 2012.
108. Ullidtz, P. *Pavement Analysis*. The Technical University of Denmark, Elsevier, Amsterdam, The Netherlands, 1987.
109. Timm, D. and A. Vargas-Nordcbeck. *Structural Coefficient of Open Graded Friction Course*. Journal of the Transportation Research Board, in press.

APPENDIX A

AS-BUILT PROPERTIES OF TEST SECTIONS

Quadrant: S
Section: 8
Sublot: 1

Laboratory Diary

General Description of Mix and Materials

Design Method: FC-5
 Compactive Effort: 50 gyrations
 Binder Performance Grade: 76-22
 Modifier Type: SBS
 Aggregate Type: Granite/RAP
 Design Gradation Type: PFC

Avg. Lab Properties of Plant Produced Mix

Sieve Size	Design	QC
25 mm (1"):	100	100
19 mm (3/4"):	100	100
12.5 mm (1/2"):	95	97
9.5 mm (3/8"):	64	71
4.75 mm (#4):	15	21
2.36 mm (#8):	9	11
1.18 mm (#16):	8	9
0.60 mm (#30):	6	7
0.30 mm (#50):	5	6
0.15 mm (#100):	4	4
0.075 mm (#200):	3.7	3.1
Binder Content (Pb):	5.5	5.1
Eff. Binder Content (Pbe):	4.9	NA
Dust-to-Binder Ratio:	0.8	NA
Rice Gravity (Gmm):	2.446	2.482
Avg. Bulk Gravity (Gmb):	2.037	NA
Avg Air Voids (Va):	16.8	NA
Agg. Bulk Gravity (Gsb):	2.613	NA
Avg VMA:	26.3	NA
Avg. VFA:	36	NA

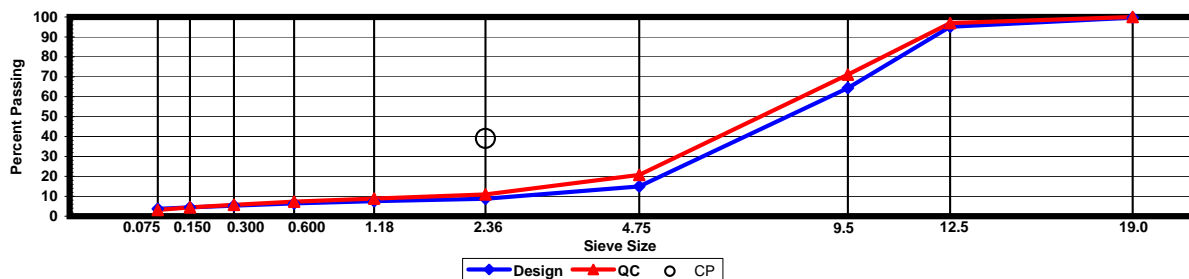
Construction Diary

Relevant Conditions for Construction

Completion Date: July 15, 2009
 24 Hour High Temperature (F): 91
 24 Hour Low Temperature (F): 74
 24 Hour Rainfall (in): 0.24
 Planned Subot Lift Thickness (in): 1.3
 Paving Machine: Spray Paver

Plant Configuration and Placement Details

Component	% Setting
Asphalt Content (Plant Setting)	5.5
78 LaGrange Granite	85.0
Coarse Fraction Local RAP	15.0
Cellulose	0.3
As-Built Sublot Lift Thickness (in):	1.3
Total Thickness of All 2009 Sublots (in):	7.0
Approx. Underlying HMA Thickness (in):	0.0
Type of Tack Coat Utilized:	NTSS-1HM
Target Tack Application Rate (gal/sy):	0.05
Approx. Avg. Temperature at Plant (F):	335
Avg. Measured Mat Compaction:	75.0%



General Notes:

- Mixes are referenced by quadrant (E=East, N=North, W=West, and S=South), section # (sequential) and subplot (top=1);
- The total HMA thickness of all structural study sections (N1-N11 and S8-S12) ranges from 5-3/4 to 14 inches by design;
- All non-structural sections are supported by a uniform perpetual foundation in order to study surface mix performance;
- SMA and OGFC refer to stone matrix asphalt and open-graded friction course, respectively; and
- All liquid asphalt purchased for use in Track reconstruction contained LOF 6500 antistrip additive at a rate of 0.5 percent

Quadrant: S
Section: 8
Sublot: 2

Laboratory Diary

General Description of Mix and Materials

Design Method: Super
 Compactive Effort: 80 gyrations
 Binder Performance Grade: 76-22
 Modifier Type: SBS
 Aggregate Type: Lms/Sand/Grn
 Design Gradation Type: Fine

Avg. Lab Properties of Plant Produced Mix

Sieve Size	Design	QC
25 mm (1"):	100	98
19 mm (3/4"):	93	94
12.5 mm (1/2"):	82	87
9.5 mm (3/8"):	71	78
4.75 mm (#4):	52	59
2.36 mm (#8):	45	47
1.18 mm (#16):	35	37
0.60 mm (#30):	24	26
0.30 mm (#50):	12	15
0.15 mm (#100):	7	9
0.075 mm (#200):	3.9	5.2
Binder Content (Pb):	4.7	4.6
Eff. Binder Content (Pbe):	4.1	4.0
Dust-to-Binder Ratio:	0.9	1.3
Rice Gravity (Gmm):	2.575	2.556
Avg. Bulk Gravity (Gmb):	2.472	2.450
Avg Air Voids (Va):	4.0	4.1
Agg. Bulk Gravity (Gsb):	2.737	2.710
Avg VMA:	13.9	13.8
Avg. VFA:	71	70

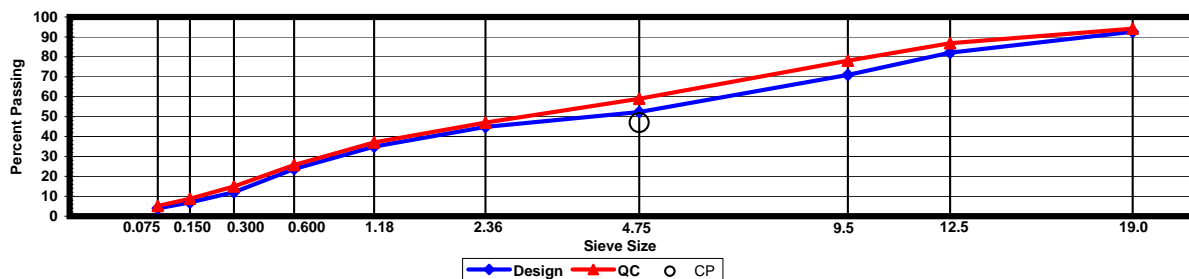
Construction Diary

Relevant Conditions for Construction

Completion Date: July 14, 2009
 24 Hour High Temperature (F): 93
 24 Hour Low Temperature (F): 72
 24 Hour Rainfall (in): 0.00
 Planned Sublot Lift Thickness (in): 2.8
 Paving Machine: Roadtec

Plant Configuration and Placement Details

Component	% Setting
Asphalt Content (Plant Setting)	4.7
78 Opelika Limestone	30.0
57 Opelika Limestone	18.0
M10 Columbus Granite	25.0
Shorter Coarse Sand	27.0
As-Built Sublot Lift Thickness (in):	3.0
Total Thickness of All 2009 Sublots (in):	7.0
Approx. Underlying HMA Thickness (in):	0.0
Type of Tack Coat Utilized:	NTSS-1HM
Target Tack Application Rate (gal/sy):	0.07
Approx. Avg. Temperature at Plant (F):	335
Avg. Measured Mat Compaction:	93.7%



General Notes:

- Mixes are referenced by quadrant (E=East, N=North, W=West, and S=South), section # (sequential) and subplot (top=1);
- The total HMA thickness of all structural study sections (N1-N11 and S8-S12) ranges from 5-3/4 to 14 inches by design;
- All non-structural sections are supported by a uniform perpetual foundation in order to study surface mix performance;
- SMA and OGFC refer to stone matrix asphalt and open-graded friction course, respectively; and
- All liquid asphalt purchased for use in Track reconstruction contained LOF 6500 antistripping additive at a rate of 0.5 percent

Quadrant: S
Section: 8
Sublot: 3

Laboratory Diary

General Description of Mix and Materials

Design Method: Super
 Compactive Effort: 80 gyrations
 Binder Performance Grade: 67-22
 Modifier Type: NA
 Aggregate Type: Lms/Sand/Grn
 Design Gradation Type: Fine

Avg. Lab Properties of Plant Produced Mix

Sieve Size	Design	QC
25 mm (1"):	100	98
19 mm (3/4"):	93	94
12.5 mm (1/2"):	84	87
9.5 mm (3/8"):	73	79
4.75 mm (#4):	55	59
2.36 mm (#8):	47	49
1.18 mm (#16):	36	39
0.60 mm (#30):	25	27
0.30 mm (#50):	14	15
0.15 mm (#100):	8	9
0.075 mm (#200):	4.6	5.3
Binder Content (Pb):	4.6	4.9
Eff. Binder Content (Pbe):	4.1	4.4
Dust-to-Binder Ratio:	1.1	1.2
Rice Gravity (Gmm):	2.574	2.532
Avg. Bulk Gravity (Gmb):	2.471	2.442
Avg Air Voids (Va):	4.0	3.6
Agg. Bulk Gravity (Gsb):	2.738	2.700
Avg VMA:	13.9	14.0
Avg. VFA:	71	75

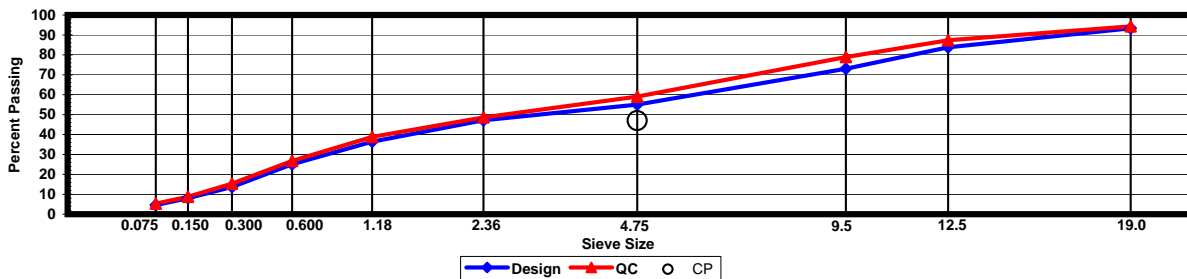
Construction Diary

Relevant Conditions for Construction

Completion Date: July 3, 2009
 24 Hour High Temperature (F): 92
 24 Hour Low Temperature (F): 69
 24 Hour Rainfall (in): 0.00
 Planned Sublot Lift Thickness (in): 3.0
 Paving Machine: Roadtec

Plant Configuration and Placement Details

Component	% Setting
Asphalt Content (Plant Setting)	4.9
78 Opelika Limestone	30.0
57 Opelika Limestone	18.0
M10 Columbus Granite	25.0
Shorter Coarse Sand	27.0
As-Built Sublot Lift Thickness (in):	2.6
Total Thickness of All 2009 Sublots (in):	7.0
Approx. Underlying HMA Thickness (in):	0.0
Type of Tack Coat Utilized:	NA
Target Tack Application Rate (gal/sy):	NA
Approx. Avg. Temperature at Plant (F):	325
Avg. Measured Mat Compaction:	91.7%



General Notes:

- Mixes are referenced by quadrant (E=East, N=North, W=West, and S=South), section # (sequential) and subplot (top=1);
- The total HMA thickness of all structural study sections (N1-N11 and S8-S12) ranges from 5-3/4 to 14 inches by design;
- All non-structural sections are supported by a uniform perpetual foundation in order to study surface mix performance;
- SMA and OGFC refer to stone matrix asphalt and open-graded friction course, respectively; and
- All liquid asphalt purchased for use in Track reconstruction contained LOF 6500 antistripping additive at a rate of 0.5 percent

Quadrant: S
Section: 9
Sublot: 1

Laboratory Diary

General Description of Mix and Materials

Design Method: Super
 Compactive Effort: 80 gyrations
 Binder Performance Grade: 76-22
 Modifier Type: SBS
 Aggregate Type: Grn/Sand/Lms
 Design Gradation Type: Fine

Avg. Lab Properties of Plant Produced Mix

Sieve Size	Design	QC
25 mm (1"):	100	100
19 mm (3/4"):	100	100
12.5 mm (1/2"):	100	100
9.5 mm (3/8"):	100	100
4.75 mm (#4):	78	81
2.36 mm (#8):	60	59
1.18 mm (#16):	46	46
0.60 mm (#30):	31	31
0.30 mm (#50):	16	16
0.15 mm (#100):	10	9
0.075 mm (#200):	5.8	6.0
Binder Content (Pb):	5.8	6.1
Eff. Binder Content (Pbe):	5.1	5.4
Dust-to-Binder Ratio:	1.1	1.1
Rice Gravity (Gmm):	2.483	2.472
Avg. Bulk Gravity (Gmb):	2.384	2.374
Avg Air Voids (Va):	4.0	4.0
Agg. Bulk Gravity (Gsb):	2.667	2.670
Avg VMA:	15.8	16.5
Avg. VFA:	75	76

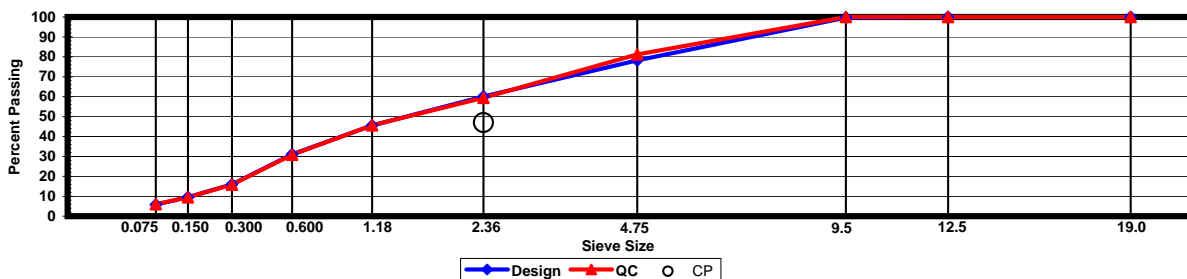
Construction Diary

Relevant Conditions for Construction

Completion Date: July 16, 2009
 24 Hour High Temperature (F): 92
 24 Hour Low Temperature (F): 74
 24 Hour Rainfall (in): 0.00
 Planned Sublot Lift Thickness (in): 1.3
 Paving Machine: Roadtec

Plant Configuration and Placement Details

Component	% Setting
Asphalt Content (Plant Setting)	6.5
89 Columbus Granite	36.0
8910 Opelika Limestone Screenings	23.0
M10 Columbus Granite	13.0
Shorter Coarse Sand	28.0
As-Built Sublot Lift Thickness (in):	1.2
Total Thickness of All 2009 Sublots (in):	7.0
Approx. Underlying HMA Thickness (in):	0.0
Type of Tack Coat Utilized:	NTSS-1HM
Target Tack Application Rate (gal/sy):	0.04
Approx. Avg. Temperature at Plant (F):	335
Avg. Measured Mat Compaction:	93.1%



General Notes:

- 1) Mixes are referenced by quadrant (E=East, N=North, W=West, and S=South), section # (sequential) and subplot (top=1);
- 2) The total HMA thickness of all structural study sections (N1-N11 and S8-S12) ranges from 5-3/4 to 14 inches by design;
- 3) All non-structural sections are supported by a uniform perpetual foundation in order to study surface mix performance;
- 4) SMA and OGFC refer to stone matrix asphalt and open-graded friction course, respectively; and
- 5) All liquid asphalt purchased for use in Track reconstruction contained LOF 6500 antistripping additive at a rate of 0.5 percent

Quadrant: S
Section: 9
Sublot: 2

Laboratory Diary

General Description of Mix and Materials

Design Method: Super
 Compactive Effort: 80 gyrations
 Binder Performance Grade: 76-22
 Modifier Type: SBS
 Aggregate Type: Lms/Sand/Grn
 Design Gradation Type: Fine

Avg. Lab Properties of Plant Produced Mix

Sieve Size	Design	QC
25 mm (1"):	100	99
19 mm (3/4"):	93	92
12.5 mm (1/2"):	82	84
9.5 mm (3/8"):	71	76
4.75 mm (#4):	52	57
2.36 mm (#8):	45	47
1.18 mm (#16):	35	38
0.60 mm (#30):	24	26
0.30 mm (#50):	12	15
0.15 mm (#100):	7	9
0.075 mm (#200):	3.9	5.3
Binder Content (Pb):	4.7	4.4
Eff. Binder Content (Pbe):	4.1	3.9
Dust-to-Binder Ratio:	0.9	1.4
Rice Gravity (Gmm):	2.575	2.551
Avg. Bulk Gravity (Gmb):	2.472	2.439
Avg Air Voids (Va):	4.0	4.4
Agg. Bulk Gravity (Gsb):	2.737	2.695
Avg VMA:	13.9	13.5
Avg. VFA:	71	68

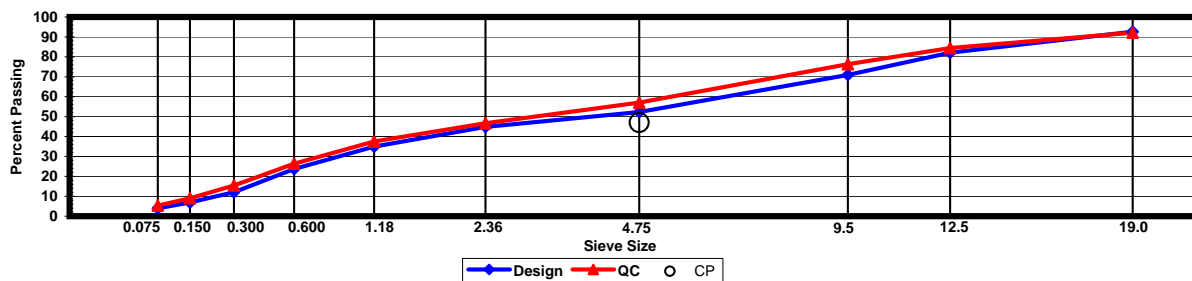
Construction Diary

Relevant Conditions for Construction

Completion Date: July 14, 2009
 24 Hour High Temperature (F): 93
 24 Hour Low Temperature (F): 72
 24 Hour Rainfall (in): 0.00
 Planned Sublot Lift Thickness (in): 2.8
 Paving Machine: Roadtec

Plant Configuration and Placement Details

Component	% Setting
Asphalt Content (Plant Setting)	4.7
78 Opelika Limestone	30.0
57 Opelika Limestone	18.0
M10 Columbus Granite	25.0
Shorter Coarse Sand	27.0
As-Built Sublot Lift Thickness (in):	2.8
Total Thickness of All 2009 Sublots (in):	7.0
Approx. Underlying HMA Thickness (in):	0.0
Type of Tack Coat Utilized:	NTSS-1HM
Target Tack Application Rate (gal/sy):	0.07
Approx. Avg. Temperature at Plant (F):	335
Avg. Measured Mat Compaction:	92.8%



General Notes:

- Mixes are referenced by quadrant (E=East, N=North, W=West, and S=South), section # (sequential) and subplot (top=1);
- The total HMA thickness of all structural study sections (N1-N11 and S8-S12) ranges from 5-3/4 to 14 inches by design;
- All non-structural sections are supported by a uniform perpetual foundation in order to study surface mix performance;
- SMA and OGFC refer to stone matrix asphalt and open-graded friction course, respectively; and
- All liquid asphalt purchased for use in Track reconstruction contained LOF 6500 antistripping additive at a rate of 0.5 percent

Quadrant: S
Section: 9
Sublot: 3

Laboratory Diary

General Description of Mix and Materials

Design Method: Super
 Compactive Effort: 80 gyrations
 Binder Performance Grade: 67-22
 Modifier Type: NA
 Aggregate Type: Lms/Sand/Grn
 Design Gradation Type: Fine

Avg. Lab Properties of Plant Produced Mix

Sieve Size	Design	QC
25 mm (1"):	100	99
19 mm (3/4"):	93	95
12.5 mm (1/2"):	84	87
9.5 mm (3/8"):	73	77
4.75 mm (#4):	55	56
2.36 mm (#8):	47	46
1.18 mm (#16):	36	37
0.60 mm (#30):	25	26
0.30 mm (#50):	14	15
0.15 mm (#100):	8	9
0.075 mm (#200):	4.6	5.1
Binder Content (Pb):	4.6	4.7
Eff. Binder Content (Pbe):	4.1	4.2
Dust-to-Binder Ratio:	1.1	1.2
Rice Gravity (Gmm):	2.574	2.540
Avg. Bulk Gravity (Gmb):	2.471	2.439
Avg Air Voids (Va):	4.0	4.0
Agg. Bulk Gravity (Gsb):	2.738	2.699
Avg VMA:	13.9	13.9
Avg. VFA:	71	71

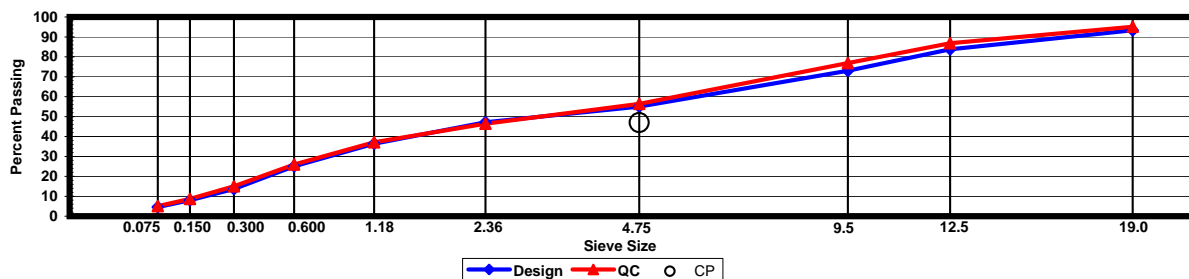
Construction Diary

Relevant Conditions for Construction

Completion Date: July 3, 2009
 24 Hour High Temperature (F): 92
 24 Hour Low Temperature (F): 69
 24 Hour Rainfall (in): 0.00
 Planned Sublot Lift Thickness (in): 3.0
 Paving Machine: Roadtec

Plant Configuration and Placement Details

Component	% Setting
Asphalt Content (Plant Setting)	4.9
78 Opelika Limestone	30.0
57 Opelika Limestone	18.0
M10 Columbus Granite	25.0
Shorter Coarse Sand	27.0
As-Built Sublot Lift Thickness (in):	3.0
Total Thickness of All 2009 Sublots (in):	7.0
Approx. Underlying HMA Thickness (in):	0.0
Type of Tack Coat Utilized:	NA
Target Tack Application Rate (gal/sy):	NA
Approx. Avg. Temperature at Plant (F):	325
Avg. Measured Mat Compaction:	92.6%



General Notes:

- 1) Mixes are referenced by quadrant (E=East, N=North, W=West, and S=South), section # (sequential) and subplot (top=1);
- 2) The total HMA thickness of all structural study sections (N1-N11 and S8-S12) ranges from 5-3/4 to 14 inches by design;
- 3) All non-structural sections are supported by a uniform perpetual foundation in order to study surface mix performance;
- 4) SMA and OGFC refer to stone matrix asphalt and open-graded friction course, respectively; and
- 5) All liquid asphalt purchased for use in Track reconstruction contained LOF 6500 antistripping additive at a rate of 0.5 percent

Quadrant: S
Section: 10
Sublot: 1

Laboratory Diary

General Description of Mix and Materials

Design Method: WMA
 Compactive Effort: 80 gyrations
 Binder Performance Grade: 76-22
 Modifier Type: Foam
 Aggregate Type: Grn/Sand/Lms
 Design Gradation Type: Fine

Avg. Lab Properties of Plant Produced Mix

Sieve Size	Design	QC
25 mm (1"):	100	100
19 mm (3/4"):	100	100
12.5 mm (1/2"):	100	100
9.5 mm (3/8"):	100	100
4.75 mm (#4):	78	81
2.36 mm (#8):	60	60
1.18 mm (#16):	46	47
0.60 mm (#30):	31	32
0.30 mm (#50):	16	17
0.15 mm (#100):	10	10
0.075 mm (#200):	5.8	6.7
Binder Content (Pb):	5.8	6.1
Eff. Binder Content (Pbe):	5.1	5.5
Dust-to-Binder Ratio:	1.1	1.2
Rice Gravity (Gmm):	2.483	2.471
Avg. Bulk Gravity (Gmb):	2.384	2.390
Avg Air Voids (Va):	4.0	3.3
Agg. Bulk Gravity (Gsb):	2.667	2.671
Avg VMA:	15.8	16.0
Avg. VFA:	75	80

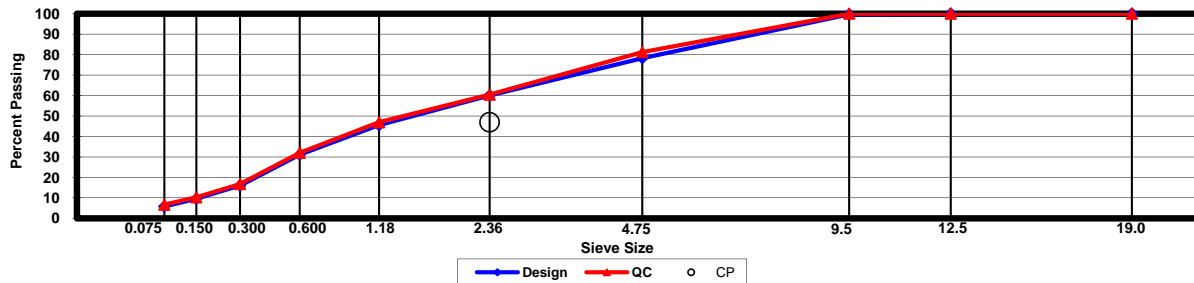
Construction Diary

Relevant Conditions for Construction

Completion Date: July 16, 2009
 24 Hour High Temperature (F): 92
 24 Hour Low Temperature (F): 74
 24 Hour Rainfall (in): 0.00
 Planned Subot Lift Thickness (in): 1.3
 Paving Machine: Roadtec

Plant Configuration and Placement Details

Component	% Setting
Asphalt Content (Plant Setting)	6.5
89 Columbus Granite	36.0
8910 Opelika Limestone Screenings	23.0
M10 Columbus Granite	13.0
Shorter Coarse Sand	28.0
As-Built Sublot Lift Thickness (in):	1.3
Total Thickness of All 2009 Sublots (in):	7.0
Approx. Underlying HMA Thickness (in):	0.0
Type of Tack Coat Utilized:	NTSS-1HM
Target Tack Application Rate (gal/sy):	0.04
Approx. Avg. Temperature at Plant (F):	275
Avg. Measured Mat Compaction:	92.3%



General Notes:

- 1) Mixes are referenced by quadrant (E=East, N=North, W=West, and S=South), section # (sequential) and subplot (top=1);
- 2) The total HMA thickness of all structural study sections (N1-N11 and S8-S12) ranges from 5-3/4 to 14 inches by design;
- 3) All non-structural sections are supported by a uniform perpetual foundation in order to study surface mix performance;
- 4) SMA and OGFC refer to stone matrix asphalt and open-graded friction course, respectively; and
- 5) All liquid asphalt purchased for use in Track reconstruction contained LOF 6500 antistripping additive at a rate of 0.5 percent

Quadrant: S
Section: 10
Sublot: 2

Laboratory Diary

General Description of Mix and Materials

Design Method: WMA
 Compactive Effort: 80 gyrations
 Binder Performance Grade: 76-22
 Modifier Type: Foam
 Aggregate Type: Lms/Sand/Grn
 Design Gradation Type: Fine

Avg. Lab Properties of Plant Produced Mix

Sieve Size	Design	QC
25 mm (1"):	100	99
19 mm (3/4"):	93	96
12.5 mm (1/2"):	82	89
9.5 mm (3/8"):	71	80
4.75 mm (#4):	52	60
2.36 mm (#8):	45	48
1.18 mm (#16):	35	39
0.60 mm (#30):	24	27
0.30 mm (#50):	12	14
0.15 mm (#100):	7	9
0.075 mm (#200):	3.9	5.3
Binder Content (Pb):	4.7	4.7
Eff. Binder Content (Pbe):	4.1	4.1
Dust-to-Binder Ratio:	0.9	1.3
Rice Gravity (Gmm):	2.575	2.550
Avg. Bulk Gravity (Gmb):	2.472	2.433
Avg Air Voids (Va):	4.0	4.6
Agg. Bulk Gravity (Gsb):	2.737	2.706
Avg VMA:	13.9	14.3
Avg. VFA:	71	68

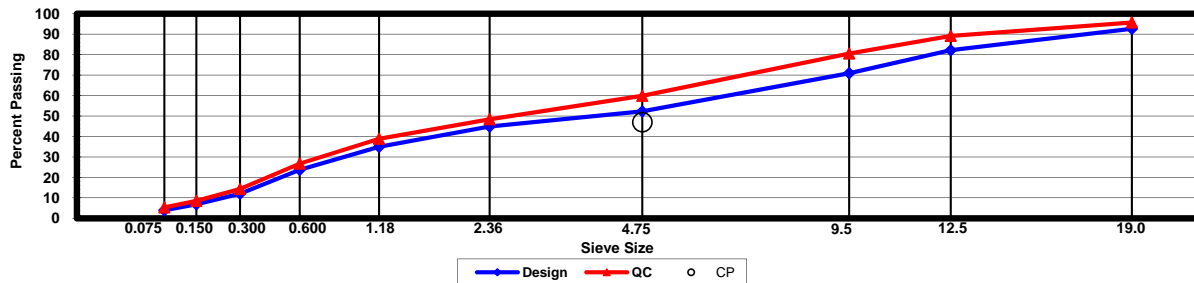
Construction Diary

Relevant Conditions for Construction

Completion Date: July 14, 2009
 24 Hour High Temperature (F): 93
 24 Hour Low Temperature (F): 72
 24 Hour Rainfall (in): 0.00
 Planned Subot Lift Thickness (in): 2.8
 Paving Machine: Roadtec

Plant Configuration and Placement Details

Component	% Setting
Asphalt Content (Plant Setting)	4.7
78 Opelika Limestone	30.0
57 Opelika Limestone	18.0
M10 Columbus Granite	25.0
Shorter Coarse Sand	27.0
As-Built Sublot Lift Thickness (in):	2.7
Total Thickness of All 2009 Sublots (in):	7.0
Approx. Underlying HMA Thickness (in):	0.0
Type of Tack Coat Utilized:	NTSS-1HM
Target Tack Application Rate (gal/sy):	0.07
Approx. Avg. Temperature at Plant (F):	275
Avg. Measured Mat Compaction:	92.9%



General Notes:

- Mixes are referenced by quadrant (E=East, N=North, W=West, and S=South), section # (sequential) and subplot (top=1);
- The total HMA thickness of all structural study sections (N1-N11 and S8-S12) ranges from 5-3/4 to 14 inches by design;
- All non-structural sections are supported by a uniform perpetual foundation in order to study surface mix performance;
- SMA and OGFC refer to stone matrix asphalt and open-graded friction course, respectively; and
- All liquid asphalt purchased for use in Track reconstruction contained LOF 6500 antistripping additive at a rate of 0.5 percent

Quadrant: S
Section: 10
Sublot: 3

Laboratory Diary

General Description of Mix and Materials

Design Method: WMA
 Compactive Effort: 80 gyrations
 Binder Performance Grade: 67-22
 Modifier Type: Foam
 Aggregate Type: Lms/Sand/Grn
 Design Gradation Type: Fine

Avg. Lab Properties of Plant Produced Mix

Sieve Size	Design	QC
25 mm (1"):	100	99
19 mm (3/4"):	93	94
12.5 mm (1/2"):	84	85
9.5 mm (3/8"):	73	76
4.75 mm (#4):	55	57
2.36 mm (#8):	47	47
1.18 mm (#16):	36	38
0.60 mm (#30):	25	21
0.30 mm (#50):	14	12
0.15 mm (#100):	8	7
0.075 mm (#200):	4.6	5.1
Binder Content (Pb):	4.6	4.7
Eff. Binder Content (Pbe):	4.1	4.2
Dust-to-Binder Ratio:	1.1	1.2
Rice Gravity (Gmm):	2.574	2.553
Avg. Bulk Gravity (Gmb):	2.471	2.448
Avg Air Voids (Va):	4.0	4.1
Agg. Bulk Gravity (Gsb):	2.738	2.715
Avg VMA:	13.9	14.0
Avg. VFA:	71	71

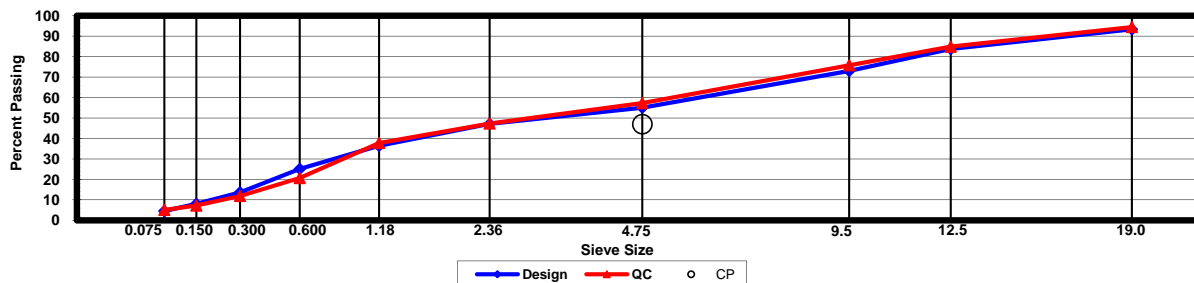
Construction Diary

Relevant Conditions for Construction

Completion Date: July 3, 2009
 24 Hour High Temperature (F): 92
 24 Hour Low Temperature (F): 69
 24 Hour Rainfall (in): 0.00
 Planned Sublot Lift Thickness (in): 3.0
 Paving Machine: Roadtec

Plant Configuration and Placement Details

Component	% Setting
Asphalt Content (Plant Setting)	4.9
78 Opelika Limestone	30.0
57 Opelika Limestone	18.0
M10 Columbus Granite	25.0
Shorter Coarse Sand	27.0
As-Built Sublot Lift Thickness (in):	3.0
Total Thickness of All 2009 Sublots (in):	7.0
Approx. Underlying HMA Thickness (in):	0.0
Type of Tack Coat Utilized:	NA
Target Tack Application Rate (gal/sy):	NA
Approx. Avg. Temperature at Plant (F):	275
Avg. Measured Mat Compaction:	92.3%



General Notes:

- Mixes are referenced by quadrant (E=East, N=North, W=West, and S=South), section # (sequential) and subplot (top=1);
- The total HMA thickness of all structural study sections (N1-N11 and S8-S12) ranges from 5-3/4 to 14 inches by design;
- All non-structural sections are supported by a uniform perpetual foundation in order to study surface mix performance;
- SMA and OGFC refer to stone matrix asphalt and open-graded friction course, respectively; and
- All liquid asphalt purchased for use in Track reconstruction contained LOF 6500 antistripping additive at a rate of 0.5 percent

Quadrant: S
Section: 11
Sublot: 1

Laboratory Diary

General Description of Mix and Materials

Design Method: WMA
 Compactive Effort: 80 gyrations
 Binder Performance Grade: 76-22+
 Modifier Type: Additive
 Aggregate Type: Grn/Sand/Lms
 Design Gradation Type: Fine

Avg. Lab Properties of Plant Produced Mix

Sieve Size	Design	QC
25 mm (1"):	100	100
19 mm (3/4"):	100	100
12.5 mm (1/2"):	100	100
9.5 mm (3/8"):	100	100
4.75 mm (#4):	78	83
2.36 mm (#8):	60	61
1.18 mm (#16):	46	47
0.60 mm (#30):	31	31
0.30 mm (#50):	16	16
0.15 mm (#100):	10	9
0.075 mm (#200):	5.8	6.1
Binder Content (Pb):	5.8	6.4
Eff. Binder Content (Pbe):	5.1	5.7
Dust-to-Binder Ratio:	1.1	1.1
Rice Gravity (Gmm):	2.483	2.464
Avg. Bulk Gravity (Gmb):	2.384	2.380
Avg Air Voids (Va):	4.0	3.4
Agg. Bulk Gravity (Gsb):	2.667	2.675
Avg VMA:	15.8	16.7
Avg. VFA:	75	80

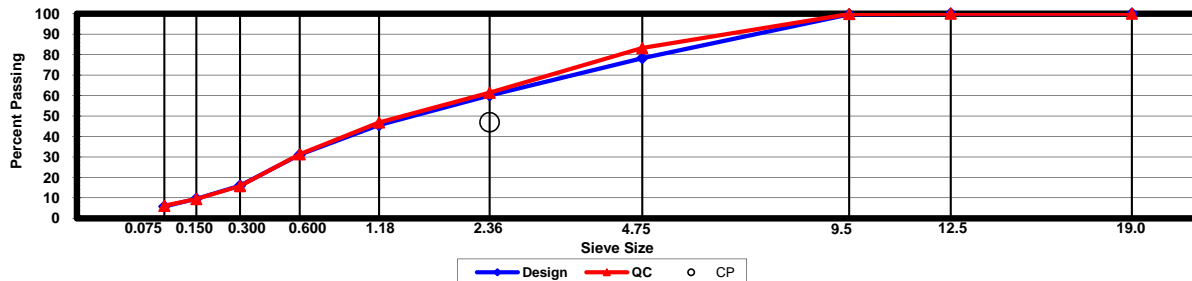
Construction Diary

Relevant Conditions for Construction

Completion Date: July 16, 2009
 24 Hour High Temperature (F): 92
 24 Hour Low Temperature (F): 74
 24 Hour Rainfall (in): 0.00
 Planned Sublot Lift Thickness (in): 1.3
 Paving Machine: Roadtec

Plant Configuration and Placement Details

Component	% Setting
Asphalt Content (Plant Setting)	6.5
89 Columbus Granite	36.0
8910 Opelika Limestone Screenings	23.0
M10 Columbus Granite	13.0
Shorter Coarse Sand	28.0
As-Built Sublot Lift Thickness (in):	1.5
Total Thickness of All 2009 Sublots (in):	6.9
Approx. Underlying HMA Thickness (in):	0.0
Type of Tack Coat Utilized:	NTSS-1HM
Target Tack Application Rate (gal/sy):	0.04
Approx. Avg. Temperature at Plant (F):	250
Avg. Measured Mat Compaction:	93.7%



General Notes:

- Mixes are referenced by quadrant (E=East, N=North, W=West, and S=South), section # (sequential) and subplot (top=1);
- The total HMA thickness of all structural study sections (N1-N11 and S8-S12) ranges from 5-3/4 to 14 inches by design;
- All non-structural sections are supported by a uniform perpetual foundation in order to study surface mix performance;
- SMA and OGFC refer to stone matrix asphalt and open-graded friction course, respectively; and
- All liquid asphalt purchased for use in Track reconstruction contained LOF 6500 antistripping additive at a rate of 0.5 percent

Quadrant: S
Section: 11
Sublot: 2

Laboratory Diary

General Description of Mix and Materials

Design Method: WMA
 Compactive Effort: 80 gyrations
 Binder Performance Grade: 76-22+
 Modifier Type: Additive
 Aggregate Type: Lms/Sand/Grn
 Design Gradation Type: Fine

Avg. Lab Properties of Plant Produced Mix

Sieve Size	Design	QC
25 mm (1"):	100	98
19 mm (3/4"):	93	94
12.5 mm (1/2"):	82	87
9.5 mm (3/8"):	71	80
4.75 mm (#4):	52	60
2.36 mm (#8):	45	48
1.18 mm (#16):	35	38
0.60 mm (#30):	24	25
0.30 mm (#50):	12	13
0.15 mm (#100):	7	8
0.075 mm (#200):	3.9	4.9
Binder Content (Pb):	4.7	4.6
Eff. Binder Content (Pbe):	4.1	4.0
Dust-to-Binder Ratio:	0.9	1.2
Rice Gravity (Gmm):	2.575	2.555
Avg. Bulk Gravity (Gmb):	2.472	2.429
Avg Air Voids (Va):	4.0	4.9
Agg. Bulk Gravity (Gsb):	2.737	2.709
Avg VMA:	13.9	14.5
Avg. VFA:	71	66

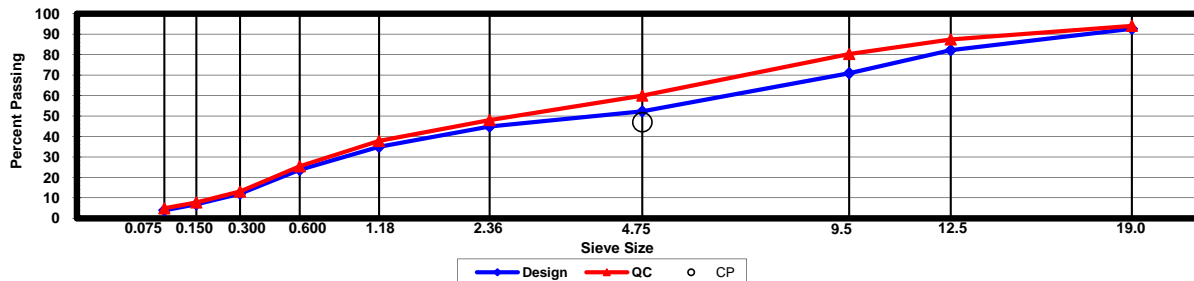
Construction Diary

Relevant Conditions for Construction

Completion Date: July 14, 2009
 24 Hour High Temperature (F): 93
 24 Hour Low Temperature (F): 72
 24 Hour Rainfall (in): 0.00
 Planned Subot Lift Thickness (in): 2.8
 Paving Machine: Roadtec

Plant Configuration and Placement Details

Component	% Setting
Asphalt Content (Plant Setting)	4.7
78 Opelika Limestone	30.0
57 Opelika Limestone	18.0
M10 Columbus Granite	25.0
Shorter Coarse Sand	27.0
As-Built Sublot Lift Thickness (in):	2.8
Total Thickness of All 2009 Sublots (in):	6.9
Approx. Underlying HMA Thickness (in):	0.0
Type of Tack Coat Utilized:	NTSS-1HM
Target Tack Application Rate (gal/sy):	0.07
Approx. Avg. Temperature at Plant (F):	250
Avg. Measured Mat Compaction:	92.9%



General Notes:

- 1) Mixes are referenced by quadrant (E=East, N=North, W=West, and S=South), section # (sequential) and subplot (top=1);
- 2) The total HMA thickness of all structural study sections (N1-N11 and S8-S12) ranges from 5-3/4 to 14 inches by design;
- 3) All non-structural sections are supported by a uniform perpetual foundation in order to study surface mix performance;
- 4) SMA and OGFC refer to stone matrix asphalt and open-graded friction course, respectively; and
- 5) All liquid asphalt purchased for use in Track reconstruction contained LOF 6500 antistripping additive at a rate of 0.5 percent

Quadrant: S
Section: 11
Sublot: 3

Laboratory Diary

General Description of Mix and Materials

Design Method: WMA
 Compactive Effort: 80 gyrations
 Binder Performance Grade: 67-22+
 Modifier Type: Additive
 Aggregate Type: Lms/Sand/Grn
 Design Gradation Type: Fine

Avg. Lab Properties of Plant Produced Mix

Sieve Size	Design	QC
25 mm (1"):	100	99
19 mm (3/4"):	93	95
12.5 mm (1/2"):	84	87
9.5 mm (3/8"):	73	80
4.75 mm (#4):	55	61
2.36 mm (#8):	47	50
1.18 mm (#16):	36	40
0.60 mm (#30):	25	28
0.30 mm (#50):	14	16
0.15 mm (#100):	8	9
0.075 mm (#200):	4.6	5.3
Binder Content (Pb):	4.6	5.0
Eff. Binder Content (Pbe):	4.1	4.5
Dust-to-Binder Ratio:	1.1	1.2
Rice Gravity (Gmm):	2.574	2.522
Avg. Bulk Gravity (Gmb):	2.471	2.447
Avg Air Voids (Va):	4.0	3.0
Agg. Bulk Gravity (Gsb):	2.738	2.693
Avg VMA:	13.9	13.7
Avg. VFA:	71	78

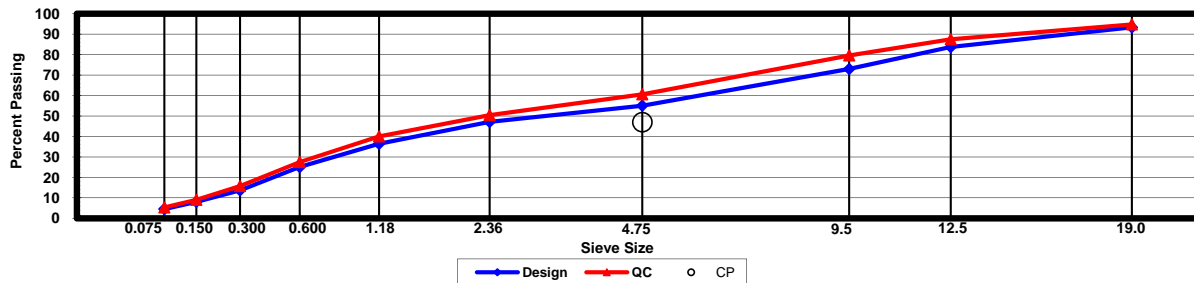
Construction Diary

Relevant Conditions for Construction

Completion Date: July 3, 2009
 24 Hour High Temperature (F): 92
 24 Hour Low Temperature (F): 69
 24 Hour Rainfall (in): 0.00
 Planned Sublot Lift Thickness (in): 3.0
 Paving Machine: Roadtec

Plant Configuration and Placement Details

Component	% Setting
Asphalt Content (Plant Setting)	4.9
78 Opelika Limestone	30.0
57 Opelika Limestone	18.0
M10 Columbus Granite	25.0
Shorter Coarse Sand	27.0
As-Built Sublot Lift Thickness (in):	2.6
Total Thickness of All 2009 Sublots (in):	6.9
Approx. Underlying HMA Thickness (in):	0.0
Type of Tack Coat Utilized:	NA
Target Tack Application Rate (gal/sy):	NA
Approx. Avg. Temperature at Plant (F):	250
Avg. Measured Mat Compaction:	93.9%



General Notes:

- 1) Mixes are referenced by quadrant (E=East, N=North, W=West, and S=South), section # (sequential) and subplot (top=1);
- 2) The total HMA thickness of all structural study sections (N1-N11 and S8-S12) ranges from 5-3/4 to 14 inches by design;
- 3) All non-structural sections are supported by a uniform perpetual foundation in order to study surface mix performance;
- 4) SMA and OGFC refer to stone matrix asphalt and open-graded friction course, respectively; and
- 5) All liquid asphalt purchased for use in Track reconstruction contained LOF 6500 antistripping additive at a rate of 0.5 percent

Quadrant: N
Section: 10
Sublot: 1

Laboratory Diary

General Description of Mix and Materials

Design Method: Super
 Compactive Effort: 80 gyrations
 Binder Performance Grade: 67-22
 Modifier Type: NA
 Aggregate Type: RAP/Sand/Grn
 Design Gradation Type: Fine

Avg. Lab Properties of Plant Produced Mix

Sieve Size	Design	QC
25 mm (1"):	100	100
19 mm (3/4"):	100	100
12.5 mm (1/2"):	100	100
9.5 mm (3/8"):	96	95
4.75 mm (#4):	64	67
2.36 mm (#8):	52	48
1.18 mm (#16):	42	39
0.60 mm (#30):	29	27
0.30 mm (#50):	14	12
0.15 mm (#100):	8	7
0.075 mm (#200):	5.2	4.7
Binder Content (Pb):	6.2	6.0
Eff. Binder Content (Pbe):	5.5	5.2
Dust-to-Binder Ratio:	0.9	0.9
Rice Gravity (Gmm):	2.447	2.450
Avg. Bulk Gravity (Gmb):	2.349	2.356
Avg Air Voids (Va):	4.0	3.8
Agg. Bulk Gravity (Gsb):	2.636	2.631
Avg VMA:	16.4	15.8
Avg. VFA:	76	76

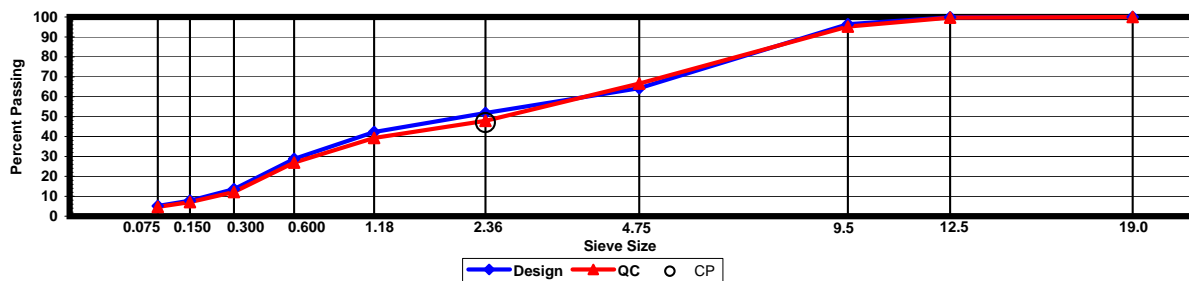
Construction Diary

Relevant Conditions for Construction

Completion Date: August 11, 2009
 24 Hour High Temperature (F): 95
 24 Hour Low Temperature (F): 76
 24 Hour Rainfall (in): 0.00
 Planned Sublot Lift Thickness (in): 1.3
 Paving Machine: Roadtec

Plant Configuration and Placement Details

Component	% Setting
Asphalt Content (Plant Setting)	5.6
89 Columbus Granite	24.0
Shorter Coarse Sand	26.0
Fine Fraction Local RAP	15.0
Coarse Fraction Local RAP	35.0
As-Built Sublot Lift Thickness (in):	1.4
Total Thickness of All 2009 Sublots (in):	7.1
Approx. Underlying HMA Thickness (in):	0.0
Type of Tack Coat Utilized:	PG67-22
Target Tack Application Rate (gal/sy):	0.05
Approx. Avg. Temperature at Plant (F):	325
Avg. Measured Mat Compaction:	92.6%



General Notes:

- Mixes are referenced by quadrant (E=East, N=North, W=West, and S=South), section # (sequential) and subplot (top=1);
- The total HMA thickness of all structural study sections (N1-N11 and S8-S12) ranges from 5-3/4 to 14 inches by design;
- All non-structural sections are supported by a uniform perpetual foundation in order to study surface mix performance;
- SMA and OGFC refer to stone matrix asphalt and open-graded friction course, respectively; and
- All liquid asphalt purchased for use in Track reconstruction contained LOF 6500 antistripping additive at a rate of 0.5 percent

Quadrant: N
Section: 10
Sublot: 2

Laboratory Diary

General Description of Mix and Materials

Design Method: Super
 Compactive Effort: 80 gyrations
 Binder Performance Grade: 67-22
 Modifier Type: NA
 Aggregate Type: RAP/Lms/Sand
 Design Gradation Type: Fine

Avg. Lab Properties of Plant Produced Mix

Sieve Size	Design	QC
25 mm (1"):	100	98
19 mm (3/4"):	94	93
12.5 mm (1/2"):	87	86
9.5 mm (3/8"):	78	79
4.75 mm (#4):	54	56
2.36 mm (#8):	46	46
1.18 mm (#16):	37	37
0.60 mm (#30):	26	26
0.30 mm (#50):	14	13
0.15 mm (#100):	8	8
0.075 mm (#200):	5.1	5.6
Binder Content (Pb):	4.8	4.4
Eff. Binder Content (Pbe):	4.2	3.8
Dust-to-Binder Ratio:	1.2	1.5
Rice Gravity (Gmm):	2.542	2.552
Avg. Bulk Gravity (Gmb):	2.440	2.436
Avg Air Voids (Va):	4.0	4.5
Agg. Bulk Gravity (Gsb):	2.698	2.695
Avg VMA:	13.9	13.6
Avg. VFA:	72	67

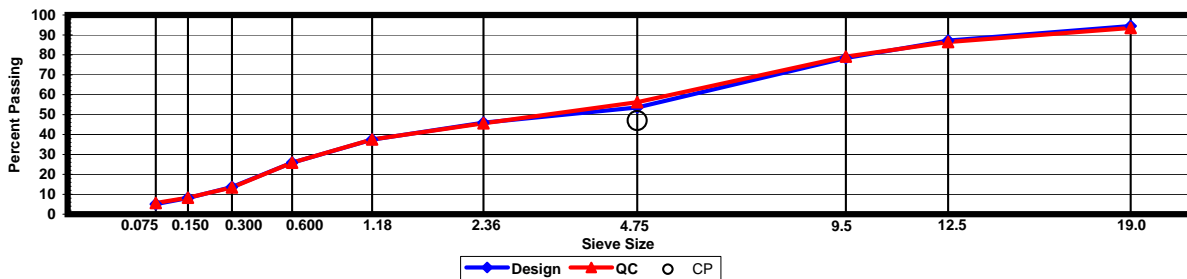
Construction Diary

Relevant Conditions for Construction

Completion Date: August 4, 2009
 24 Hour High Temperature (F): 94
 24 Hour Low Temperature (F): 73
 24 Hour Rainfall (in): 0.00
 Planned Sublot Lift Thickness (in): 2.8
 Paving Machine: Roadtec

Plant Configuration and Placement Details

Component	% Setting
Asphalt Content (Plant Setting)	5.8
78 Opelika Limestone	15.0
57 Opelika Limestone	15.0
Shorter Coarse Sand	20.0
Fine Fraction Local RAP	20.0
Coarse Fraction Local RAP	30.0
As-Built Sublot Lift Thickness (in):	2.7
Total Thickness of All 2009 Sublots (in):	7.1
Approx. Underlying HMA Thickness (in):	0.0
Type of Tack Coat Utilized:	NTSS-1HM
Target Tack Application Rate (gal/sy):	0.05
Approx. Avg. Temperature at Plant (F):	325
Avg. Measured Mat Compaction:	92.9%



General Notes:

- Mixes are referenced by quadrant (E=East, N=North, W=West, and S=South), section # (sequential) and subplot (top=1);
- The total HMA thickness of all structural study sections (N1-N11 and S8-S12) ranges from 5-3/4 to 14 inches by design;
- All non-structural sections are supported by a uniform perpetual foundation in order to study surface mix performance;
- SMA and OGFC refer to stone matrix asphalt and open-graded friction course, respectively; and
- All liquid asphalt purchased for use in Track reconstruction contained LOF 6500 antistripping additive at a rate of 0.5 percent

Quadrant: N
Section: 10
Sublot: 3

Laboratory Diary

General Description of Mix and Materials

Design Method: Super
 Compactive Effort: 80 gyrations
 Binder Performance Grade: 67-22
 Modifier Type: NA
 Aggregate Type: RAP/Lms/Sand
 Design Gradation Type: Fine

Avg. Lab Properties of Plant Produced Mix

Sieve Size	Design	QC
25 mm (1"):	100	99
19 mm (3/4"):	94	95
12.5 mm (1/2"):	87	89
9.5 mm (3/8"):	78	82
4.75 mm (#4):	54	58
2.36 mm (#8):	46	47
1.18 mm (#16):	37	39
0.60 mm (#30):	26	27
0.30 mm (#50):	14	14
0.15 mm (#100):	8	9
0.075 mm (#200):	5.1	5.8
Binder Content (Pb):	4.8	4.7
Eff. Binder Content (Pbe):	4.2	4.1
Dust-to-Binder Ratio:	1.2	1.4
Rice Gravity (Gmm):	2.542	2.537
Avg. Bulk Gravity (Gmb):	2.440	2.431
Avg Air Voids (Va):	4.0	4.2
Agg. Bulk Gravity (Gsb):	2.698	2.688
Avg VMA:	13.9	13.8
Avg. VFA:	72	70

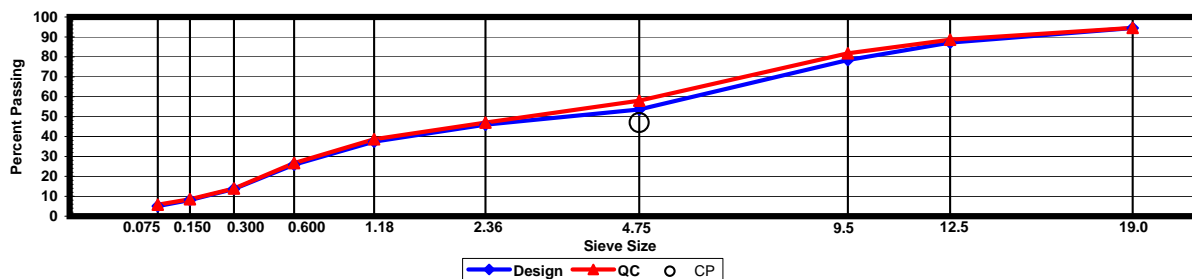
Construction Diary

Relevant Conditions for Construction

Completion Date: August 4, 2009
 24 Hour High Temperature (F): 94
 24 Hour Low Temperature (F): 73
 24 Hour Rainfall (in): 0.00
 Planned Subot Lift Thickness (in): 3.0
 Paving Machine: Roadtec

Plant Configuration and Placement Details

Component	% Setting
Asphalt Content (Plant Setting)	5.8
78 Opelika Limestone	15.0
57 Opelika Limestone	15.0
Shorter Coarse Sand	20.0
Fine Fraction Local RAP	20.0
Coarse Fraction Local RAP	30.0
As-Built Sublot Lift Thickness (in):	3.0
Total Thickness of All 2009 Sublots (in):	7.1
Approx. Underlying HMA Thickness (in):	0.0
Type of Tack Coat Utilized:	NA
Target Tack Application Rate (gal/sy):	NA
Approx. Avg. Temperature at Plant (F):	325
Avg. Measured Mat Compaction:	95.0%



General Notes:

- Mixes are referenced by quadrant (E=East, N=North, W=West, and S=South), section # (sequential) and subplot (top=1);
- The total HMA thickness of all structural study sections (N1-N11 and S8-S12) ranges from 5-3/4 to 14 inches by design;
- All non-structural sections are supported by a uniform perpetual foundation in order to study surface mix performance;
- SMA and OGFC refer to stone matrix asphalt and open-graded friction course, respectively; and
- All liquid asphalt purchased for use in Track reconstruction contained LOF 6500 antistripping additive at a rate of 0.5 percent

Quadrant: N
Section: 11
Sublot: 1

Laboratory Diary

General Description of Mix and Materials

Design Method: Super
 Compactive Effort: 80 gyrations
 Binder Performance Grade: 67-22
 Modifier Type: NA
 Aggregate Type: RAP/Sand/Grn
 Design Gradation Type: Fine

Avg. Lab Properties of Plant Produced Mix

Sieve Size	Design	QC
25 mm (1"):	100	100
19 mm (3/4"):	100	100
12.5 mm (1/2"):	100	99
9.5 mm (3/8"):	96	95
4.75 mm (#4):	64	69
2.36 mm (#8):	52	51
1.18 mm (#16):	42	41
0.60 mm (#30):	29	27
0.30 mm (#50):	14	12
0.15 mm (#100):	8	7
0.075 mm (#200):	5.2	4.8
Binder Content (Pb):	6.2	6.1
Eff. Binder Content (Pbe):	5.5	5.3
Dust-to-Binder Ratio:	0.9	0.9
Rice Gravity (Gmm):	2.447	2.449
Avg. Bulk Gravity (Gmb):	2.349	2.371
Avg Air Voids (Va):	4.0	3.2
Agg. Bulk Gravity (Gsb):	2.636	2.633
Avg VMA:	16.4	15.5
Avg. VFA:	76	79

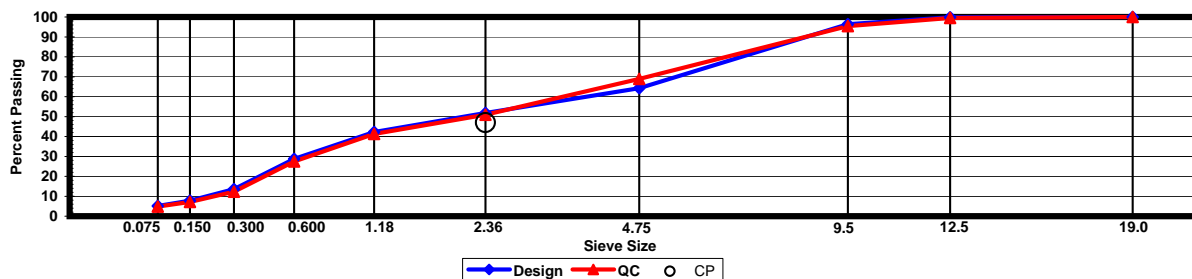
Construction Diary

Relevant Conditions for Construction

Completion Date: August 11, 2009
 24 Hour High Temperature (F): 95
 24 Hour Low Temperature (F): 76
 24 Hour Rainfall (in): 0.00
 Planned Subot Lift Thickness (in): 1.3
 Paving Machine: Roadtec

Plant Configuration and Placement Details

Component	% Setting
Asphalt Content (Plant Setting)	5.6
89 Columbus Granite	24.0
Shorter Coarse Sand	26.0
Fine Fraction Local RAP	15.0
Coarse Fraction Local RAP	35.0
As-Built Sublot Lift Thickness (in):	1.2
Total Thickness of All 2009 Sublots (in):	7.1
Approx. Underlying HMA Thickness (in):	0.0
Type of Tack Coat Utilized:	PG67-22
Target Tack Application Rate (gal/sy):	0.05
Approx. Avg. Temperature at Plant (F):	275
Avg. Measured Mat Compaction:	92.1%



General Notes:

- Mixes are referenced by quadrant (E=East, N=North, W=West, and S=South), section # (sequential) and subplot (top=1);
- The total HMA thickness of all structural study sections (N1-N11 and S8-S12) ranges from 5-3/4 to 14 inches by design;
- All non-structural sections are supported by a uniform perpetual foundation in order to study surface mix performance;
- SMA and OGFC refer to stone matrix asphalt and open-graded friction course, respectively; and
- All liquid asphalt purchased for use in Track reconstruction contained LOF 6500 antistripping additive at a rate of 0.5 percent

Quadrant: N
Section: 11
Sublot: 2

Laboratory Diary

General Description of Mix and Materials

Design Method: Super
 Compactive Effort: 80 gyrations
 Binder Performance Grade: 67-22
 Modifier Type: NA
 Aggregate Type: RAP/Lms/Sand
 Design Gradation Type: Fine

Avg. Lab Properties of Plant Produced Mix

Sieve Size	Design	QC
25 mm (1"):	100	99
19 mm (3/4"):	94	93
12.5 mm (1/2"):	87	86
9.5 mm (3/8"):	78	79
4.75 mm (#4):	54	58
2.36 mm (#8):	46	47
1.18 mm (#16):	37	39
0.60 mm (#30):	26	27
0.30 mm (#50):	14	14
0.15 mm (#100):	8	8
0.075 mm (#200):	5.1	5.7
Binder Content (Pb):	4.8	4.7
Eff. Binder Content (Pbe):	4.2	4.1
Dust-to-Binder Ratio:	1.2	1.4
Rice Gravity (Gmm):	2.542	2.541
Avg. Bulk Gravity (Gmb):	2.440	2.446
Avg Air Voids (Va):	4.0	3.7
Agg. Bulk Gravity (Gsb):	2.698	2.697
Avg VMA:	13.9	13.6
Avg. VFA:	72	72

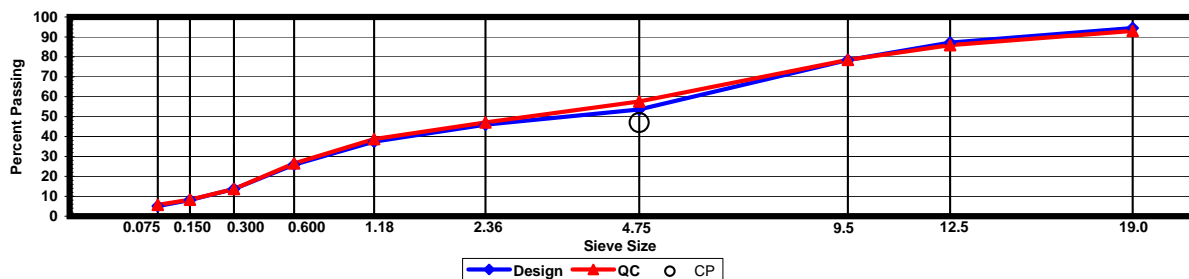
Construction Diary

Relevant Conditions for Construction

Completion Date: August 4, 2009
 24 Hour High Temperature (F): 94
 24 Hour Low Temperature (F): 73
 24 Hour Rainfall (in): 0.00
 Planned Sublot Lift Thickness (in): 2.8
 Paving Machine: Roadtec

Plant Configuration and Placement Details

Component	% Setting
Asphalt Content (Plant Setting)	5.8
78 Opelika Limestone	15.0
57 Opelika Limestone	15.0
Shorter Coarse Sand	20.0
Fine Fraction Local RAP	20.0
Coarse Fraction Local RAP	30.0
As-Built Sublot Lift Thickness (in):	3.0
Total Thickness of All 2009 Sublots (in):	7.1
Approx. Underlying HMA Thickness (in):	0.0
Type of Tack Coat Utilized:	NTSS-1HM
Target Tack Application Rate (gal/sy):	0.05
Approx. Avg. Temperature at Plant (F):	275
Avg. Measured Mat Compaction:	93.1%



General Notes:

- Mixes are referenced by quadrant (E=East, N=North, W=West, and S=South), section # (sequential) and subplot (top=1);
- The total HMA thickness of all structural study sections (N1-N11 and S8-S12) ranges from 5-3/4 to 14 inches by design;
- All non-structural sections are supported by a uniform perpetual foundation in order to study surface mix performance;
- SMA and OGFC refer to stone matrix asphalt and open-graded friction course, respectively; and
- All liquid asphalt purchased for use in Track reconstruction contained LOF 6500 antistripping additive at a rate of 0.5 percent

Quadrant: N
Section: 11
Sublot: 3

Laboratory Diary

General Description of Mix and Materials

Design Method: Super
 Compactive Effort: 80 gyrations
 Binder Performance Grade: 67-22
 Modifier Type: NA
 Aggregate Type: RAP/Lms/Sand
 Design Gradation Type: Fine

Avg. Lab Properties of Plant Produced Mix

Sieve Size	Design	QC
25 mm (1"):	100	97
19 mm (3/4"):	94	89
12.5 mm (1/2"):	87	83
9.5 mm (3/8"):	78	75
4.75 mm (#4):	54	54
2.36 mm (#8):	46	44
1.18 mm (#16):	37	37
0.60 mm (#30):	26	25
0.30 mm (#50):	14	13
0.15 mm (#100):	8	8
0.075 mm (#200):	5.1	5.3
Binder Content (Pb):	4.8	4.6
Eff. Binder Content (Pbe):	4.2	4.0
Dust-to-Binder Ratio:	1.2	1.3
Rice Gravity (Gmm):	2.542	2.544
Avg. Bulk Gravity (Gmb):	2.440	2.439
Avg Air Voids (Va):	4.0	4.1
Agg. Bulk Gravity (Gsb):	2.698	2.695
Avg VMA:	13.9	13.7
Avg. VFA:	72	70

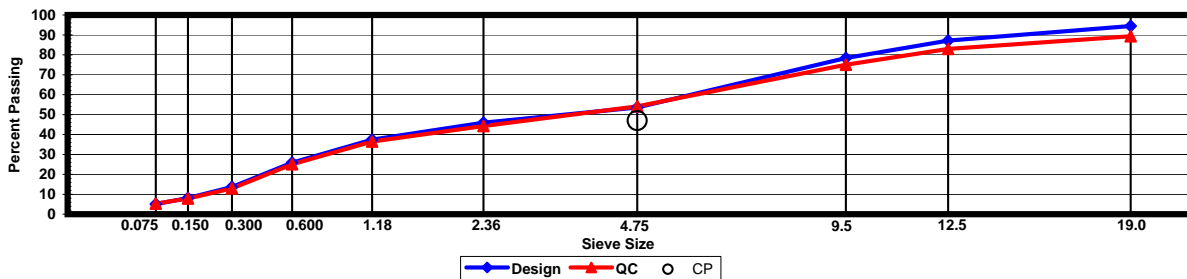
Construction Diary

Relevant Conditions for Construction

Completion Date: August 4, 2009
 24 Hour High Temperature (F): 94
 24 Hour Low Temperature (F): 73
 24 Hour Rainfall (in): 0.00
 Planned Subot Lift Thickness (in): 3.0
 Paving Machine: Roadtec

Plant Configuration and Placement Details

Component	% Setting
Asphalt Content (Plant Setting)	5.8
78 Opelika Limestone	15.0
57 Opelika Limestone	15.0
Shorter Coarse Sand	20.0
Fine Fraction Local RAP	20.0
Coarse Fraction Local RAP	30.0
As-Built Sublot Lift Thickness (in):	2.9
Total Thickness of All 2009 Sublots (in):	7.1
Approx. Underlying HMA Thickness (in):	0.0
Type of Tack Coat Utilized:	NA
Target Tack Application Rate (gal/sy):	NA
Approx. Avg. Temperature at Plant (F):	275
Avg. Measured Mat Compaction:	94.2%



General Notes:

- Mixes are referenced by quadrant (E=East, N=North, W=West, and S=South), section # (sequential) and subplot (top=1);
- The total HMA thickness of all structural study sections (N1-N11 and S8-S12) ranges from 5-3/4 to 14 inches by design;
- All non-structural sections are supported by a uniform perpetual foundation in order to study surface mix performance;
- SMA and OGFC refer to stone matrix asphalt and open-graded friction course, respectively; and
- All liquid asphalt purchased for use in Track reconstruction contained LOF 6500 antistrip additive at a rate of 0.5 percent